A Unique and Species-Rich Assemblage of Freshwater Glassfishes (Teleostei: Ambassidae: Dapalis) from the lower Oligocene of the Central Paratethys with the Description of Four New Species

Harald Ahnelt, Katarina Bradić-Milinović

taxonomy

MDPI

Article

A Unique and Species-Rich Assemblage of Freshwater Glassfishes (Teleostei: Ambassidae: *Dapalis*) from the lower Oligocene of the Central Paratethys with the Description of Four New Species †

Harald Ahnelt [1,2,*] and Katarina Bradić-Milinović [3]

[1] Department of Evolutionary Biology, University of Vienna, Djerassiplatz 1, 1030 Vienna, Austria
[2] First Zoological Department, Natural History Museum Vienna, Burgring 7, 1010 Vienna, Austria
[3] Department of Regional Geology, Faculty of Mining and Geology, University of Belgrade, Kamenička 6, 11000 Belgrade, Serbia; katarina.bradic.milinovic@rgf.bg.ac.rs
* Correspondence: harald.ahnelt@univie.ac.at
† urn:lsid:zoobank.org:pub:A836201B-E17A-4364-AD68-6504CA9521E9; urn:lsid:zoobank.org:act:C60EE4E0-C67D-4678-B125-A916B029870; urn:lsid:zoobank.org:act: 1CB14345-5A37-4E1C-8D9C-8FA0D0FC74C7; urn:lsid:zoobank.org:act:DF983A46-4DEE-476C-9AE1-E96FAB07739E; urn:lsid:zoobank.org:act: A57C5831-F7C3-45EF-A31D-F122C9F66D09.

Abstract: We describe four new species of the fossil genus *Dapalis* (Ambassidae), *Dapalis absconditus* sp. nov., *Dapalis octospinus* sp. nov., *Dapalis parvus* sp. nov. and *Dapalis quintus* sp. nov., based on articulated skeletons with otoliths in situ from a freshwater habitat of the lower Oligocene of Raljin/Strelac (Serbia). Besides in body shape (e.g., body length, body depth, head length, preanal length), the species differ in morphological characters like, e.g., the serration of the preopercle, the length of the first two spines of the first dorsal and the anal fin and the morphology of the sagittal otoliths (e.g., ratio of otolith height to otolith length, ratio of otolith width to otolith length). Together with *D. pauciserratus*, also described from Raljin, these four species represent the most species-rich assemblage of freshwater *Dapalis* known so far. The compartmentalization of the internal structure of the spines reveals the close relationship of *Dapalis* and extant Ambassidae. Additionally, we discuss a new character from the ventral field of the otolith, a ventral depression, only found in species from Raljin. This new character is unique among the European *Dapalis* species and allows us to separate these five species into two species groups.

Keywords: Ambassidae; otoliths in situ; fossil record; cenozoic; Serbia

Citation: Ahnelt, H.; Bradić-Milinović, K. A Unique and Species-Rich Assemblage of Freshwater Glassfishes (Teleostei: Ambassidae: *Dapalis*) from the lower Oligocene of the Central Paratethys with the Description of Four New Species. *Taxonomy* **2024**, *4*, 805–849. https://doi.org/10.3390/taxonomy4040044

Academic Editor: Mathias Harzhauser

Received: 1 October 2024
Revised: 9 November 2024
Accepted: 11 November 2024
Published: 20 November 2024

1. Introduction

Dapalis Gistel, 1848, is an extinct genus of the glass perch family Ambassidae Klunzinger, 1870 (formerly Chandidae Fowler, 1905). The genus existed in Europe from the middle Eocene to the middle Miocene [1]. Three species occurred in the Eocene of Europe, two brackish water species (*Dapalis hungaricus* (Schubert, 1912) and *D. ventricosus* Nolf & Reichenbacher, 1999) and one (*D. praecursor* Gaudant, 2007) freshwater species. The radiation of this genus especially during the early Oligocene resulted in a number of freshwater species like, e.g., *D. angustus* Reichenbacher & Weidmann, 1992 [2], *D. borkensis* (Weiler, 1961) [3] or *D. pauciserratus* Ahnelt, Bradić-Milinović & Schwarzhans, 2024 [4] (Table 1). Although paleontological evidence suggests a marine origin of this genus in the Indo-West Pacific (discussed in [4]), so far, records of *Dapalis* in Europe are only known from brackish and/or freshwater habitats.

During the middle and late Eocene, when the first Ambassidae occurred in Europe, freshwater habitats were island-bound, with few primary freshwater fishes and a high number of marine immigrants were able to adapt to waters of low salinity [5] like, e.g., the

brackish water ambassid species *D. hungaricus* [6] and *D. ventricosus* [7] or the freshwater species *D. praecursor* [8]. This trend to occupy brackish and freshwater habitats continued throughout the entire Oligocene and the late early Miocene and resulted in a remarkable radiation, especially in the early Oligocene, i.e., the freshwater species *D. borkensis* [3] and *D. pauciserratus* [4], the brackish/freshwater species *D. angustus* Reichenbacher & Weidmann, 1992, and *D. transylvanicus* Reichenbacher & Codrea, 1999, or the brackish water species *D. macrurus* (Agassiz, 1836). Many more than the currently recognized 17 species of *Dapalis* were described in Europe. However, most of them are now placed with other generic names in different fish families. For a detailed list of these species, we refer to Ahnelt et al. [4].

Species descriptions of *Dapalis* in Europe based on skeletons are rare [8–12], as are descriptions of specimens with otoliths in situ [4,11,13]. The majority of *Dapalis* species are only known from otoliths, e.g., [1,2,14–18]. Only five of the so far seventeen species are known from articulated skeletons, *D. formosus* [10,11,19,20], *D. macrurus* [13,21–23], *D. minutus* [12], *D. pauciserratus* [4] and *D. praecursor* [8] (Table 1).

It has to be noted that many so-called *Dapalis* species were described from skeletons as *Smerdis* but are now placed with other generic names in various fish families like, e.g., *Smerdis budensis* Heckel, 1856, in Percoidei *incertae* [24], *S. isabellae* Gaudry, 1862, in Moronidae [25], *S. micracanthus* Agassiz, 1835, in Centropomidae [26], *Smerdis rotundus* Weiler, 1963, in Atherinidae [17] or *Smerdis sieblosensis* in "Percichhtyiidae" [17,27]. The geology and the fossil lagerstätten with their fish remains, including *Dapalis*, of the Koritinica–Babušnica basin in southeast Serbia are well studied, e.g., [28–34]. Recently, the mammalian fauna from Raljin/Strelac of the Babušnica basin was studied in detail [32,33,35]. These authors showed that the lacustrine sediments of these localities are of early Oligocene (Rupelian) age. Fishes identified as *D. formosus*, *D. macrurus* and *D. minutus* by Anđelković [31] at localities nearby were shown to be misidentified and were placed in other fish families [26,36,37]. The deposits of this basin were variously dated from the early Oligocene to the early Miocene (summarized in [31,36]). However, the lacustrine sediments in the area of Raljin/Strelac were recently dated as of early Oligocene (Rupelian) age [32,34].

The Geological Survey of Serbia (GZS) obtained two specimens of the genus *Dapalis* which turned out to be a new species, *D. pauciserratus* [4]. Recently, four additional skeletons with otoliths in situ from the same locality were donated to the GZS. Here, we describe these specimens as four new species of *Dapalis* from the early Oligocene (Rupelian). These records are remarkable as they document a species-rich assemblage of *Dapalis* species from freshwater deposits.

2. Materials and Methods

Four articulated skeletons with otoliths in situ, collected by Mr. Žarko Petrović near the site "Raljin" (43°0′1″ N, 22°27′56″ E), close to the village Strelac, Babušnica basin (Serbia), were deposited in the Paleontological Collection of the Geološki Zavod Srbije (GZS) (Geological Survey of Serbia), Belgrade, Serbia. These specimens were catalogued as GZS-RA3, GZS-RA21, GZS-RA25 and GZS-RA34. The fishes were embedded in lacustrine marlstone.

We describe the skeletons and the otoliths in detail. Vertebra counts include the urostyle (terminal centrum).

Geological setting.

The Babušnica basin is a 520 km long narrow basin which is part of the tectonic unit of the Carpatho-Balkanides (Figure 1). It extends in the NW-SE direction along a fault zone (Ridan–Krepoljin dislocation) and is located in southeastern Serbia between Koritnica (43°09′ N, 22°19′ E) and Babušnica (43°04′ N, 22°25′ E) [32,38]. The following tectonic sequence is recognized: (i) formation of grabens of Eocene to Oligocene age, (ii) subvolcanic intrusions and dykes, 32–29 Ma, (iii) formation of coal-bearing basin during the late Oligocene–early Miocene and (iv) extensional tectonic during the middle Miocene [39].

The Cenozoic sedimentation of the Babušnica basin is divided into a lower level of sedimentation represented by red conglomerate and sand with large grains of up to

50 cm. This sedimentation is followed by lake deposits which consist of grey marlstone, sandstone and marly limestone. The final phase of sedimentation in the Babušnica basin is characterized by claystone which houses fossil fishes and plants [40].

Paleontological investigations in the area resulted in conflicting age estimates, e.g., Oligocene (Pantić, 1956), early Oligocene [29,30,41] and Oligo-Miocene [42]. However, recent micromammal remains from the locality Raljin were identified to be of early Oligocene (Rupelian) age [32,34,35].

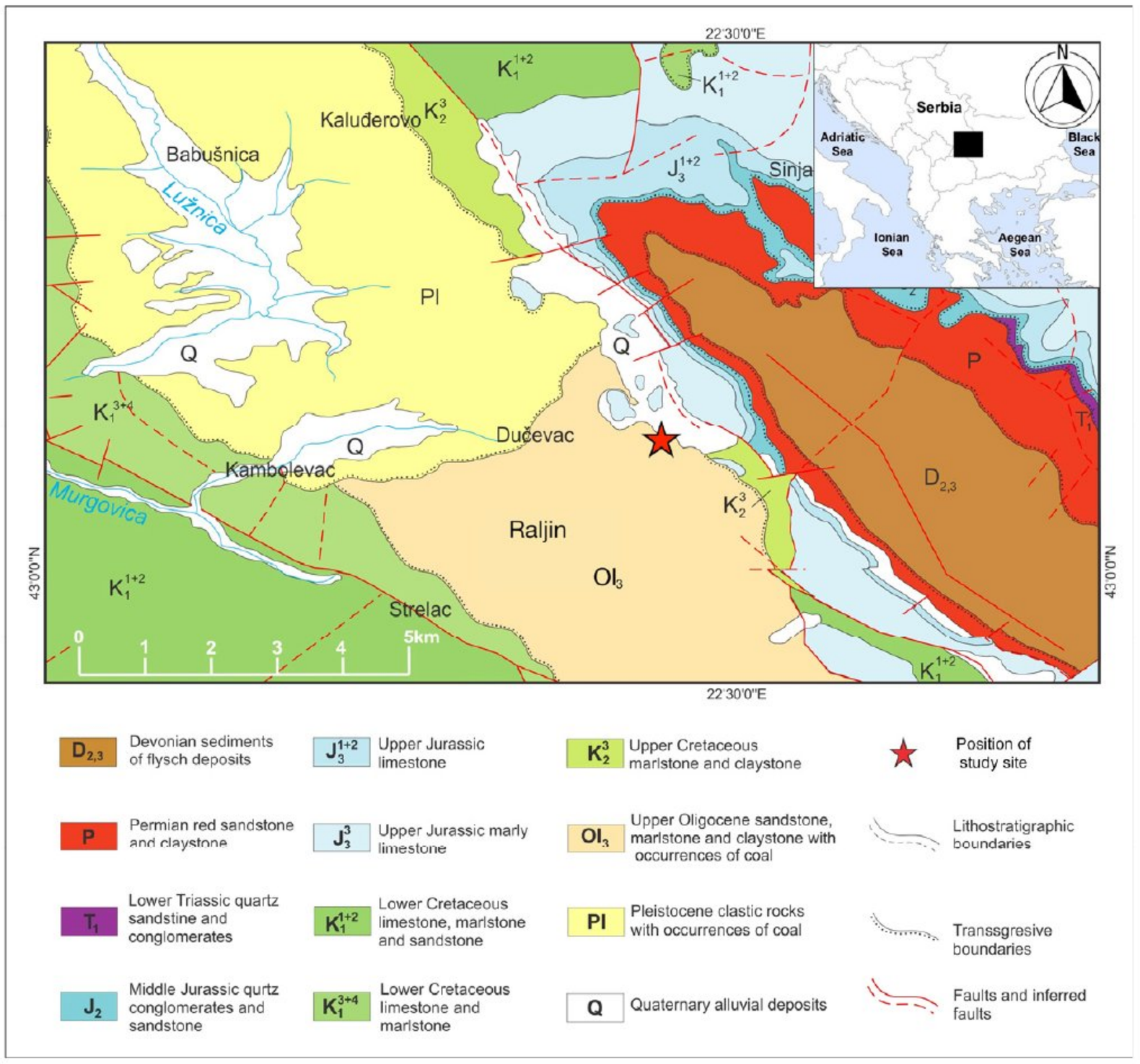

Figure 1. Location and stratigraphy. Simplified geological map of the Babušnica basin, modified from [43–45], with the position of the study site marked as a red star.

Stratigraphic setting.

Two series of sedimentation of the Babušnica basin are recognized in the Cenozoic area: first, a lower level of sedimentation characterized by sand and conglomerate, which is, second, followed by lake deposits of grey marlstone, sandstone and marly limestone. The final phase of sedimentation in the basin contains paleoflora and fossil fishes [40].

Comparative skeletal materials of Dapalis:

Dapalis formosus (Meyer, 1852): SMNS 002960; Unterkirchberg, Deutschland.

Dapalis macrurus (Agassiz, 1834): NHMW 1913/II/115; Aiguebelle près Aubenas-les-Alpes, France; SMNS 55544, Céreste, Alpes de Haute, France. *Dapalis minutus* (Agassiz, 1834): NHMUK P76287, NHMW 1850/XVIII/282, NHMW 1850/XVIII/283, NHMW 1913/II/114 and MNHN Aix-243 (photography); Aix-en-Provence, France. *Dapalis pauciserratus* Ahnelt, Bradić-Milinović, Schwarzhans (2024): GZS-RA1 and GZS-RA5, Raljin, Serbia. *Dapalis praecursor* Gaudant 2007, from [8].

Comparative skeletal material of Ambassidae:

Comparison of the internal structure of the fin spines:

Ambassis ambassis (Lacpéde, 1802), NMW 34591, NMW 34592 and NMW 94593; *Ambassis agrammus* Günther, 1867, US 173828; *Ambassis buruensis* Bleeker, 1856, UF 237575; *Ambassis dussumieri* Cuvier, 1828, IE 16526, NMW 78317 and NMW 86931; *Ambassis macleayi* (Castelnau, 1878), US 173817; *Ambassis nalua* (Hamilton, 1922), NMW 58733; *Ambassis natalensis* Gilchrist & Thompson, 1908, NMW 29529; *Chanda nama* Hamilton 1822, NMW 78319; *Chanda ranga* Hamiton, 1822, NMW 34615; *Denariusa australis* (Steindachner, 1867), US 173814; *Gymnochanda ploegi* Tan & Lim, 2014, IE 15773; *Parambassis baculis* (Hamilton, 1892), UF 178036; *Parambassis lala* (Hamilton, 1822), IE 11182; *Parambassis piratica* (Roberts, 1989), UF 166901; *Parambassis siamensis* (Fowler, 1937), IE 15611; *Parambassis thomassi* (Day, 1870), NMW 76654; *Parambassis wolffi* (Bleeker, 1850).

Comparison of Dapalis otoliths from the early Oligocene: Dapalis pauciserratus Ahnelt, Bradić-Milinović, Schwarzhans (2024): GZS-RA1 and GZS-RA5, Raljin, Serbia.

Comparison of Dapalis otoliths from the early Oligocene based on the literature: Dapalis angustus from [2,18,46], *Dapalis borkensis* from [3,47], *Dapalis macrurus* from [13,48] and *Dapalis transylvanicus* from [18].

The serrations of the opercular, suborbital (infraorbital) and supraorbital bones are of taxonomic importance for ambassid fishes [49,50] including *Dapalis* [4,22] (Figure 2). In the nomenclature of these bones and their ridges, we follow [49]; in the predorsal formula, we follow [51]: each slash represents a neural spine, each 0 represents a supraneural (predorsal) and the numerals represent a pterygiophore and its spine, for example, /0/1/ means one supraneural (=0) between the first and second neural spine (=/) and a pterygiophore supporting one spine (=1) between the second and the third neural spine.

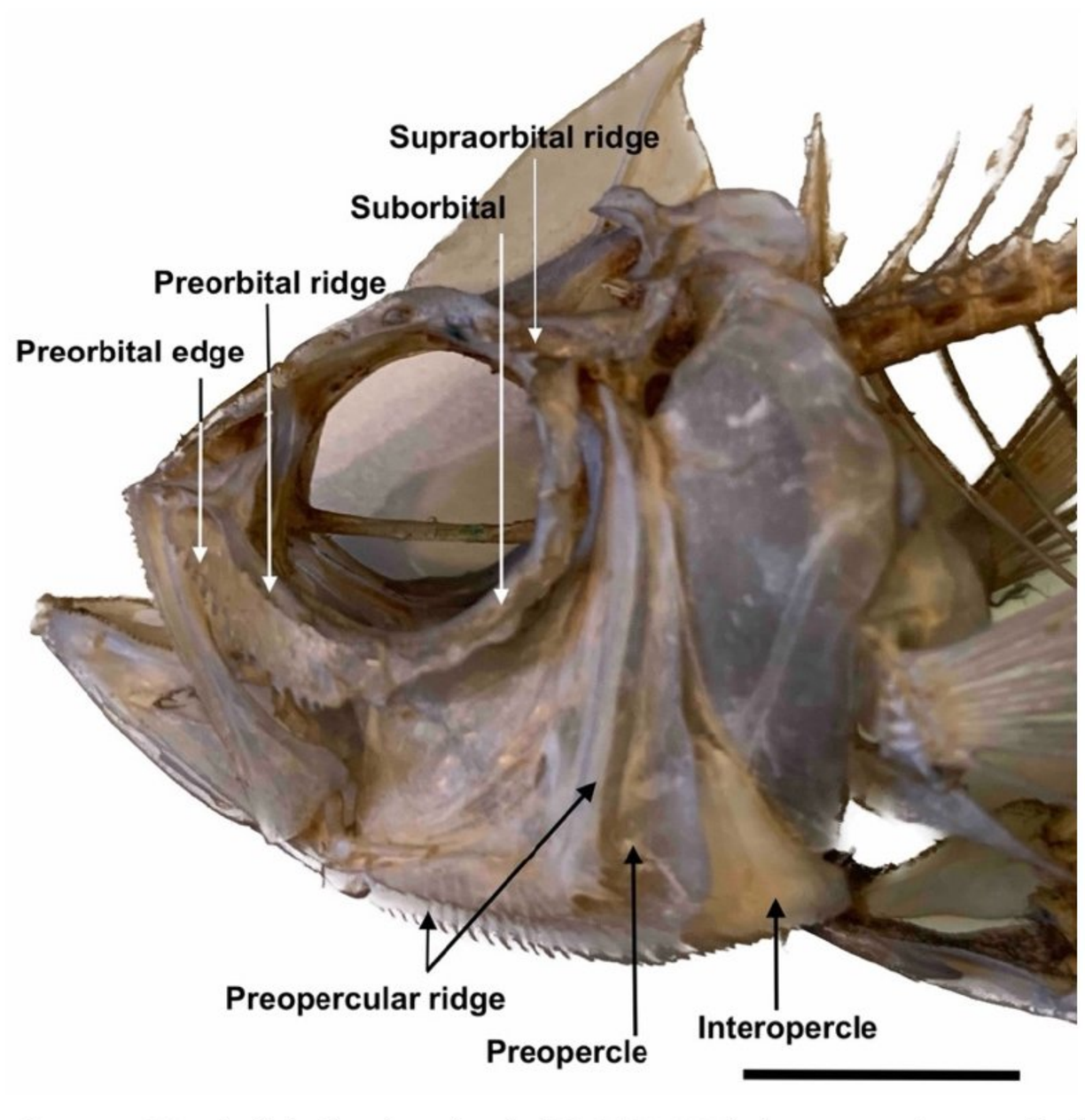

Figure 2. Head of *Ambassis ambassis* (NMW 93975) showing ridges and edges of taxonomic importance. Scale bar is 10 mm. From [4]. Photo H. Ahnelt.

Table 1. Species of the genus *Dapalis* from the Eocene to the Miocene in Europe. Species from the early Oligocene are shaded in grey. The new species are shown in bold. bra-brackish water; fre-fresh water. MP, MN-mammal zones. O = otolith; S = skeleton. [1] [20], [2] [52], [3] [46], [4] [18], [5] [53], [6] [1], [7] [2], [8] [17], [9] [19], [10] [12], [11] [26], [12] [23], [13] [21], [14] [54], [15] [55], [16] [6], [17] [56], [18] [8], [19] [14], [20] [15], [21] [57], [22] [58], [23] [4], [24] [7].

Species	Facies	Age	Biostratigraphic Correlation	Otolith-/Skeleton-Based
D. kuehni [15]	fre–bra	Middle Miocene	MN 5–MN 6	Otolith
D. formosus [1,5,6,8,9,19,20]	bra	Early Miocene	MN 2–MN 4	Otolith/skeleton
D. crassirostris [8,19,20]	fre–bra	Early Miocene	MN 4	Otolith
D. curvirostris [7,8,9,19,20]	bra	Early Miocene	MN 2–MN 4	Otolith
D. kaelini [8]	bra	Early Miocene	MN 2–MN 4	Otolith
D. rhenanus [14,17,21,22]	bra	Early Miocene	MN 2	Otolith
D. carinatus [7]	fre–bra	Late Oligocene–early Miocene	MP 28–29, MN 1	Otolith
D. minutus [10,11]	fre–bra	Late Oligocene–early Miocene	MP 26–MN 2	Skeleton
D. rhomboidalis [7]	fre–bra	Late Oligocene–early Miocene	MP 28–MN 1	Otolith
D. borkensis [4]	fre	Early Oligocene	MP 24	Otolith
D. transylvanicus [4]	fre–bra	Early Oligocene	MP 24	Otolith
***D. absconditus* n. sp.**	fre	Early Oligocene	MP 23	Otolith/skeleton
***D. octospinus* n. sp.**	fre	Early Oligocene	MP 23	Otolith/skeleton
***D. parvus* n.sp.**	fre	Early Oligocene	MP 23	Otolith/skeleton
D. pauciserratus [23]	fre	Early Oligocene	MP 23	Otolith/skeleton
***D. quintus* n. sp.**	fre	Early Oligocene	MP 23	Otolith/skeleton
D. angustus [1,2,3,4,7]	fre–bra	Early Oligocene	MP 21–MP 23	Otolith
D. macrurus [11,12,13]	bra	Early–late Oligocene	MP 21–MP30	Otolith/skeleton
D. ventricosus [24]	bra	Middle Eocene	MP 13–MP 14	Otolith
D. praecursor [18]	fre	Middle Eocene	MP 13–MP 14	Otolith/skeleton
D. hungaricus [16]	bra	Middle Eocene	MP 12–MP 13	Otolith

A final definition of the genus *Dapalis* is challenging because till recently only 5 of the 17 described species were known from their skeletons, the other 12 just by their otoliths [4]. Although the skeletons of four of the five species (Table 1) are well documented (e.g., [8,12,13]), only two attempts have been made to define the genus *Dapalis* [9,13]. The first definition of *Dapalis* (as *Smerdis*) was provided by [9] based on a species which is actually a member of another fish family (Centropomidae) [26]. The second definition was provided by [13] but focused only on generalized percomorph characters. Weiler [13] included some traits of the otolith morphology, but there is, to our best knowledge, no generic definition of this genus based on the sagittal otolith [2–4,7,8,13,16,18]. This is possibly the reason why all European extinct ambassid fishes are summarized in the genus *Dapalis*. As already mentioned by Ahnelt et al. [4], a revision of *Dapalis* is needed, but additional material, especially well-preserved skeletons also from regions outside of Europe, is needed to do so. However, we give a comprehensive description of the genus *Dapalis*.

A common character of extinct and extant Ambassidae is the compartmentalization of the internal structure of the fin spines [4]. The external surface of the spines of the four specimens examined was not splintered, as was the case with the holotype of *D. pauciserratus* from the same locality [4]. Fortunately, one of us (K. B.-M.) was given permission to remove the external-most layer of spines of the first dorsal fin. However, we are now able to show the typical compartmentalized structure of Ambassidae in three of the four new specimens. It was not possible to remove this external sheet in the fourth specimen. Due to the high risk of irreversibly damaging the fin of the holotype, this attempt was postponed until more specimens are available. However, all morphological structures indicate that it is a congener of the other Raljin species.

Because three specimens in this study exhibit a unique morphology of the ventral field of the sagittal otolith, a character not known for the other European species of *Dapalis*, we

also provide sketches of the interpretative surface relief of the ventral area of the otoliths for all of them and additionally for all other species from the early Oligocene (Table 1).

Abbreviations: IE, Deutsches Meeresmuseum, Stralsund; GZS, Geološki Zavod Srbije, Belgrade; MNHN, Muséum national d'histoire naturelle, Paris; NHMUK, Natural History Museum, London; NHMW, Naturhistorisches Museum Wien; NMW, a traditional abbreviation for the Ichthyological collection of NHMW catalogue numbers; UF, Florida Museum of Natural History, Gainesville; USNM, National Museum of Natural History, Washington.

3. Results

The classification of the genus examined in this study is as follows:

- Class Actinopterygii Woodward, 1891;
- Subclass Neopterygii Regan, 1923;
- Infraclass Teleostei Müller, 1845;
- Division Acanthopterygii Artedi, 1738;
- Clade Percomorpha Hay, 1903;
- Family Ambassidae Klunzinger, 1870;
- Genus *Dapalis* Gistel, 1848.

Diagnosis of the genus *Dapalis*:

The genus is characterized by the combination of the following characters: body laterally compressed, of various height; head generally large; mouth terminal; teeth small, conical; cycloid scales; preopercle and preorbital (first suborbital) generally with serrations; preopercle without spine at angle; generally three supraneurals; 10 precaudal vertebrae and 14 caudal vertebrae including the urostyle (compound center); first and second dorsal fin connected at their bases; first dorsal fin with seven strong and rigid spines, anal fin with three strong and rigid spines and pelvic fin with a single, strong spine; the spines are internally compartmentalized; pelvic fins insert just slightly posterior to the pectoral fins; caudal fin deeply forked; sagittal otolith deep to elongate with a wide, more or less rounded and deep ostium followed by a long, narrower and straight cauda not bent ventrally at its end; and the ventral field is convex or with a more or less large ventral depression.

Dapalis absconditus Bradić-Milinović and Ahnelt sp. nov. (Figures 1–10; Tables 2–4).

Holotype: registration number GZS-RA3 (Figure 3).

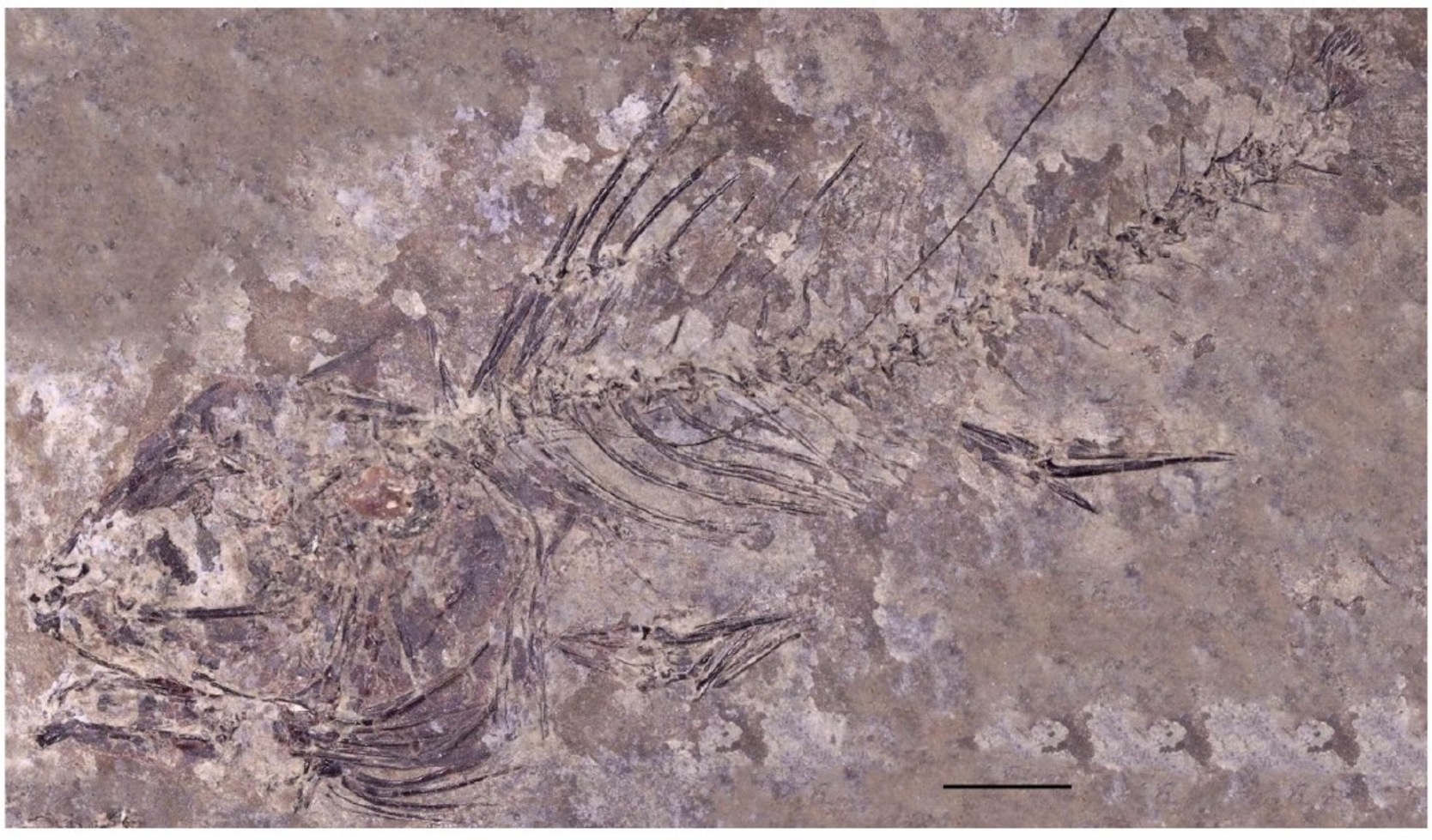

Figure 3. *Dapalis absconditus* sp. nov., articulated skeleton, holotype GZS-RA3. Scale bar is 3 mm. Photo K. Bradić-Milinović.

Type locality: Raljin, Babušnica basin, Serbia: 43°0′1″ N, 22°27′56″ E.

Distribution: the new species is only known from Serbia, Raljin, Babušnica basin; early Oligocene, Rupelian.

Etymology: the new species is named *absconditus*, a Latin adjective meaning hidden, with reference to the posterior edge of the preopercle which is hidden below scales and bony fragments.

Diagnosis: *Dapalis absconditus* is distinguished from its congeners by a combination of the following characters: two supraneural (predorsal) bones; length of first spine of the dorsal fin 38.8% of length of the second spine of the dorsal fin; first spine of anal fin short, 35.3% in length of second anal fin spine; second spine of the anal fin 13% of SL; body shape elongate, body depth 29.7% of SL and head depth 27.5% of SL; head long, 35.3% of SL; preorbital (infraorbital one) with two narrow, pointed serrations; two serrations, pointed and narrow on the preopercle, but most of the posterior rim of the preopercle is not visible; otolith oval, deep (ratio of otolith length to otolith height = 1.42) and thin (otolith length to otolith width = 3.61); sulcus moderately short (ratio of otolith length to sulcus length is 1.17) with ostium shorter than cauda (ratio of ostium length to cauda length = 0.80); cauda ending distant from posterior rim; and a short and narrow ventral depression.

Dapalis absconditus is distinguished from the remaining sympatric species of *Dapalis* (*D. octospinus*, *D. parvus*, *D. pauciserratus* and *D. quintus*) from Raljin by (i) a preorbital with two posteriorly directed spine-like serrations, (ii) a moderately high and thin otolith, (iii) a large and round ostium, (iv) a bulbous antirostrum and (v) a narrow and short ventral depression dorsal to the distinctly dome-shaped ventral field.

Description: A deep-bodied species with body depth increasing to the origin of the first dorsal fin. Counts and measurements are reported in Tables 2 and 3. The skeleton of the specimen is completely preserved. However, the bones of the head are only partly discernable (Figure 3).

Table 2. Body proportions in % standard length of the five *Dapalis* species from Raljin (Babušnica basin, Serbia). Values are mean and, in parentheses, range. D1I and DII length, length of the first and second spines of the first dorsal fin; AI and AII length, length of the first and second spines of the anal fin. Values for the holotype of *D. pauciserratus* from [4].

	***Dapalis abscondidus* sp. nov.**	***Dapalis octospinus* sp. nov.**	***Dapalis parvus* sp. nov.**	***Dapalis quintus* sp. nov.**	***Dapalis pauciserratus***
	GZS-RA3	GZS-RA21	GZS-RA34	GZS-RA25	GZS-RA1
SL (mm)	45.5	34.3	32.7	–	42.0
% SL					
Predorsal length	43.0	42.7	41.9	–	41.2
Preanal length	71.5	68.4	67.2	–	66.0
Tail length	38.2	35.1	41.9	–	36.3
Head length	35.3	30.3	–	–	31.4
Head depth	27.5	23.7	22.8	–	23.9
Snout length	–	9.6	8.0	–	7.8
Orbit diameter	–	12.2	9.1	–	11.8
Postorbital length	–	12.6	–	–	13.4
Cheek depth	–	8.6	–	–	7.2
Body depth	29.7	24.0	–	–	24.2
Caudal peduncle length	–	–	–	–	24.2
First dorsal fin base	15.1	17.4	14.1	–	14.4
D1I length	6.0	6.3	5.6	–	5.2
D1II length	16.2	15.2	–	–	Damaged
AI length	4.8	5.1	7.3	–	8.1
AII length	13.7	15.2	14.1	–	12.1

Table 2. *Cont.*

	***Dapalis abscondidus* sp. nov.**	***Dapalis octospinus* sp. nov.**	***Dapalis parvus* sp. nov.**	***Dapalis quintus* sp. nov.**	***Dapalis pauciserratus***
% head length					
Head depth	88.8	78.4	–	–	77.0
Snout length	–	29.4	–	30.7	23.7
Orbit diameter	–	30.0	–	22.7	35.4
Postorbital length	–	39.8	–	46.7	42.6
Cheek depth	–	25.4	–	24.7	23.0
First dorsal fin base	42.6	55.8	–	–	45.9
% D1II					
D1I	38.3	38.7	–	–	–
% AII					
AI	35.3	45.6	51.8	–	69.4

Table 3. Meristic information of the five *Dapalis* species from Raljin (Babušnica basin, Serbia). Values for the holotype of *D. pauciserratus* from [4].

	***Dapalis abscondidus* sp. nov.**	***Dapalis octospinus* sp. nov.**	***Dapalis parvus* sp. nov.**	***Dapalis quintus* sp. nov.**	***Dapalis pauciserratus***
Register numbers	GZS-RA3	GZS-RA21	GZS-RA34	GZS-RA25	GZS-RA1
SL (mm)	45.5	34.3	32.7	–	42.0
First dorsal fin	VII	VIII	VII	–	VII
Second dorsal fin	I/x	I/x	Missing	–	I/6+
Anal fin	III/	III/x	III/?	–	III/x
Pectoral fin	Missing	Parts present	Missing	Missing	Missing
Pelvic fin	I/5	I/5	–	I/5	I/5
Caudal fin (d/v)	10/9	10/9	Missing		Missing
Vertebra	24	24	24?	–	24
Precaudal vertebra	10	10	10?	–	10
Caudal vertebra	14	14	14	–	14
Supraneuralia	2	–	–	–	–
Preopercle	Serrated	Serrated	Missing	Serrated	Serrated
Preopercular ridge	Smooth	Smooth	–	Smooth	Smooth
Preorbital ridge	Smooth	Smooth	–	–	Smooth
Preorbital edge	Serrated	Serrated	–	Serrated	Smooth
Suborbital	Smooth?	Smooth	–	Smooth	Smooth
Interopercle	–	–	Missing	–	Smooth
Supraorbital ridge	–	Smooth	–		Smooth
Teeth premaxilla	–	Villiform and conical	Villiform and conical	Villiform and conical	Villiform and conical
Teeth dentary	Caniniform and villiform	Villiform and conical	–	Caniniform and villiform	Villiform and conical
Gill rakers	–	–	Narrow and long	Narrow and long	–

Neurocranium: The skull is large and massive. Many bones are fragmented, and their borders are not discernable. The parasphenoid is long, and only the part ventral to the orbit is visible; its anterior end is covered by the large lacrimal, its posterior part by the preopercle. The dorsal limits of the orbit are formed by the frontal; its posterior wide and plate-like part is posteroventrally pointed; anteriorly, the frontal narrows rapidly contacting the small nasal bone. The elevated supraoccipital, which originates dorsal to the posterior third of the orbit, is only partly visible: the anterior convex part and the triangular-shaped posterior-most part (Figure 4).

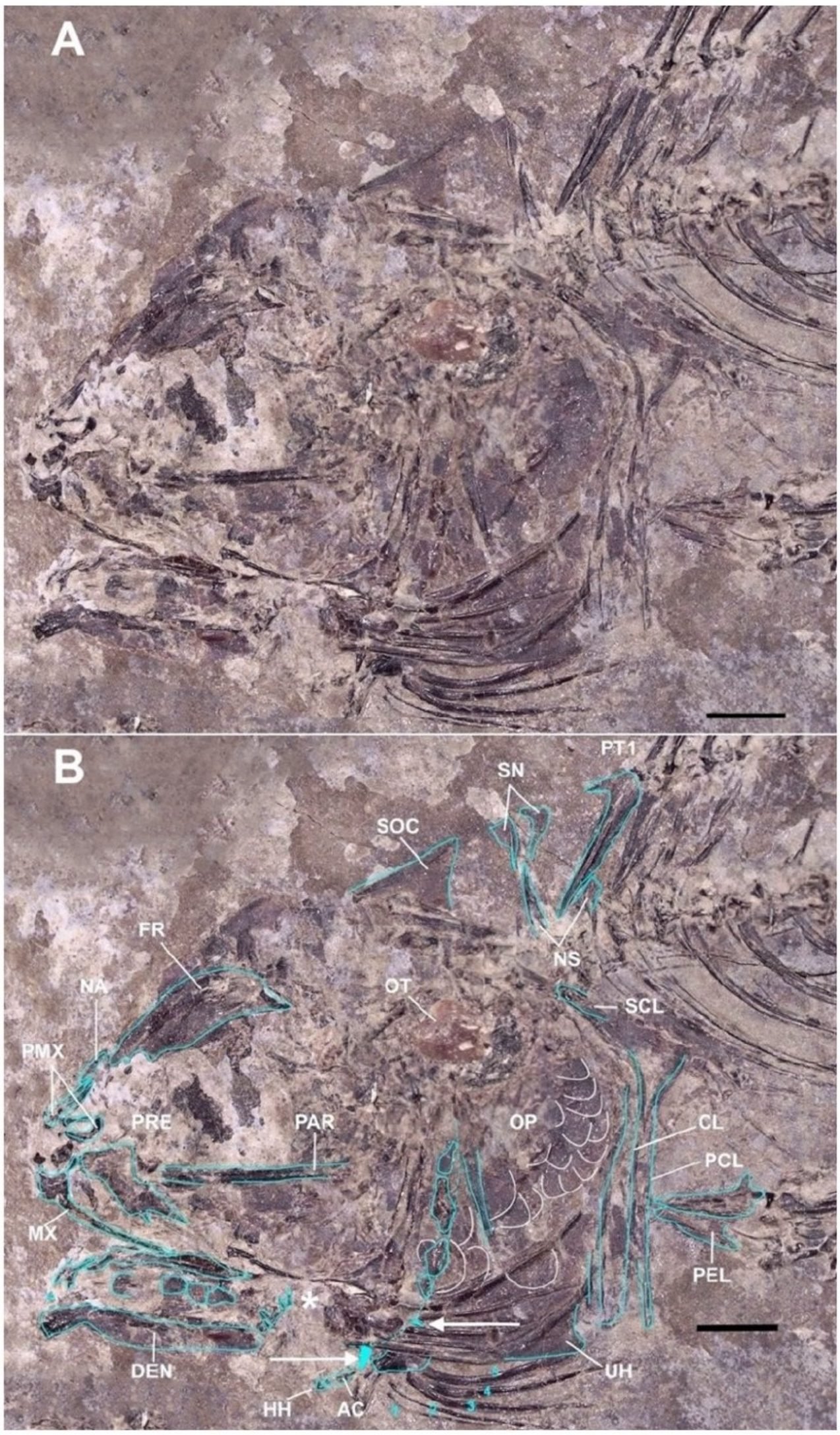

Figure 4. *Dapalis absconditus* sp. nov., head of the holotype GZS-RA3 (**A**). Outline of the skeletal elements (**B**). AC = anterior ceratohyal; CL = cleithrum; DEN = dentary; FR = frontal; HH = hypohyalia; MX = maxilla; NA = nasal; NS = neural spines of first and second vertebra (tip of second neural spine is missing); OP = opercle; OT = otolith; PAR = parasphenoid; PEL = pelvis; PMX = premaxilla; PRE = preorbital (lacrimal); PT1 = first dorsal pterygiophore; SN = supraneural; SOC = suparaoccipital; UH = urohyal; turquoise dashed line = estimated posterior outline of the preopercle which is largely hidden below bony fragments. Numbers 1–5 = branchiostegal rays. White arrows point to two spine-like serrations of the preopercle. * = see text of preopercle for explanation. Scales of the opercular series are shown in white. Scale bars are 2 mm. Photo K. Bradić-Milinović.

Circumorbitalia (suborbitalia + supraorbitalia): The first suborbital, the preorbital (the infraorbital bone 1, lacrimal), is large, laminar and elongated with a longer dorsal edge and shorter ventral; the preorbital edge carries two spine-like serrations, a posterior long and

massive one and an anterior-positioned short and small one; the preorbital ridge is smooth (Figure 5). Other suborbitalia are fragmented or not visible.

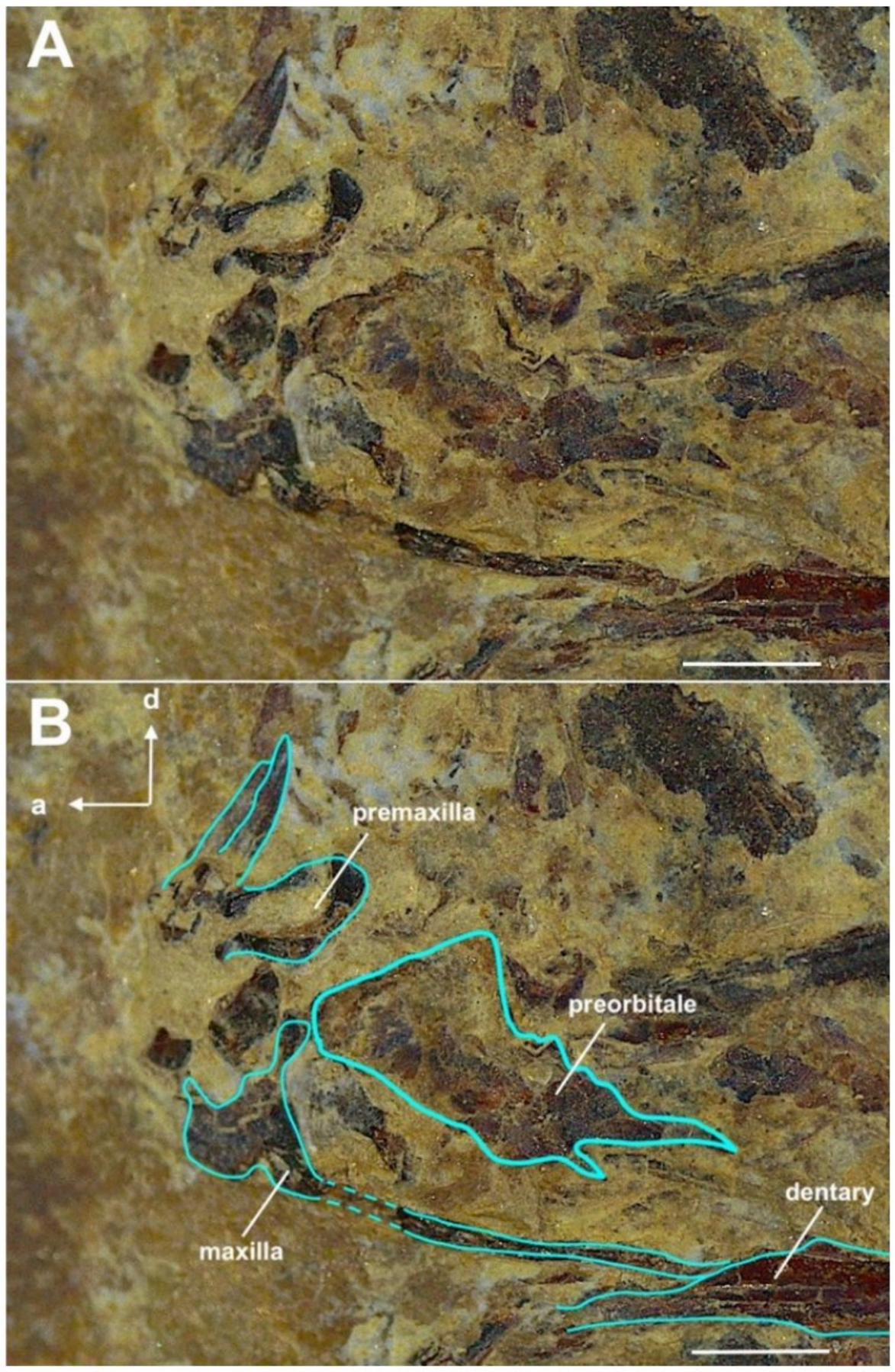

Figure 5. *Dapalis absconditus* sp. nov., maxilla and premaxilla of the upper jaw and the preorbital (lacrimal) of the holotype GZS-RA3 (**A**). Outline of the skeletal elements (**B**). a = anterior; d = dorsal. Scale bars are 0.5 mm. Photo K. Bradić-Milinović.

Jaws: The tooth-bearing part of the premaxilla is lost; only its most anterior part with the narrow but distinct ascending process and the large, oval articular process is present; both processes are separated by a distinct gap (Figure 4). The maxilla is displaced anteriad; the head of the maxilla is massive, which, in place, would contact the articular process of the premaxilla with its wide lateral process; the median process, the contact to the maxillary process of the palatine, is long and narrow; the shaft of the maxilla is long, straight and narrow; the posterior end of the maxilla is covered by the tilted and displaced left dentary (Figure 4).

The tooth-bearing part of the dentary is long and narrow; shortly after the symphysis, it is broken (Figures 6 and 7); the posterior part of the dentary with the coronoid process is, like the anguloarticular and the retroarticular, not preserved or fragmented beyond recognition. Two detached conical teeth are recognizable dorsal to the symphysis of the dentary, and there is a series of small, villiform teeth close to the symphysis (Figure 7).

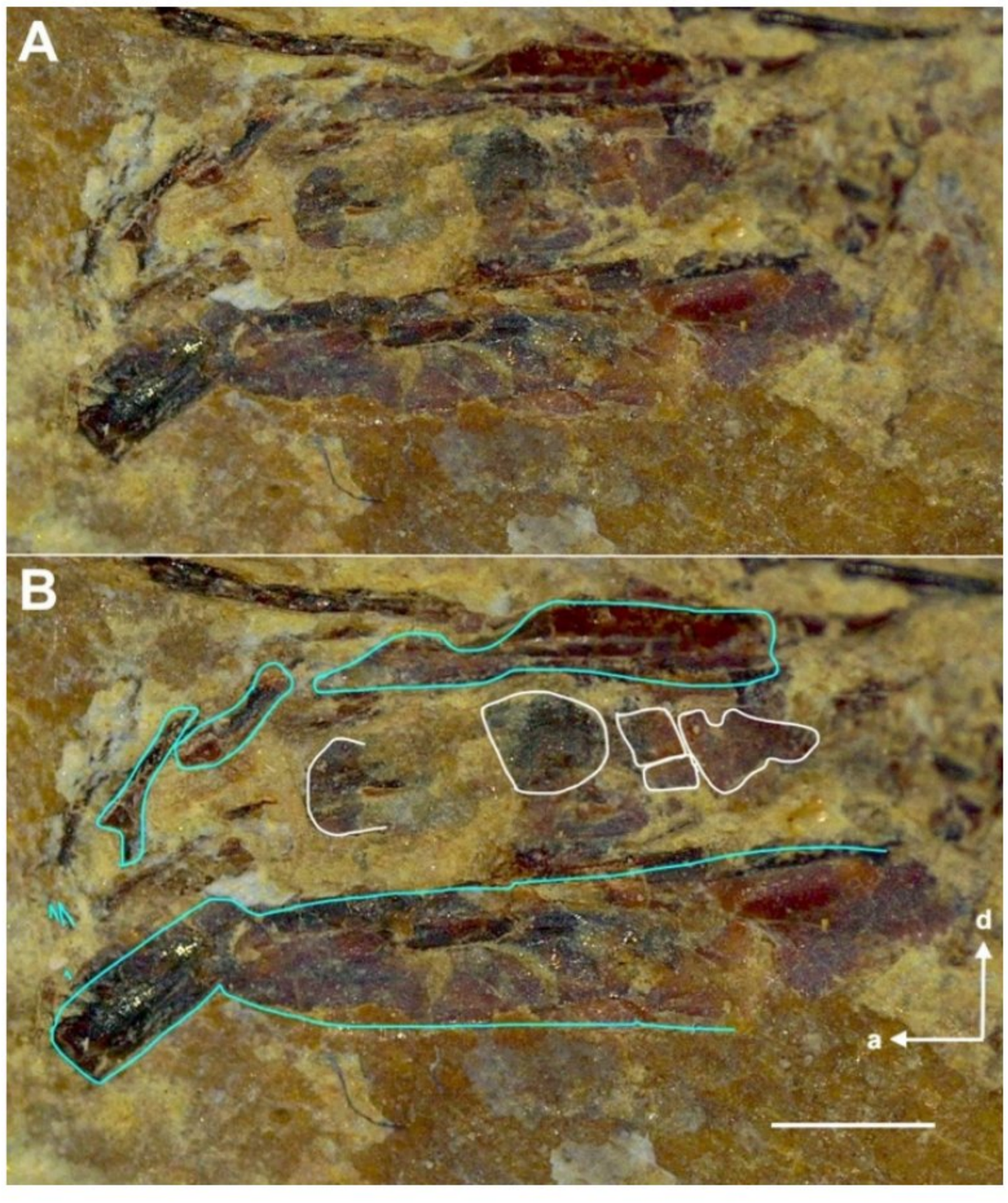

Figure 6. *Dapalis absconditus* sp. nov., dentary of the lower jaw of the holotype GZS-RA3 in dorsolateral view (**A**). Outline of the skeletal elements (**B**). Fragments of the branchial basket are shown in white; white arrows point to teeth. Left dentary is broken at the tip (see Figure 7). a = anterior; d = dorsal. Scale bar is 0.5 mm. Photo K. Bradić-Milinović.

Suspensorium: the bones of the suspensory are not discernable.

Opercular series: The opercle and the subopercle form a large, triangular plate, dorsally wide, ventrally narrowing. The interopercle is not discernable. The preopercle has the shape of a reverse "L". Only its vertical arm is preserved but is in large part covered by scales and by bony fragments. Therefore, it is not clear if and to what extent the posterior edge is serrated. A single short and narrow spine-like serration is discernible where the vertical arm would merge with the horizontal arm pointing posteroventrally (Figure 4). Another single and somewhat larger narrow and pointed spine-like serration is discernable anteroventrally; it extends in the ventral direction (Figure 4). From the horizontal arm, only the most posterior part is visible but fragmented. Seemingly a vertically dislocated piece of the ventral edge of the horizontal arm lies vertical immediately posterior to the lower jaw. It carries 3–4 short, narrow and pointed serrations (Figure 4). The preopercular ridge is smooth in its entire length (Figure 4).

Hyoid bar: Only fractions of the posterior and the anterior ceratohyals are preserved. Of the five branchiostegal rays, the two anterior-most rays are narrow; the following three are approximately twice as wide and all of a similar width. Medial to the left branchiostegal rays and ventral to the opercular plate, the urohyal is partly discernable; its posterior edge is concave (Figure 4).

Scales: Small, roundish cycloid scales cover the opercle, subopercle, preopercle and the cheek. Some detached scales lie between the two lower jaws (Figure 4).

Axial skeleton: The vertebral column comprises 24 vertebrae, 10 abdominal (precaudal) and 14 caudal, including the urostyle (compound center); the parapophysis of the last abdominal vertebra is long and ventrally directed; the abdominal portion of the vertebral

column is in length 85% of the caudal portion; the neural spines and the somewhat longer hemal spines are narrow, emerging from the anterior part of the centra, subsequently shifting posteriorly from caudal vertebra 6 (neural spines) and caudal vertebra 7 (hemal spines) on; the neural spines and the hemal spines of the preural vertebra 3–4 are elongated and more oblique than the preceding ones; no neural spine and no parhypural were discernable on the preural vertebra 2.

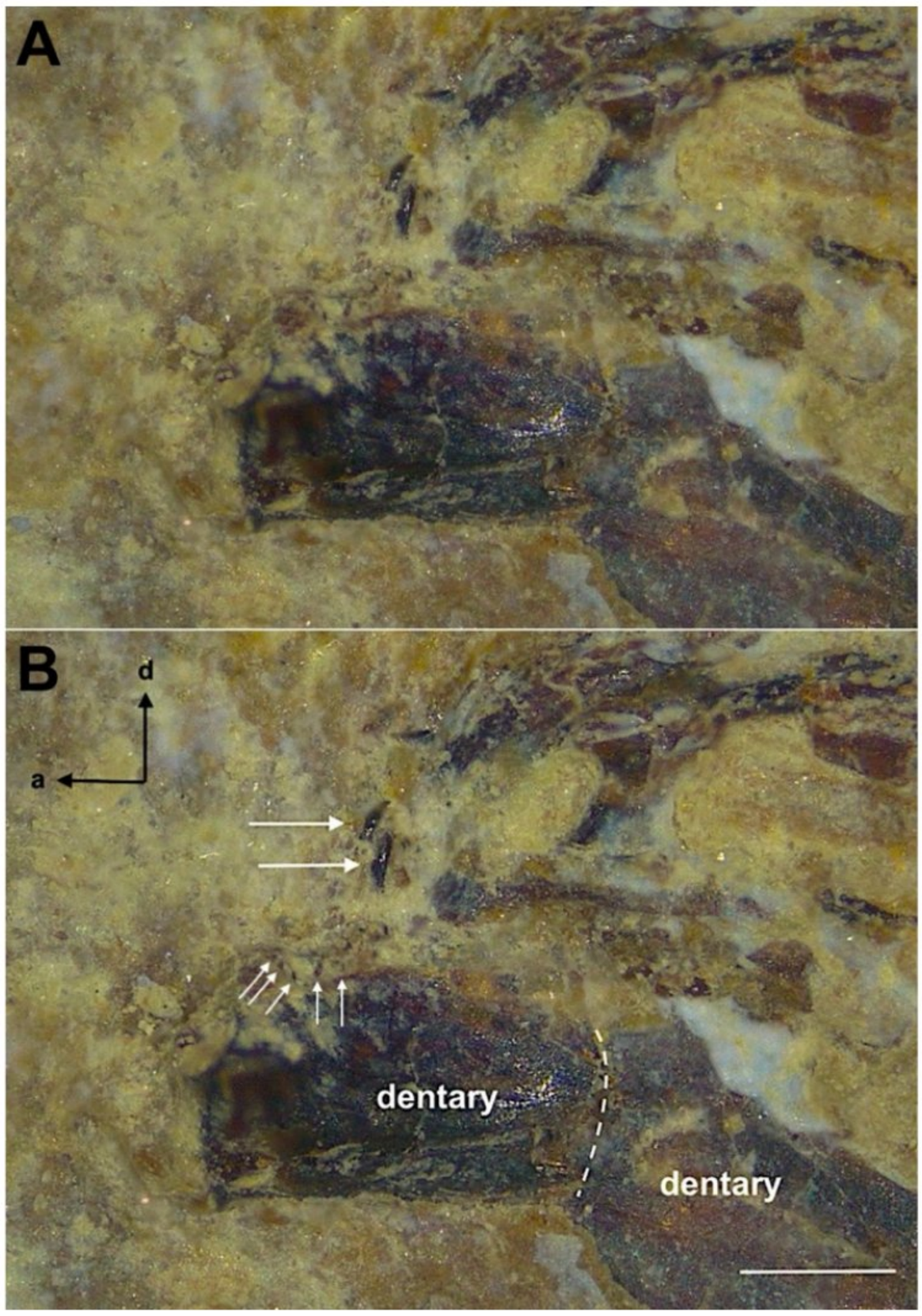

Figure 7. *Dapalis absconditus* sp. nov., anterior-most part of the dentary of the holotype GZS-RA3 (**A**). Outline of the skeletal elements (**B**). Horizontal white arrows point to detached caniniform teeth; oblique and vertical white arrows point to tiny, villiform teeth; dashed line = fracture of dentary (**B**). a = anterior; d = dorsal. Scale bar is 0.5 mm. Photo K. Bradić-Milinović.

Seven pairs of long pleural ribs extend from the abdominal vertebrae 3–9; the long, ventrally directed parapophysis of the last abdominal vertebra carries no rib. Epipleural ribs are only discernable on vertebra 2 (Figures 3 and 4).

Caudal skeleton + caudal fin: From the hypuralia, only the dorsal hypural plate (formed by the hypurals 3 + 4), in close contact with the compound center (urostyle), and the hypural 5 are discernable (Figure 9); the ventral hypural plate (hypurals 1 + 2) is missing. Ten rays of the dorsal lobe of the caudal fin are preserved; the ventral lobe is somewhat displaced ventrally, and imprints of nine fin rays are visible (Figure 9). The dorsal lobe of the caudal fin is slightly displaced dorsally. Large parts of the caudal fin skeleton are missing like the epurals, the parhypural and the ventral hypural plate (hypural 1 + 2), as well as the neural spine of the second preural center, which is generally short and wide

in ambassid fishes. The neural and hemal spines of two caudal vertebrae anterior to the urostyle (compound center) are included in the caudal fin skeleton.

Median fins: There are two dorsal fins. The first dorsal fin is composed of seven spines, the second dorsal fin of one spine and soft rays (7+) (Figure 3). The first dorsal fin originates dorsal to the fourth vertebra; the seven spines are moderately strong and acute; the internal structure of the spines is compartmentalized (Figure 8); each spine is associated with one pterygiophore; the first three pterygiophores are long and strong, the following gradually decreasing in length and strength; between two neural spines, a single pterygiophore is inserted; the first pterygiophore inserts in the interneural space between the neural spines of the vertebrae 2 and 3, the seventh pterygiophore between the neural spines of the vertebrae 7 and 8. The first spine is short (38.8% of the length of the second spine), and the seventh is slightly shorter than the first and therefore the shortest (34.5% of the length of the second spine); the length of the second to the penultimate spine, which is of about the same length as the last one, rapidly decreases (Figure 3). There are two supraneurals (predorsal bones), with the first immediately anterior of the first neural spine of the first vertebra and the second immediately posterior to this spine; the supraneurals are laminar with a strong dorsal rim and a vertical strut; the first supraneural is triangular-shaped with a straight anterior margin; the second supraneural is narrower, slightly hook-shaped and with a concave anterior margin (Figure 4). The first dorsal pterygiophore inserts in the interneural space between the neural spines one and two, the second pterygiophore in the interneural space between the neural spines two and three and the third in the interneural space between the neural spines three and four; the dorsal part of the first pterygiophore is anteriorly spine-like and extended (Figure 4). The predorsal formula is 0/0 + 1/.

Figure 8. *Dapalis absconditus* sp. nov. (GZS-RA3), compartmentalization of the second spine of the first dorsal fin. External-most sheet of the spine is partly removed. Scale bar is 2 mm. Photo K. Bradić-Milinović.

The anal fin originates ventral to the third caudal vertebra; three spines precede the soft part of this fin; the first spine is short (35.3 of the length of the second anal spine), and the second and third spines are of about the same length (Figure 3); the anal spines are moderately strong and acute; the second spine is the strongest and somewhat shorter than the third spine; the spines are followed by soft rays, of which the imprints of six are discernable. The pterygiophores of the first two spines are very long and strong, of equal length and strength; distally, they are wider; proximally, they end in a narrow tip; both pterygiophores lie close together and form a long, narrow, club-shaped structure in this way (Figure 3); the third pterygiophore is hard to discern (only a small fraction

is preserved) and seemingly shorter than the preceding two pterygiophores; these spine-bearing pterygiophores are strongly inclined posteriorly; the first two pterygiophores insert immediately anterior to the first hemal spine.

Paired fins and girdles: The pectoral fin is not preserved. From the bones of the shoulder girdle, the cleithrum is covered by opercular bones; a narrow supracleithrum and the long postcleithra are discernable (Figure 4). The pelvic girdle is well preserved; the two triangular basipterygia carry the pelvic fins; these fins are formed by a spine and five soft rays; from the right fin, only the soft rays are visible; from the left fin, which is folded, the spine and three rays are discernable; the spine is moderately strong, acute and shorter than the fin rays (Figure 3).

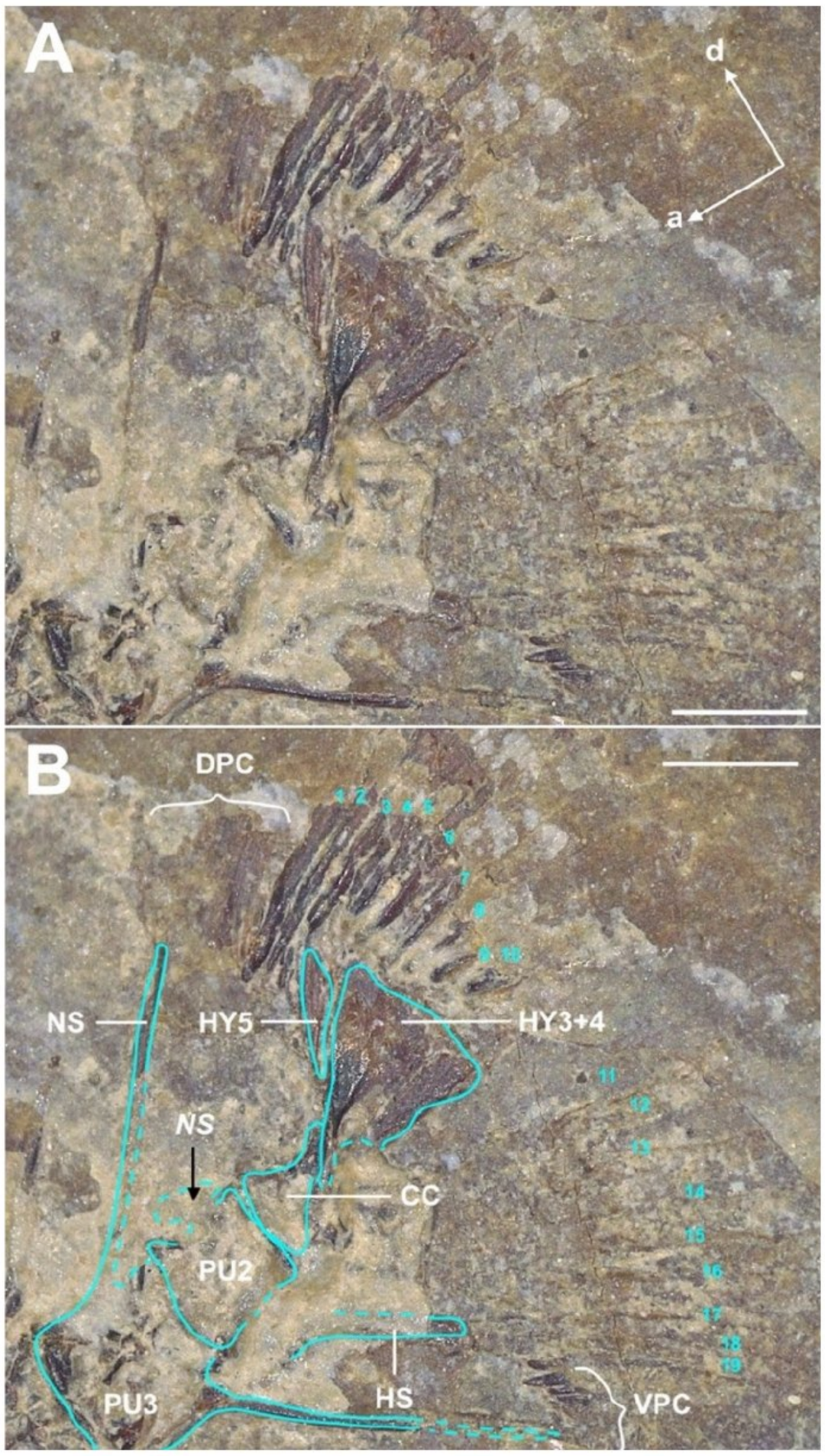

Figure 9. *Dapalis absconditus* sp. nov., caudal skeleton of the holotype GZS-RA3 (**A**). Outline of the skeletal elements (**B**). CC = compound center (urostyle); DPC = dorsal procurrent rays; HS = hemal spine of second preural vertebra; HY3 + 4 = hypurals 3 and 4; HY5 = hypural 5; NS = neural spine of third preural center; *NS* = hypothetical outline of neural spine of the second preural center (see text for explanation); PU2 = second preural center; PU3 = third preural center; VPC = ventral procurrent rays. Numbers = fin rays of the caudal fin, 1–10 of the dorsal fin lobe and 11–19 of the ventral fin lobe. Black arrow points to the hypothetical neural spine of the second preural center. a = anterior; d = dorsal. Scale bars are 0.5 mm. Photo K. Bradić-Milinović.

Otolith (sagitta): The otolith is 2.7 mm long and 1.9 mm high; the ratio of the otolith length to the height is 1.42. It has an oval shape and is moderately elongated but relatively deep. The otolith is highest in the anterior third (Figure 10). Anteriorly, it is distinctly pointed; posteriorly, it is straight with a short but wide caudal projection. The rostrum is massive with a pointed tip and asymmetrical with concave dorsal and convex ventral margins. The antirostrum is massive, rounded and symmetrical. The excisura is well expressed. The inner and the outer face of the otolith are convex: the outer face slightly, the inner face more prominently. The dorsal rim is straight. The ventral rim is regularly curved and slightly undulating (Figure 10). The ventral furrow is distinct and runs close to and along the ventral rim. This furrow separates the narrow ventral rim from a large dome-shaped area of the ventral field. Between the ventral boundary of the cauda and the dome-shaped area, there extends a narrow and relatively short ventral depression. The posterior rim of the otolith is nearly vertical with a very slight postcaudal depression immediately dorsal to the short but long-based caudal projection. The overall shape of the well-defined sulcus is characteristic of *Dapalis*. The ostium is large and roundish; its ventral boundary is expanded, and its upper dorsal boundary is nearly straight; the ostium is distinctly wider than the cauda. The cauda is straight, posteriorly closed and ends distant from the posterior rim; its terminal part is slightly widened and ends narrowed ventrally; the crista superior, the dorsal boundary of the cauda, is massive, bulbous and elevated along its entire length; the crista inferior, the ventral boundary, is well expressed but not distinctly elevated and straight (Figure 10). The ostium is shorter than the cauda; the ratio of the ostium length to the cauda length is 0.80. The ratio of the otolith length to the sulcus length is 1.17. On the dorsal field, dorsal to the sulcus, extends the long and narrow dorsal depression, which is drop-like, wide anteriorly and narrowing posteriorly (Figure 10).

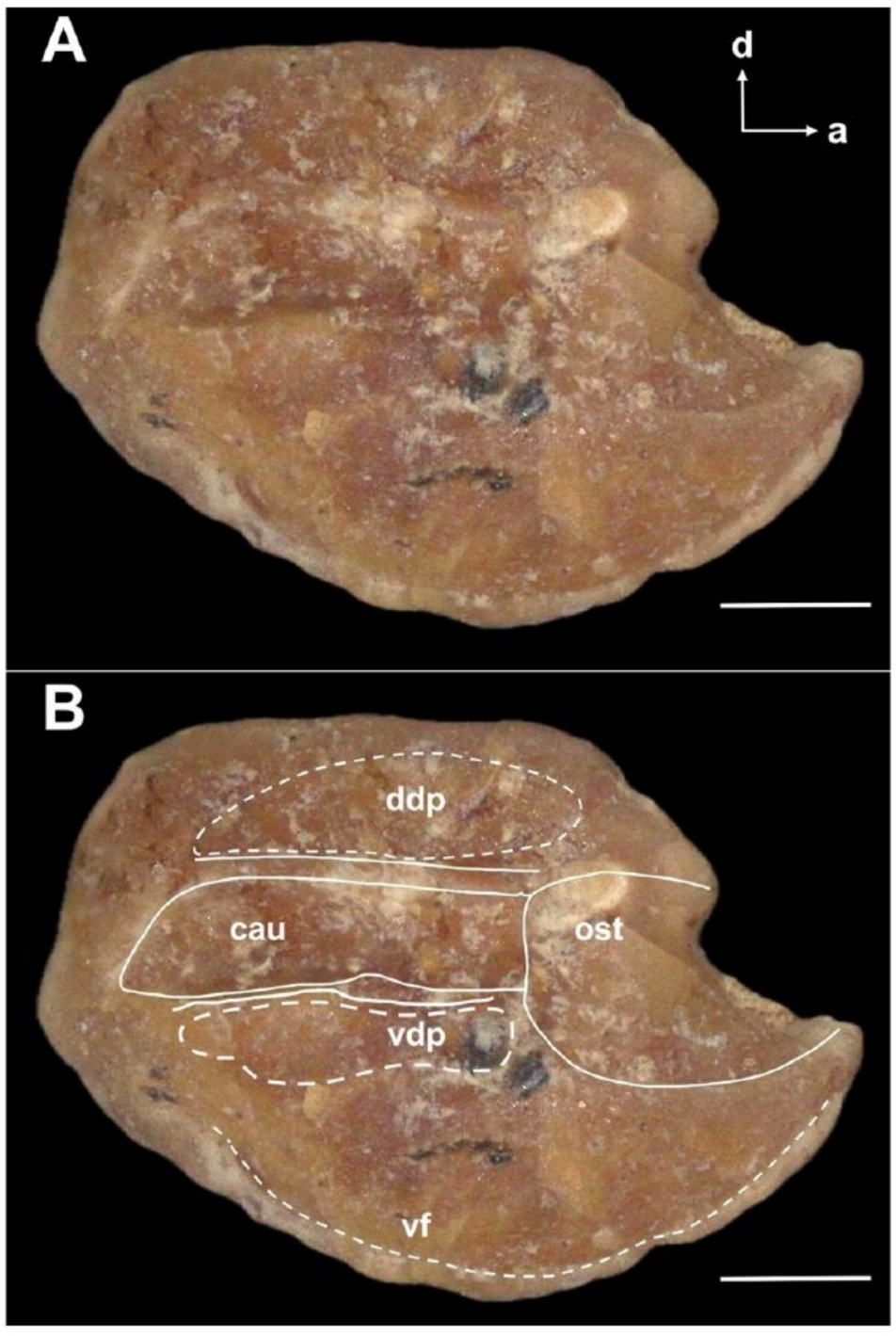

Figure 10. *Dapalis absconditus* sp. nov. Otolith GZS-RA3, from holotype (**A**); interpretative outline of inner face (**B**). cau = cauda; ddp = dorsal depression; ost = ostium; vdp = ventral depression; vf = ventral furrow; a = anterior; d = dorsal. Scale bars are 0.5 mm. Photo K. Bradić-Milinović.

Dapalis octospinus Ahnelt and Bradić-Milinović nov. sp. (Figures 11–20; Tables 2–4). Holotype: registration number GZS-RA21 (Figure 11).

Figure 11. *Dapalis octospinus* sp. nov., articulated skeleton, holotype GZS-RA21. Scale bar is 2 mm. Photo K. Bradić-Milinović.

Type locality: Raljin, Babušnica basin, Serbia: 43°0′1″ N, 22°27′56″ E.

Distribution: the new species is only known from Raljin, Babušnica basin; early Oligocene, Rupelian.

Etymology: the new species is named *octospinus* (Latin: having eight spines), with reference to the first dorsal fin which consists of eight spines, with the seventh spine in the row being accessory.

Diagnosis: *Dapalis octospinus* is distinguished from its congeners by a combination of the following characters: first dorsal fin with eight spines; spine VII of first dorsal fin accessorial; length of the first spine is 38.7% of the length of the second spine; first spine of anal fin is long, 45.6% of the length of the second spine; body shape elongated and narrow with body depth 24.0% of SL and head depth 23.7% of SL; head relatively short, 30.3% of SL; mouth terminal; strong, pointed, spine-like serrations with narrow bases on the preopercle; otolith oval, elongated (ratio of otolith length to height = 1.59) and moderately thick (ratio of otolith length to otolith width = 4.20); sulcus moderately long, with the ostium shorter than the cauda (ratio of ostium length to cauda length = 0.82); cauda ending distant from posterior rim; ventral furrow extends very close to the ventral rim; and a wide and short ventral depression.

Dapalis octospinus is distinguished from the remaining sympatric species of *Dapalis* from Raljin by (i) a smooth preorbital, (ii) an elongate and narrow otolith, (iii) a deep ostium, (iv) a short and convex antirostrum and (v) an elongate, wide and short ventral depression.

Description: A slender and elongate species. Counts and measurements are reported in Tables 2 and 3. The skeleton of the specimen is completely preserved. However, the bones of the head are fragmented and are only partly discernible (Figure 11).

Neurocranium: The skull is large. Many bones are fragmented beyond recognition, and their borders are not discernible. The parasphenoid is long and narrow; its anterior and posterior ends (posterior to the lateral wings) are fragmented. The dorsal limits of the orbit are formed by fragments of the frontal bone with the characteristic wide and plate-like part missing; anteriorly, the frontal contacts the small nasal bone (Figure 12). From the elevated supraoccipital, which originates dorsal to the posterior third of the orbit, only the ventral part is visible (Figure 12).

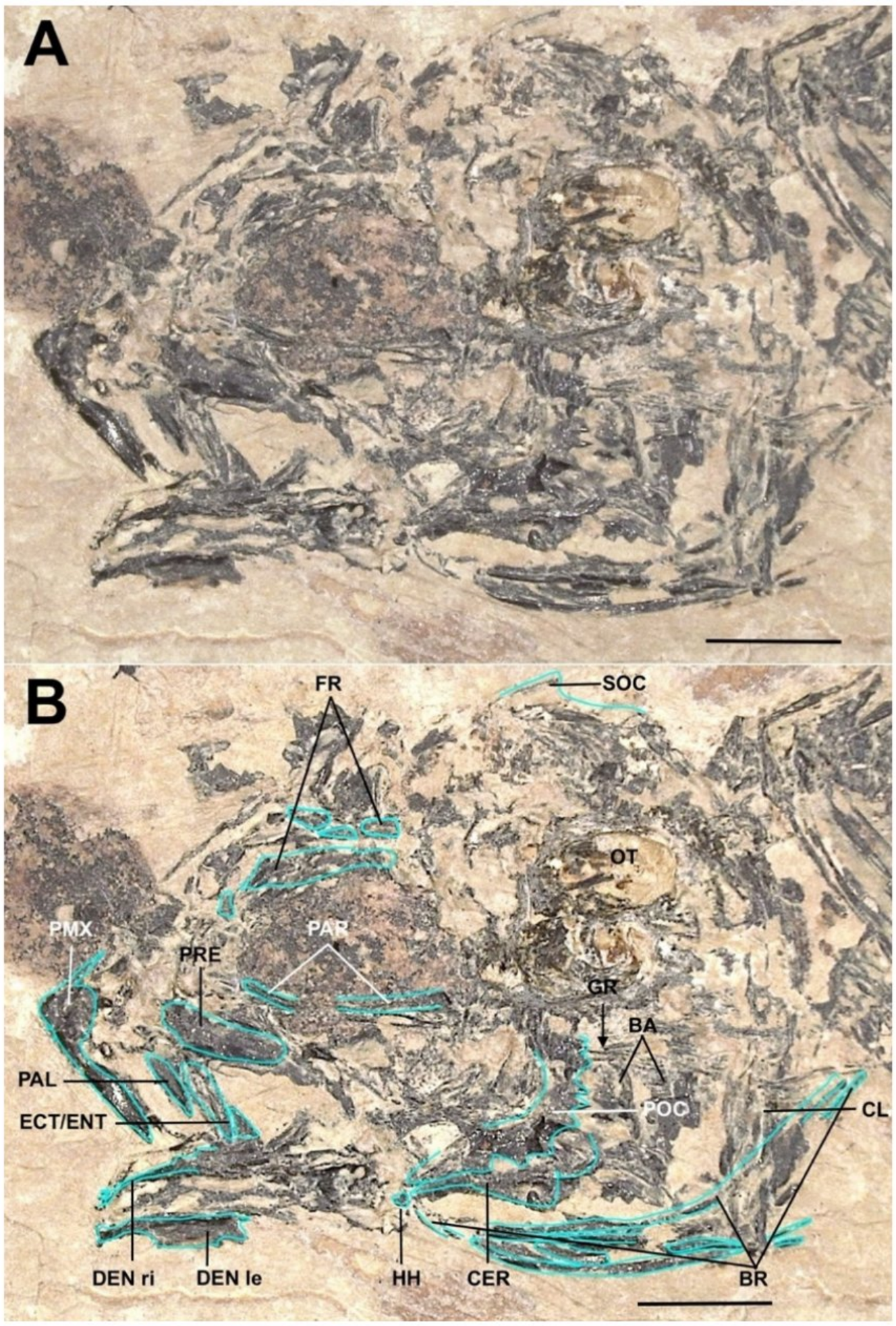

Figure 12. *Dapalis octospinus* sp. nov., head of the holotype GZS-RA21 (**A**). Outline of the skeletal elements (**B**). BA = branchial arch; BR = branchiostegal ray; CER = ceratohyal; CL = cleithrum; DEN le = left dentary; DEN ri = right dentary; ECT/ENT = fragments of the ectopterygoid and the endopterygoid; GR = gill raker; FR = frontal bone; HH = hypohyal; OT = otolith; PAL = palatine; PAR = parasphenoid; PMX = premaxilla; POC = preopercle; PRE = preorbital (lacrimal). Scale bars are 2 mm. Photo K. Bradić-Milinović.

Circumorbitalia (suborbitalia + supraorbitalia): The first suborbital, the preorbital, is large, elongated and narrow; its ventral edge, the preorbital edge, and its dorsal edge, the preorbital ridge, carry no serrations and are smooth (Figure 12). Other infraorbitalia and supraorbitalia are fragmented or not preserved.

Jaws: The premaxilla carries three processes, a narrow ascending process followed by a large, roundish articulating process; in about the middle of the premaxilla, the narrow, triangular postmaxillary process rises; the premaxilla ends with a tip (Figure 12); a few, tiny, villiform teeth are visible on the ventral edge immediately posterior to the articulating process (Figure 12). The maxilla is in large part missing; only a few fragments of its posterior part are possibly preserved.

The lower jaw is tilted to the left; the ventral part of the dentary is partly lost; its posterior-most part and the adjacent anguloarticular and the retroarticular are fragmented beyond recognition; small, conical teeth are visible on the dentaries (Figures 12 and 13).

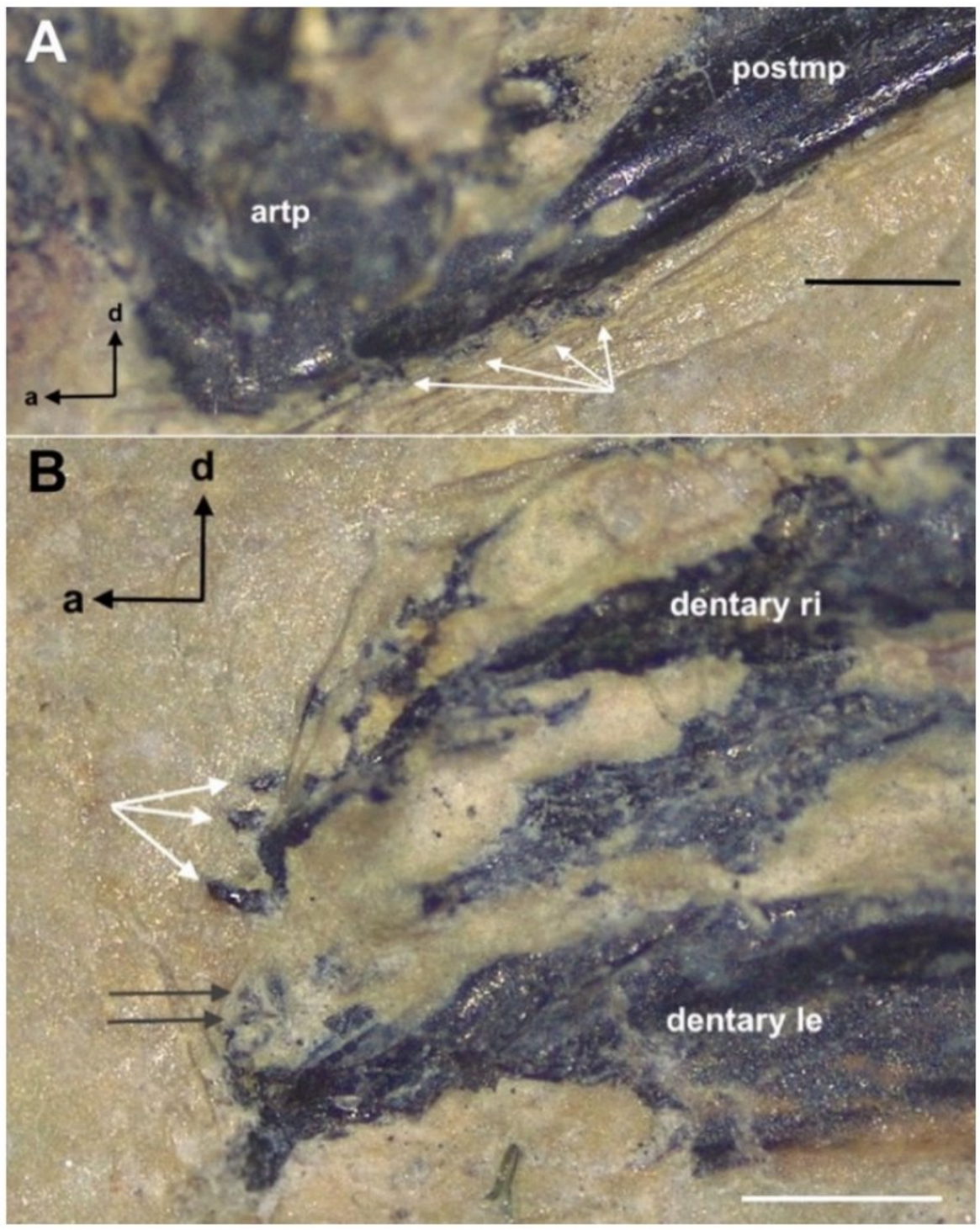

Figure 13. *Dapalis octospinus* sp. nov., head of the holotype GZS-RA21. Anterior part of premaxilla: white arrows point to tiny, villiform teeth (**A**). Anterior part of the lower jaw: white arrows point to conical teeth on the right dentary; grey arrows point to two conical, pointed and depressed teeth with their tips facing inwards in the mouth (**B**). artp = articulating process; le = left; postmp = postmaxillary process; ri = right. a = anterior; d = dorsal. Scale bars are 0.5 mm. Photo K. Bradić-Milinović.

Suspensorium: A large fragment of the palatine carrying a few small conical teeth on its ventral side is preserved; it is positioned anterior to the elongate ectocoracoid (Figure 14). It is possible that the fragment immediately posterior to the ventral end of the ectocoracoid is the rest of the endocoracoid. The metapterygoid, quadratum, symplecticum and hyomandibula are not discernible.

Opercular series: If at all, only tiny fragments of the opercle, subopercle and interopercle are left. The preopercle is a robust bone; it is halfmoon-shaped with large parts of the anterior part of the ventral (horizontal) arm missing; the vertical arm carries strong, spine-like serrations with narrow bases and pointed tips (Figures 12 and 14); the ventral edge of the ventral arm, so far preserved, is smooth; the preopercular ridge is smooth (Figure 12); some depressions appear to be pores of the preopercular canal of the head's lateral line canal system (Figure 14).

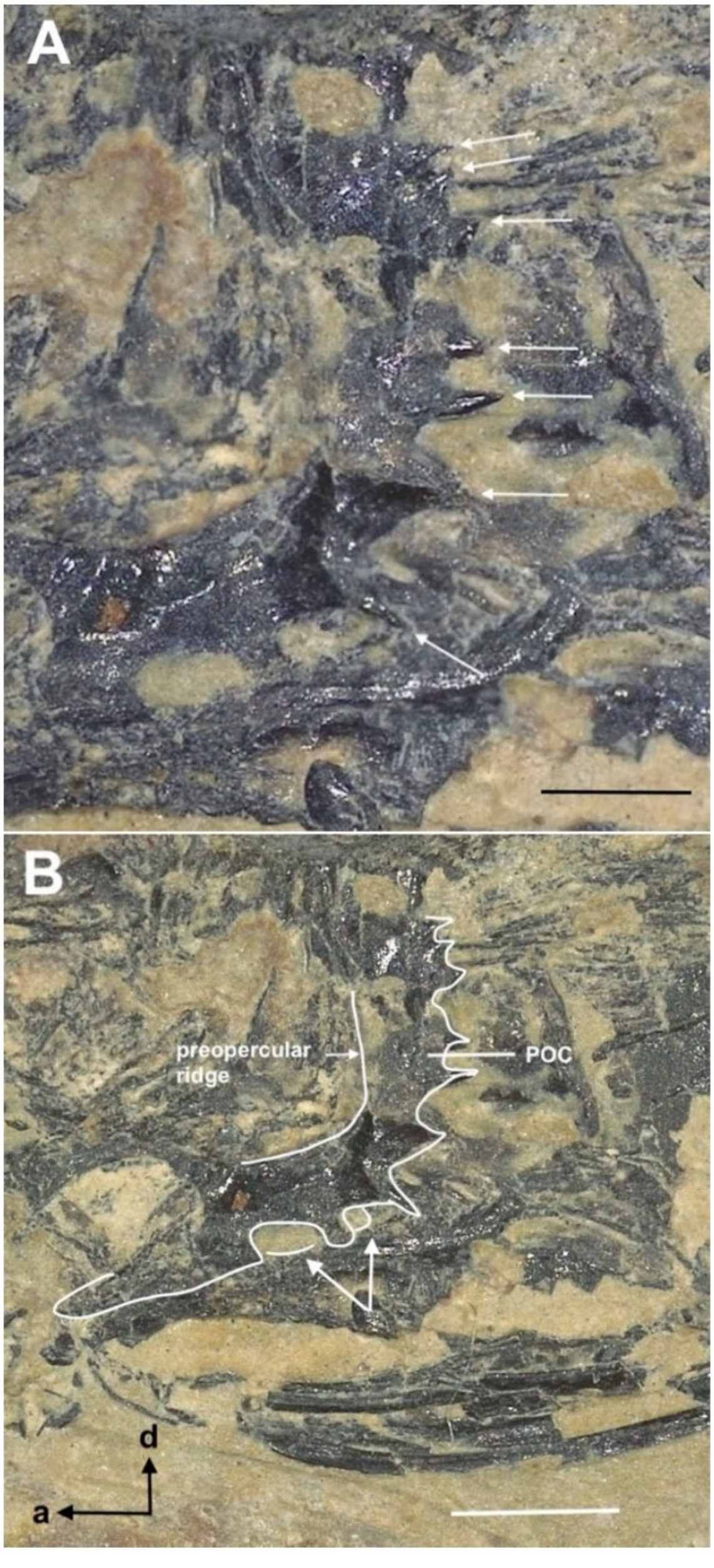

Figure 14. *Dapalis octospinus* sp. nov., preopercle of the holotype GZS-RA21. Spine-like serrations of the preopercle are marked by white arrows (**A**). Outline of the preopercle; white arrows point to two pores of the preopercular canal of the head's lateral line system (**B**). POC = preopercle. a = anterior; d = dorsal. Scale bars are 0.5 mm. Photo K. Bradić-Milinović.

Hyoid bar and branchial basket: The anterior ceratohyal bone with its narrow, elongated anterior part and the laminar posterior part is dorsally partly covered by the left preopercle, but its posterior part is discernible on the right counterpart. Five branchiostegal rays lie

ventral to the anterior ceratohyal. The anterior tip of the anterior ceratohyal bone carries the dorsal and the ventral hypohyals (Figure 12).

Posterior to the preopercle and the ceratohyal lie two–three elongated structures; at their anterior edges, a few anterior-pointing spine-like projections, short and strong, are visible, possibly parts of gill arches with their gill rakers (Figure 12).

Axial skeleton: The vertebral column comprises 24 vertebrae, 10 precaudal and 14 caudal, including the urostyle (compound center); the parapophysis of the last precaudal vertebra (vertebra 10) is long, ventrally directed and pointed; the abdominal portion of the vertebral column is in length 90% of the caudal portion; the neural spines and the somewhat longer hemal spines are narrow, emerging from the anterior part of the centra, subsequently shifting posteriorly from caudal vertebra 6 (neural spines) and caudal vertebra 7 (hemal spines) on and becoming more and more oblique and elongated; the neural spine of the preural vertebra 2 is short and wide; the hemal spine of the preural vertebra 2 and the parhypural are partly visible, long and narrow. Immediately dorsal to the compound center (urostyle) are fragments of the second epural and likely also of the uroneural 1 (Figure 15).

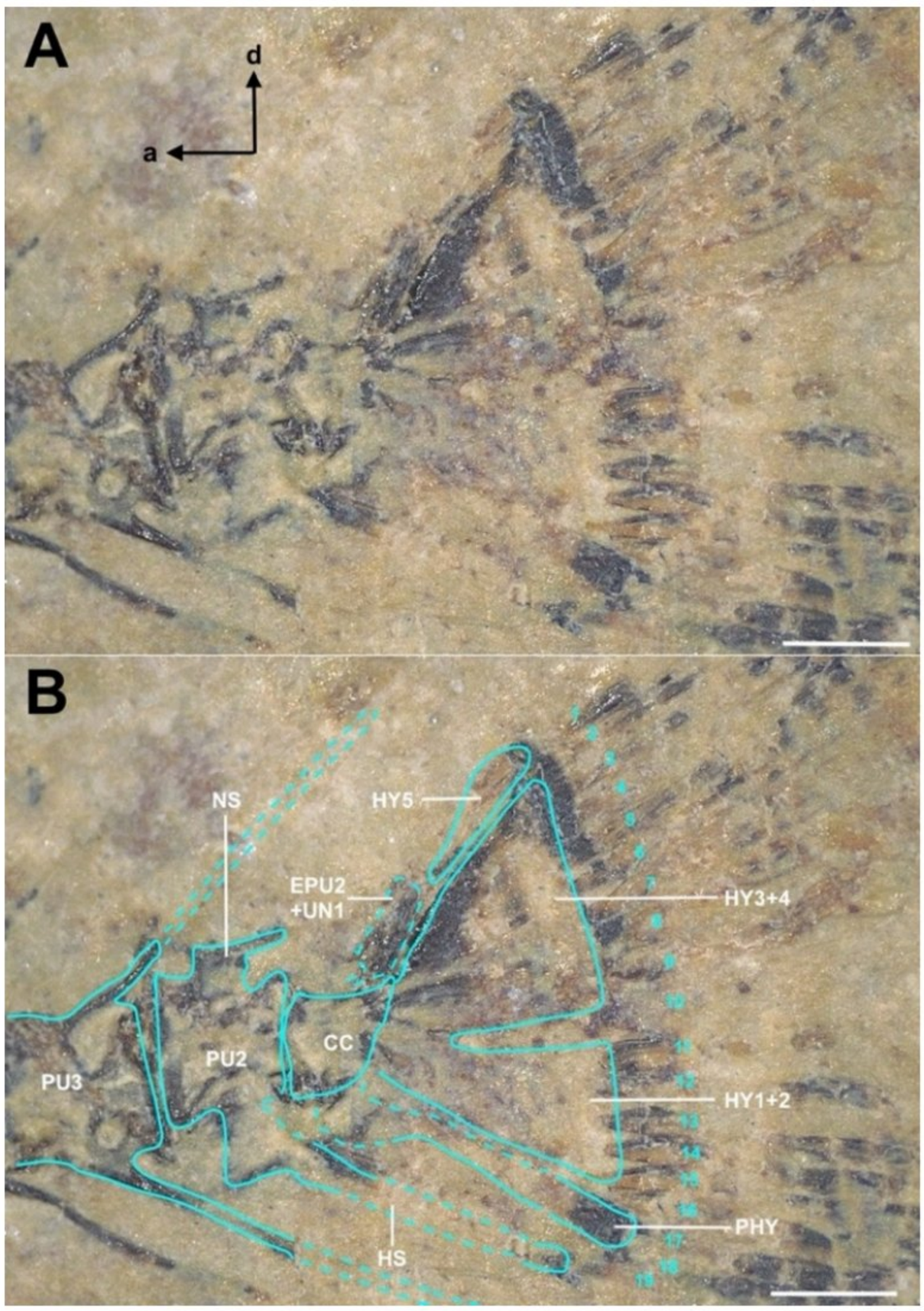

Figure 15. *Dapalis octospinus* sp. nov., caudal fin skeleton of the holotype GZS-RA21 (**A**). Outline of the skeletal elements (**B**). CC = compound center; EPU2 = second epural; HS = hemal spine of the second preural vertebra; HY = hypural; NS = neural spine of the second preural vertebra; PHY = parhypural; PU2 = second preural center; PU3 = third preural center; UN1 = first uroneural. Numbers = fin rays of the caudal fin, 1–10 of the dorsal fin lobe and 11–19 of the ventral fin lobe. a = anterior; d = dorsal. Scale bars are 0.5 mm. Photo K. Bradić-Milinović.

Seven pairs of long pleural ribs extend from the abdominal vertebrae 3–9; the long parapophysis of the last abdominal vertebra carries no rib. At the abdominal vertebrae 6–7 (8?), epiplueral ribs are recognizable.

Caudal skeleton + caudal fin: The caudal skeleton is formed by the parhypural (partly visible): the ventral hypural plate is formed by the hypurals 1–2 (only partly visible where this plate contacts with the urostyle and where the caudal fin rays attach to it), and the dorsal hypural plate is formed by the hypurals 3–4 and the hypural 5; immediately anterior to the hypural 5, remnants of the uroneural 1 are positioned (Figure 15).

Principal caudal fin rays are carried by the parhypural, the lower hypural plate (HY1 + 2), the upper hypural plate (HY3 + 4) and the hypural 5. The dorsal lobe of the caudal fin is formed by ten rays, the ventral lobe by nine rays. The caudal fin is emarginate (Figures 11 and 15).

Median fins: There are two dorsal fins. The first dorsal fin is composed of eight spines, with the seventh of these eight spines being accessory; the inner structure of the spines is compartmentalized (Figure 16); the second dorsal fin is composed of one spine and soft rays (3+) (Figure 11). The first dorsal fin originates dorsal to the fourth vertebra; the eight spines are strong and acute; each spine is associated with one pterygiophore; the first three pterygiophores are the longest and strongest, the following gradually decrease in length and strength (Figures 11 and 17); between two neural spines, a single pterygiophore is inserted, except for the interneural space between the neural spines of the vertebrae 6 and 7; here, two pterygiophores, those of the sixth and the seventh, supernumerary, dorsal spines, are inserted (Figure 17); the first pterygiophore inserts in the interneural space between the neural spines of the vertebrae 2 and 3; the eighth pterygiophore inserts between the neural spines of the vertebrae 7 and 8. The first dorsal spine is short (38.7% of the length of the second dorsal spine); the eighth spine is slightly shorter than the first and therefore the shortest (37.7% of the length of the second dorsal spine); the length of the dorsal fin spines, from the second to the last, rapidly decreases (Figure 17). No supraneurals are preserved.

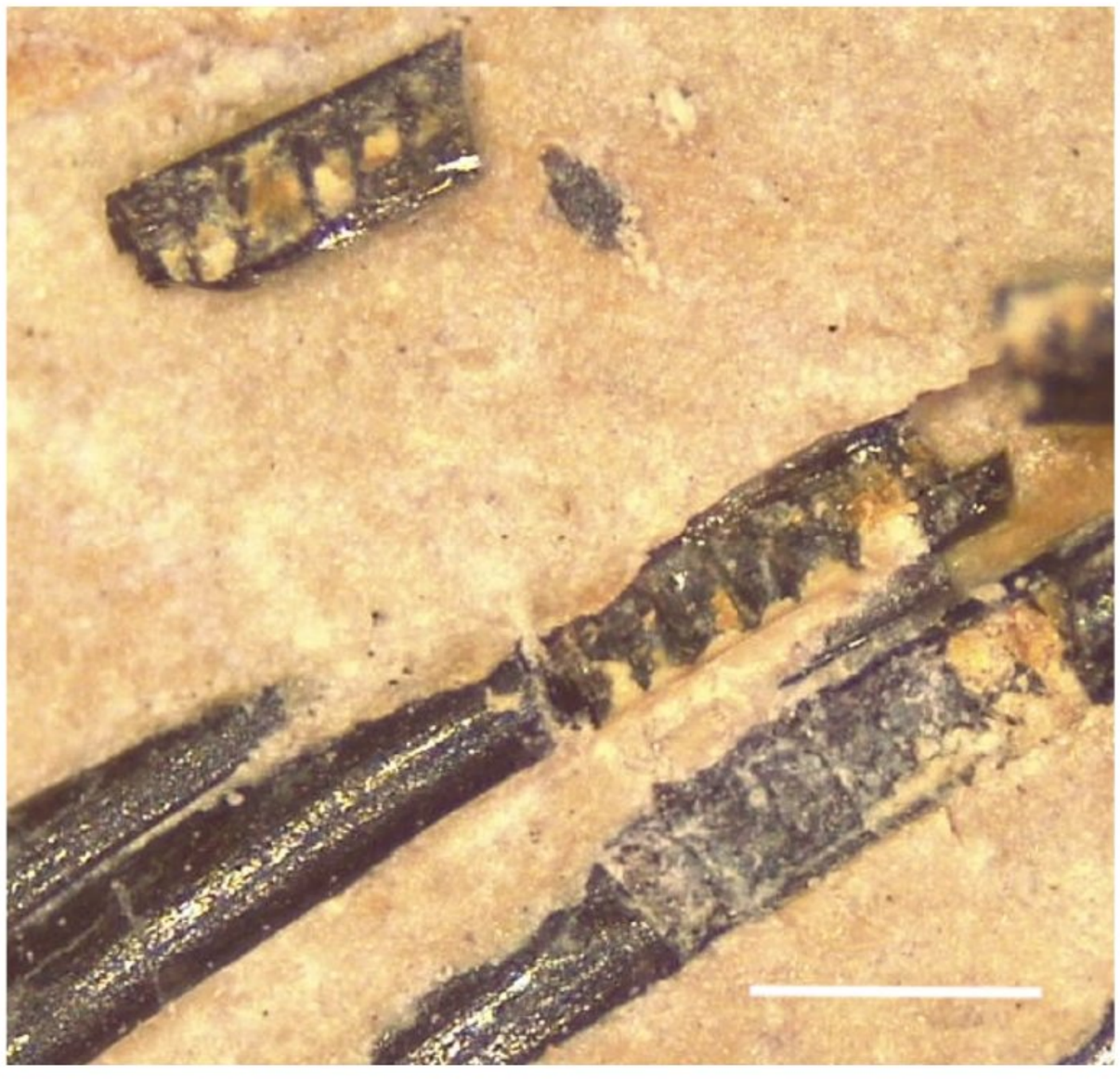

Figure 16. *Dapalis octospinus* sp. nov. (GZS-RA21), compartmentalization of the second and third spines of the first dorsal fin. External-most sheet of these spines is partly removed. Scale bar is 2 mm. Photo K. Bradić-Milinović.

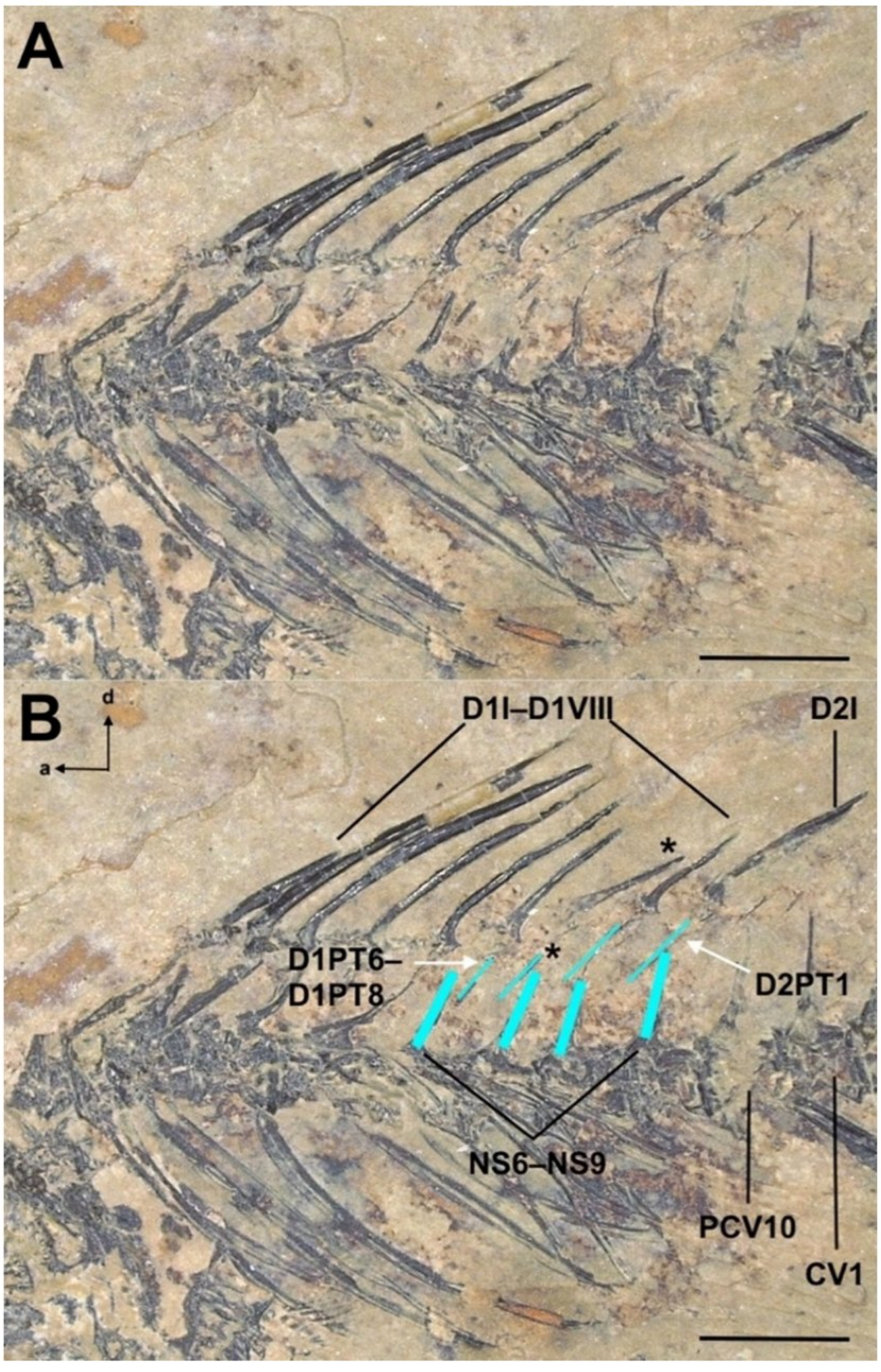

Figure 17. *Dapalis octospinus* sp. nov., dorsal fins and pterygiophores of the holotype GZS-RA21 (**A**). Outline of the skeletal elements (**B**). CV1 = first caudal vertebra; D1I–D1VII = first to eighth spine of the first dorsal fin; D1PT6–D1PT8 = sixth to eighth pterygiophore of the first dorsal fin; D2I = first (and only) spine of the second dorsal fin; D2PT1 = first pterygiophore of the second dorsal fin; NS6–NS9 = sixth to ninth neural spine; PCV10 = tenth precaudal vertebra. Asterisks = supernumerary dorsal spine and its pterygiophore. a = anterior; d = dorsal. Scale bars are 2 mm. Photo K. Bradić-Milinović.

The anal fin originates ventral to the third caudal vertebra; three spines precede the soft part of this fin; the first anal fin spine is long (45.6% of the length of the second spine); the second and the third spines are of about the same length (Figure 18); the anal spines are strong and acute; the second and the third spines are of about equal length; the second spine is the strongest one (Figure 18); the spines are followed by soft rays from which the imprints of four are discernable; the pterygiophores of the first two spines are very long and strong, of equal length and strength; distally, they are wider; proximally, they end in a narrow tip; both pterygiophores lie close together and form a long, narrow, club-shaped structure in this way; the third pterygiophore is narrow and distinctly shorter than the

preceding two pterygiophores; these spine-bearing pterygiophores are strongly inclined posteriorly; seemingly, the anal fin is slightly displaced with the first two pterygiophores covering the hemal spine of the first caudal vertebra (Figure 11).

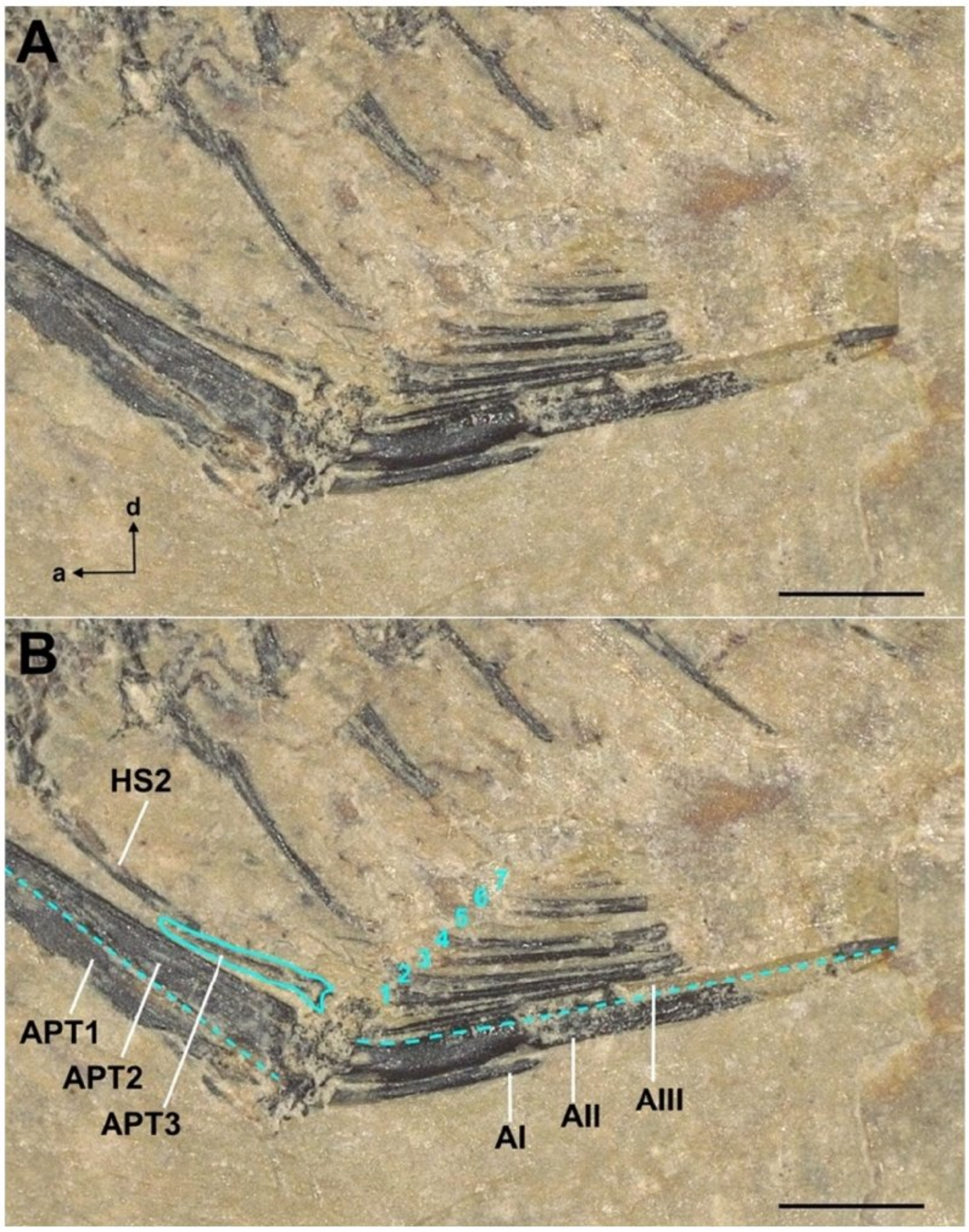

Figure 18. *Dapalis octospinus* sp. nov., dorsal fins and pterygiophores of the holotype GZS-RA21 (**A**). Outline of the skeletal elements (**B**). AI–AIII = first to third anal spine; APT1–APT3 = first to third anal pterygiophore; HS2 = hemal spine of the second caudal vertebra. Dashed lines separate the first from the second anal pterygiophore and the second from the third anal spine. Numbers indicate anal soft fin rays. a = anterior; d = dorsal. Scale bars are 0.5 mm. Photo K. Bradić-Milinović.

Paired fins and girdles: The pectoral fin is partly preserved with the four proximal radialis and four fin rays discernible (Figure 19). From the bones of the shoulder girdle, the cleithrum is preserved but fragmented. The pelvic fins are well preserved; they are formed by a spine and five soft rays which are somewhat longer than the strong and acute spine (Figure 19).

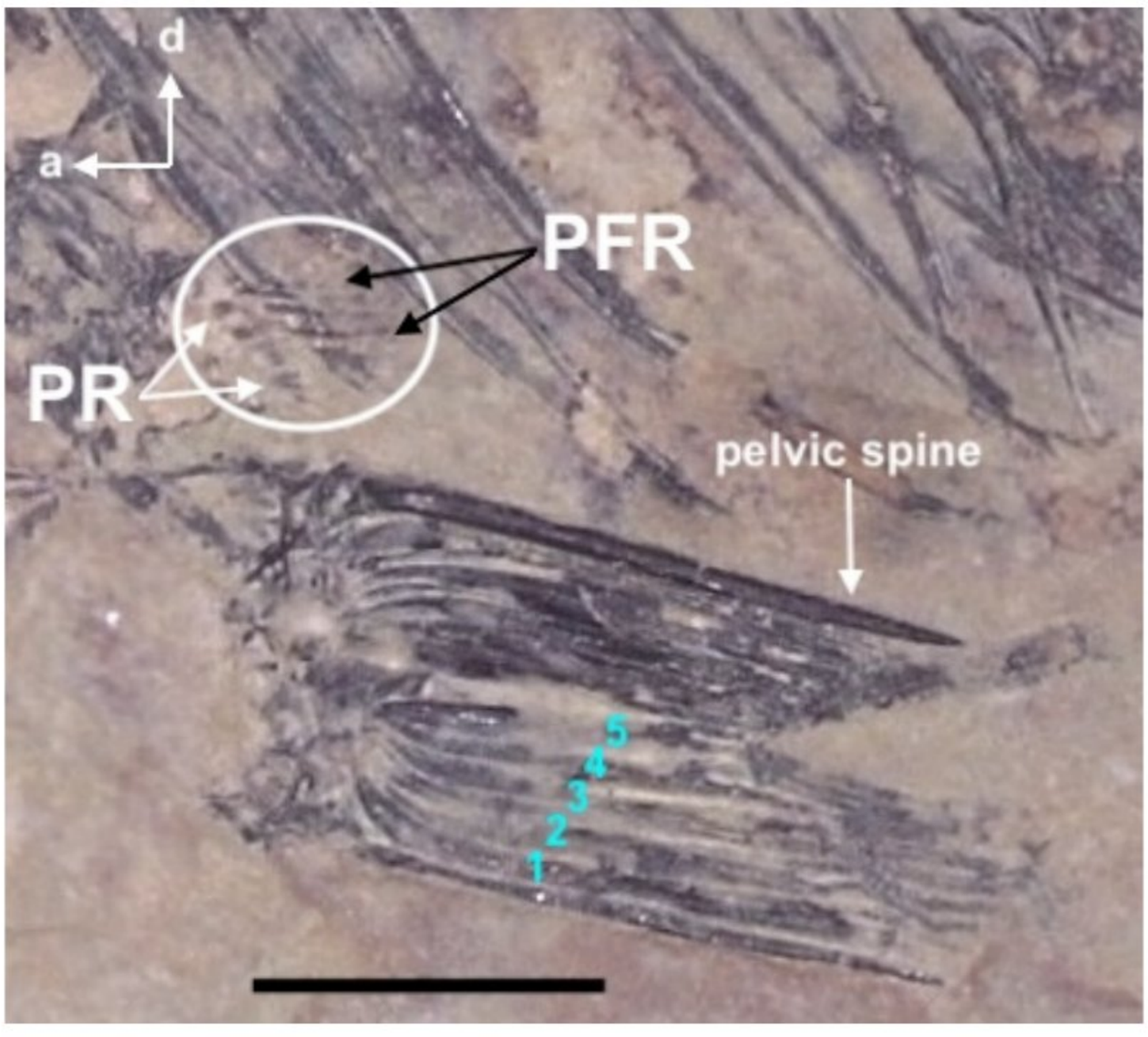

Figure 19. *Dapalis octospinus* sp. nov., pectoral and pelvic fin of the holotype GZS-RA21. Pectoral fin in lateral view; pelvic fins in ventral view. PFR = pectoral fin ray; PR = proximal radial. Remnants of the pectoral fin are within the white circle. White arrows point to the dorsal-most and ventral-most proximal radial of the pectoral fin; black arrows point to pectoral fin rays. Numbers indicate the five soft fin rays of the pelvic fin. a = anterior; d = dorsal. Scale bar is 1 mm. Photo K. Bradić-Milinović.

Otolith (*sagitta*): The otolith is 2.1 mm long and 1.3 mm high; the ratio of the otolith length to the otolith height is 1.6. It has an oval and very elongated shape. The otolith is highest in about the middle (Figure 20). Anteriorly, it is distinctly pointed and posteriorly rounded. The rostrum is massive with a rounded tip and asymmetrical with concave dorsal and convex ventral margins. The antirostrum is short, massive and bulbous. The excisura is weakly expressed. The inner face of the otolith is distinctly convex; the outer face slightly convex, nearly flat. The dorsal rim and the ventral rim are regularly curved and not undulating (Figure 20). The ventral furrow is distinct and runs close to and along the ventral rim. This furrow separates the narrow ventral rim from a relatively narrow dome-shaped area of the ventral field. Between the ventral boundary of the cauda and the narrow dome-shaped area, there extends an elongate, wide and relatively short ventral depression. The posterior rim of the otolith is rounded; there is no postcaudal depression.

The overall shape of the well-defined sulcus is characteristic of *Dapalis*. The ostium is large and elongate; both of its boundaries are expanded, the ventral boundary less so; the ostium is wider than the cauda. The cauda is straight, gradually narrowing in its length, posteriorly closed and ends distant to the posterior rim; the crista superior, the dorsal boundary of the cauda, is elevated along its entire length; the crista inferior, the ventral boundary, is well expressed but not elevated and straight (Figure 20). The ostium is shorter than the cauda but deep, the ratio of the ostium length to the cauda length is 0.82. The ratio of the otolith length to the sulcus length is 1.17. Dorsal to the sulcus, there extends the elongated dorsal depression, which reaches its greatest extent in about its middle; the shape of the depression is asymmetric, with the anterior part narrowing; its dorsal boundary runs along and close to the dorsal rim (Figure 20).

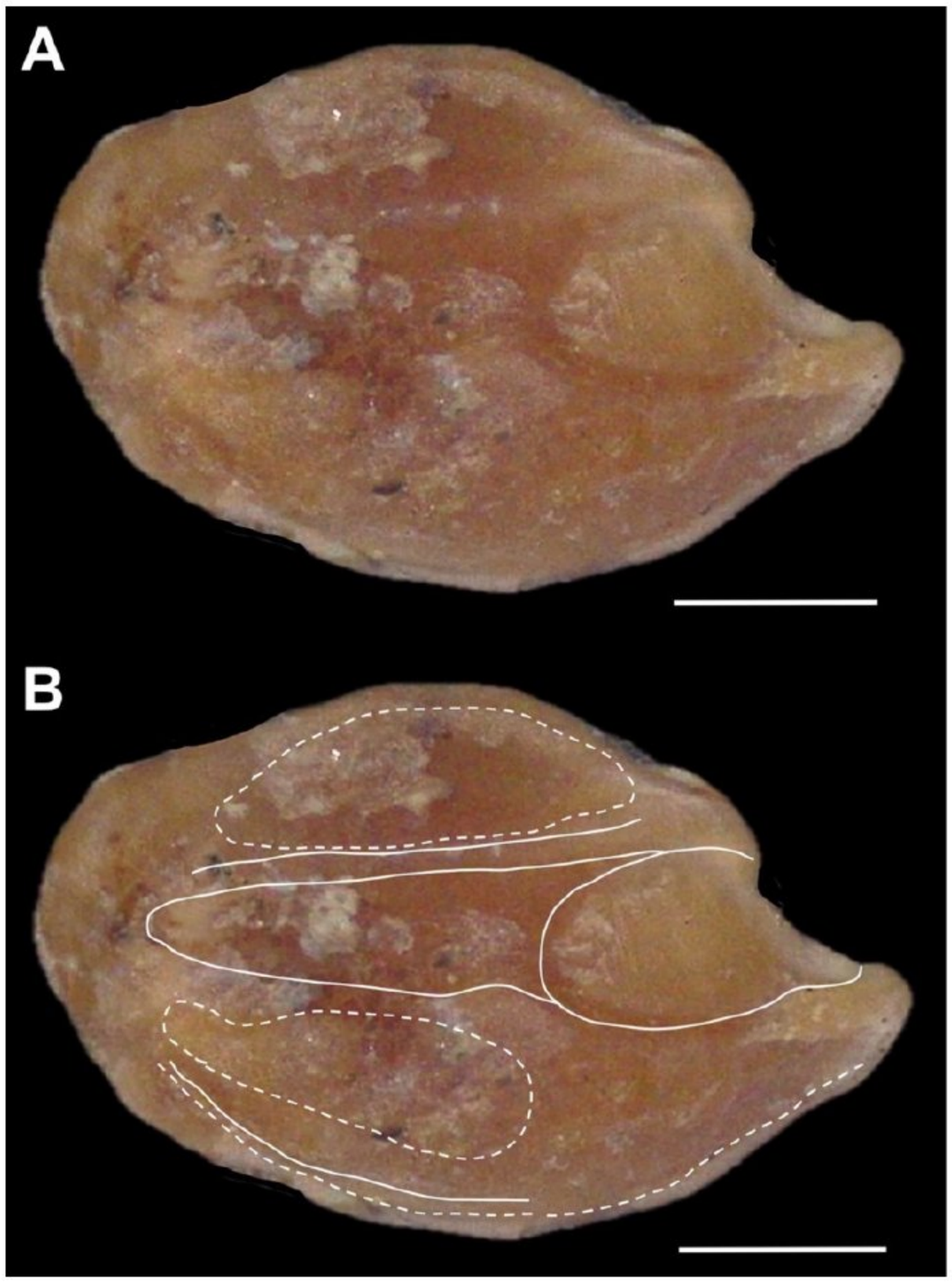

Figure 20. *Dapalis octospinus* sp. nov. Otolith GZS-RA21, from holotype (**A**); interpretative outline of inner face (**B**). Scale bars are 0.5 mm. Photo K. Bradić-Milinović.

Dapalis parvus Ahnelt and Bradić-Milinović nov. sp. (Figures 21–27; Tables 2–4). Holotype: registration number GZS-RA34 (Figure 21).

Figure 21. *Dapalis parvus* sp. nov., articulated skeleton, holotype GZS-RA34. White scale bar is 2 mm. Photo K. Bradić-Milinović.

Type locality: Raljin, Babušnica basin, Serbia: 43°0′1″ N, 22°27′56″ E.

Distribution: only known from Raljin, Babušnica basin; early Oligocene, Rupelian.

Etymology: the new species is named *parvus* (Latin: meaning small), with reference to the small body size.

Diagnosis: *Dapalis parvus* is distinguished from its congeners by a combination of the following characters: the length of the first spine of the first dorsal fin is short (5.6% of SL); the first spine of the anal fin is long, 51.8% of the length of the second spine; head is narrow (22.8% of SL); strong, pointed, spine-like serrations with narrow bases on the preopercle; otolith is almost roundish (otolith length to height = 1.36) and thin (otolith length to otolith

width = 4.74); sulcus is short (otolith length to sulcus length = 1.22), with the ostium and cauda of similar length (ostium length to cauda length = 0.96); between both, there rises a distinct and wide ridge; cauda ends gradually and distant from posterior rim; and no ventral depression developed.

Dapalis parvus is distinguished from the remaining sympatric species of *Dapalis* from Raljin by (i) a preorbital with one ventral-directed spine-like serration, (ii) a roundish and high otolith, (iii) a small, indistinct antirostrum, (iv) a long ostium, nearly as long as the cauda, and (v) the entire ventral area of the otolith dorsal to the ventral furrow being dome-shaped, with no ventral depression.

Description: Slender and elongate. Counts and measurements are reported in Tables 2 and 3. The skeleton of the specimen is completely preserved but strongly discarded. Most bones of the head are poorly preserved if at all, and large parts of the postcranial skeleton are hard to discern (Figure 21).

Neurocranium: no bones of the neurocranium are preserved except the long and narrow parasphenoid (Figure 22).

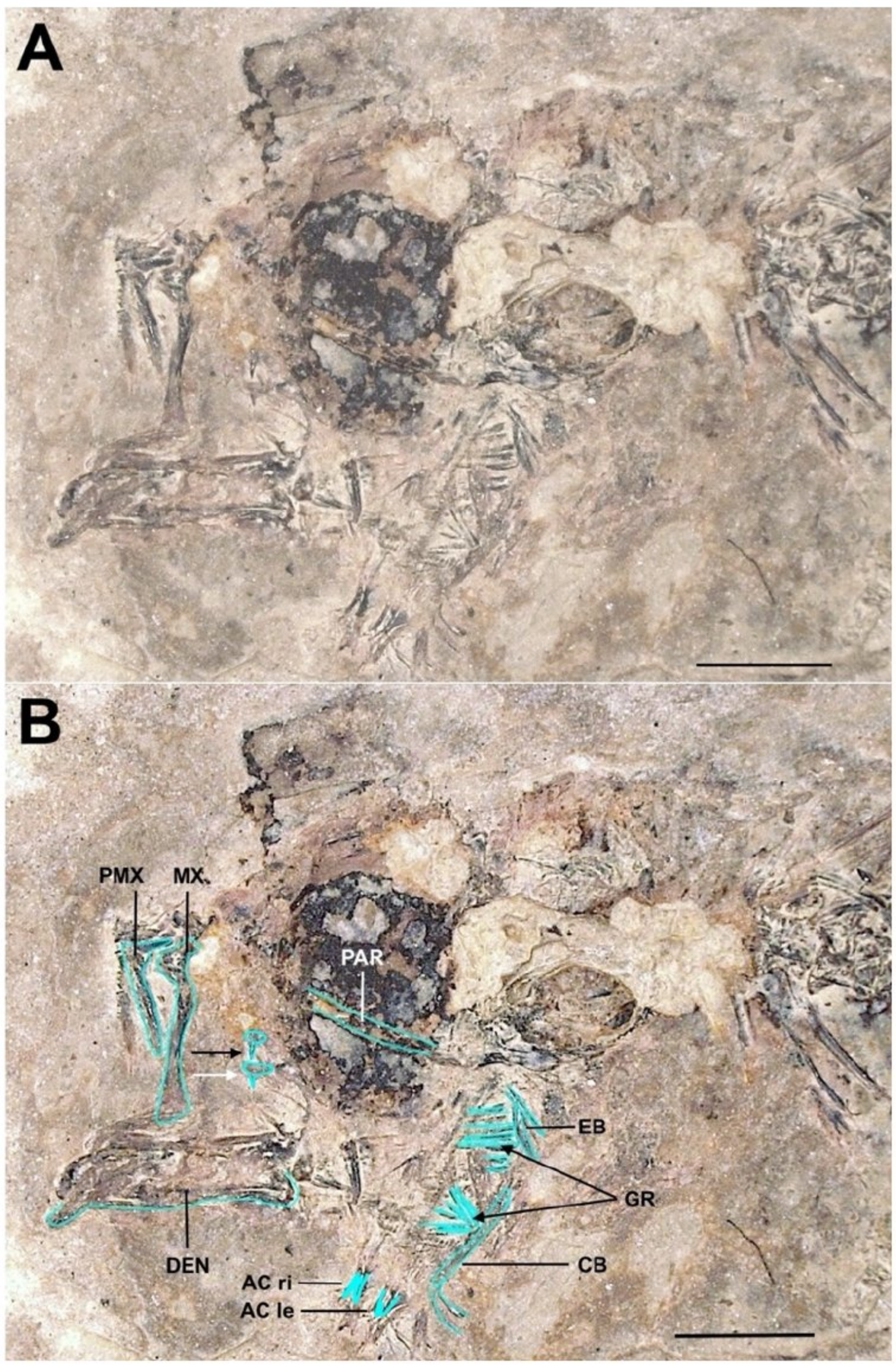

Figure 22. *Dapalis parvus* sp. nov., head of the holotype GZS-RA34 (**A**). Outline of the skeletal elements (**B**). AC = anterior ceratohyal; CB = ceratobranchiale; DEN = dental; EB = epibranchial; GR = gill raker; le = left; MX = maxilla; PAR = parasphenoid; PMX = premaxilla; ri = right. The black arow points to the left preorbital (lacrimal); the white arrow points to the right preorbital. Scale bars are 2 mm. Photo K. Bradić-Milinović.

Circumorbitalia (suborbitalia + supraorbitalia): No circumorbital bones are preserved. From the left and the right, preorbital bone fragments, each with one large spine-like serration of the preorbital edge, are visible (Figure 22).

Jaws: The upper jaw is tilted. The premaxilla anteriorly carries two processes, a distinct ascending process and a small articular process; posteriorly, the shaft of the premaxilla gradually thickens and has a roundish appearance; from its highest point, in about the middle of the shaft, the premaxilla gradually narrows, ending in a narrow and pointed tip; at the symphysis, a single strong caniniform tooth, narrow and pointed, is placed, followed by a series of smaller teeth of the same shape which decrease in length along the ventral edge of the premaxilla; these teeth are detached and reversed in their position with the tips pointing dorsally (Figure 23); it is not clear if these teeth are from the left or from the right premaxilla or from both bones. The maxilla has a rod-like shape and extends posterior to the premaxilla in the anteroposterior direction; it is separated into two parts: a head and a long and narrow shaft; the head is massive and carries two short and wide processes, an anterolateral process which contacts the articular process of the premaxilla and an anteromedian process (palatine process) which connects to the maxillary process of the palatine (Figure 23); the shaft of the maxilla is long, straight and narrow and widens at its end to a triangular plate-like extension (Figure 23); at its very end, the maxilla is covered by the right lower jaw; shortly after the head, the shaft of the maxilla is broken; because the lower jaw is tilted to the left and because it is covering the end of the maxilla, this likely caused the maxilla to crack (Figure 21).

The lower jaw is tilted to the left; the left and right lower jaw can only be viewed ventrolaterally; the right dentary, in medial view, carries a series of small, conical teeth, six of them well recognizable (Figure 24); only a fragment of the anguloarticular, detached from the Meckelian fossa of the dentary, is recognizable.

Suspensory: The bones of the suspensory are nearly completely missing. From the palatine, its very anterior end is preserved, with the maxillary process contacting the anteromedian process of the maxilla and an opposite projection, possibly the process which contacts the ethmoid (Figure 23).

Hyoid bar and branchial basket: Two elongate structures in close vicinity to remnants of branchiostegal rays are possibly the anterior ends of the left and right anterior ceratohyal bones (Figure 22).

Remnants of a branchial arch (epi- and ceratobranchial) carry long and narrow gill rakers: four on the epibranchial, one at the corner where the epibranchial and ceratobranchial meet and two at the dorsal end of the ceratobranchial are recognizable (Figure 22); another eight long and thin gill rakers are visible more anteroventrally on the ceratobranchial.

Axial skeleton: Eight precaudal and fourteen caudal vertebrae, including the urostyle (compound center), are preserved (Figure 22); the abdominal part of the vertebral column is twisted; therefore, vertebrae 3–5 are seen ventrally and vertebrae 6–7 ventrolaterally (Figures 22 and 25); the following three caudal vertebra, including those of the caudal part of the vertebral column, are in a lateral position; the neural spines and the longer hemal spines are narrow, emerging from the anterior part of the centra, subsequently shifting posteriorly from caudal vertebra 7 (neural spines) and caudal vertebra 8 (hemal spines) on; the neural spines of the caudal vertebra 11–12 are more oblique than the preceding ones. Six pairs of long pleural ribs, extending from the abdominal vertebrae 3–8, are recognizable, together with six epipleural ribs (Figures 22 and 25).

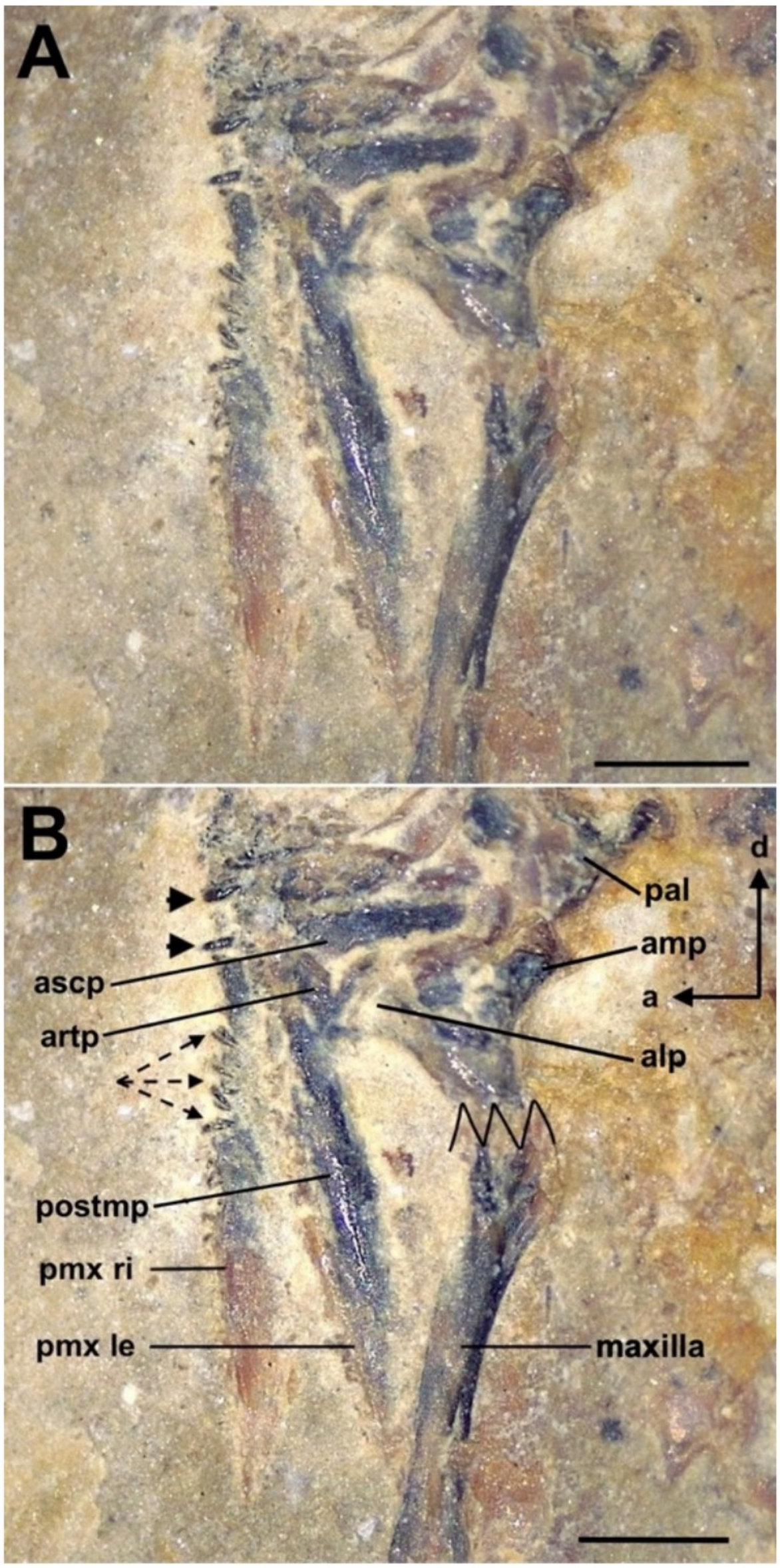

Figure 23. *Dapalis parvus* sp. nov., upper jaw of the holotype GZS-RA34 (**A**). Labeling of the skeletal elements (**B**). alp = anterolateral process; amp = anteromedian process; artp = articulating process; ascp = ascending process; le = left; pal = palatinum; pmx = premaxilla; postmp = postmaxillary process; ri = right. Arrow heads point to the caniniform teeth of both premaxillas; dashed arrows point to detached teeth which look inwards; zigzag symbolizes the region where the maxilla is broken. a = anterior; d = dorsal. Scale bars are 0.5 mm. Photo K. Bradić-Milinović.

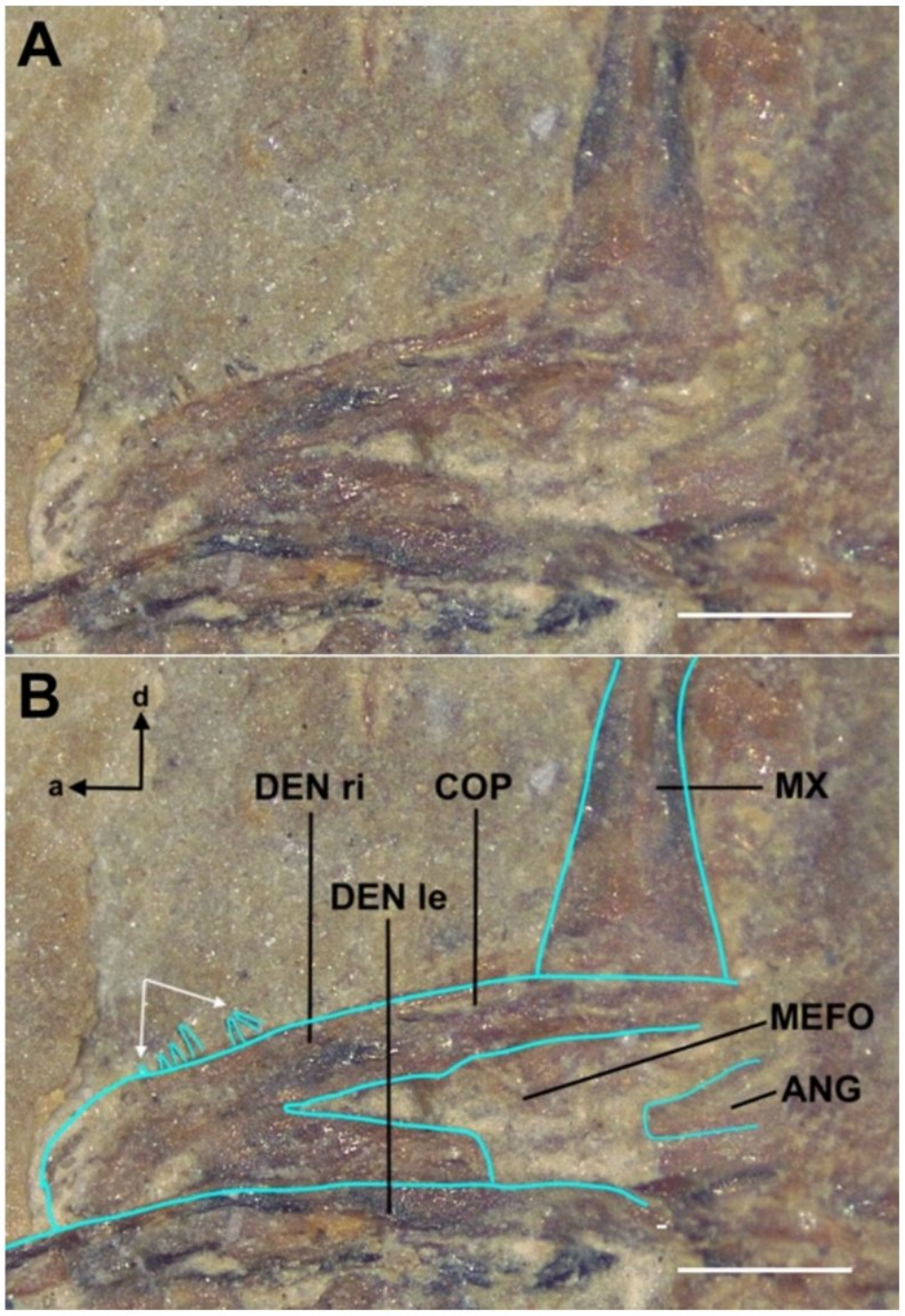

Figure 24. *Dapalis parvus* sp. nov., upper jaw of the holotype GZS-RA34 (**A**). Outline of the skeletal elements (**B**). ANG = anguloarticular; COP = coronoid process; DEN = dentary; le = left; MEFO = Meckelian fossa; MX = maxilla; ri = right. a = anterior; d = dorsal. Scale bars are 0.5 mm. Photo K. Bradić-Milinović.

Median fins: Only the first dorsal fin and the anterior part of the anal fin are preserved (Figures 22 and 25). From the first dorsal fin, the first six spines are preserved; the internal structure of the spines is compartmentalized (Figure 26); the first spine is short; the tips of the second to fourth spines are missing; the spines are moderately strong and, where visible, acute; the first dorsal fin originates dorsally to the fourth vertebra (Figure 22). The first four pterygiophores carry a single spine; the first two pterygiophores are long and strong; the following two decrease in length and strength gradually; the first pterygiophore inserts immediately anterior to the neural spine of the third vertebra, and the second inserts in the interneural space between the neural spines of the vertebrae 3–4 (Figure 25).

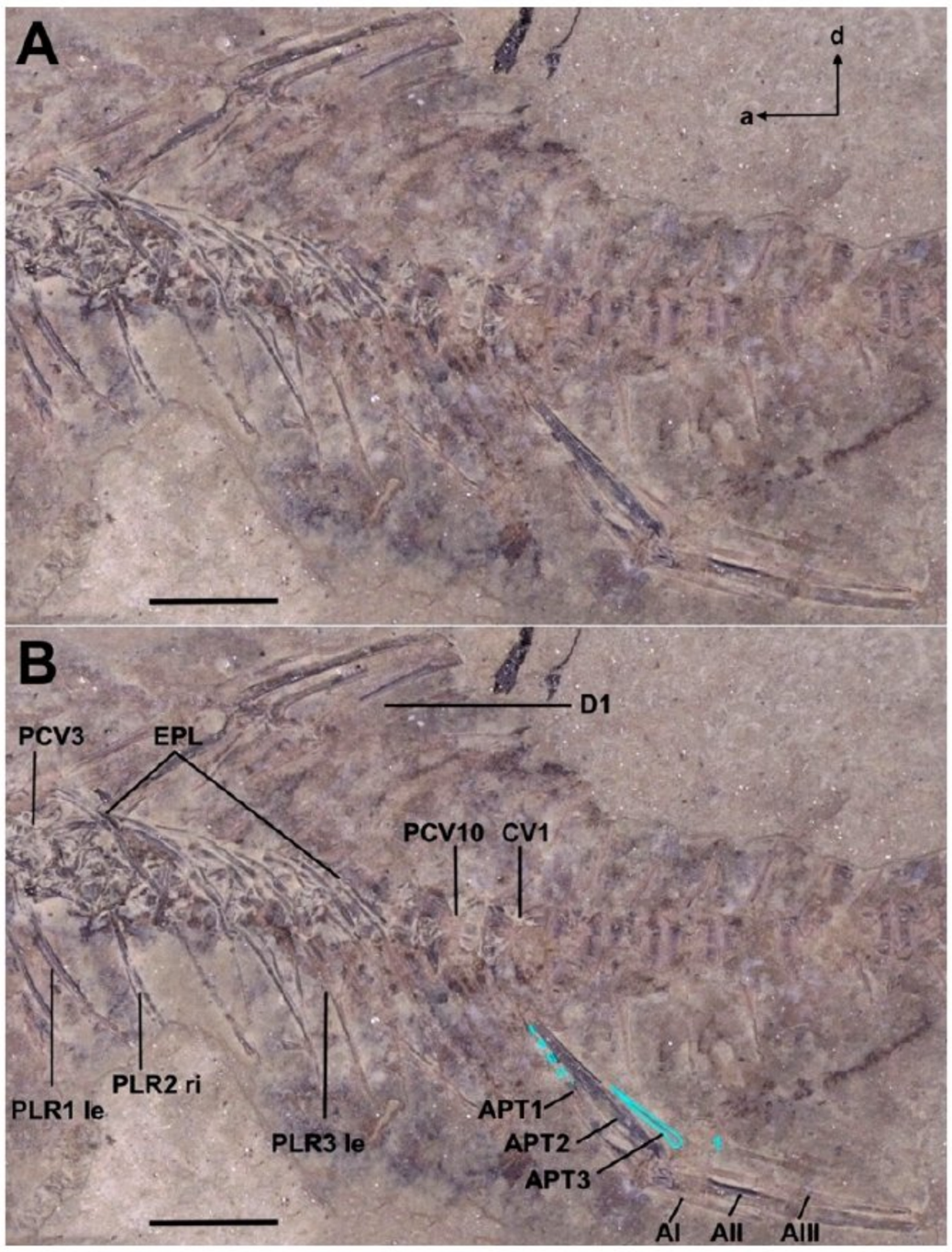

Figure 25. *Dapalis parvus* sp. nov., axial skeleton, GZS-RA34 (**A**). Labeling and outline of skeletal elements (**B**). AI–AIII = first to third anal fin spines; APT1–APT3 = first to third anal fin pterygiophores; CV1 = first caudal vertebra; D1 = first dorsal fin; EPL = epipleural rib; le = left; PLR = pleural rib; PCV10 = tenth (last) precaudal (abdominal) vertebra; ri = right. a = anterior; d = dorsal. Scale bars are 2 mm. Photo K. Bradić-Milinović.

Figure 26. *Dapalis parvus* sp. nov. (GZS-RA34), compartmentalization of the third and fourth spines of the first dorsal fin. External-most sheet of these spines is partly removed. Scale bar is 2 mm. Photo K. Bradić-Milinović.

The anal fin originates ventral to the third caudal vertebra (Figure 25); three spines precede the soft part of this fin; all three are moderately strong and acute; the first anal fin spine is relatively long (51.8% of the length of the second); the second spine is the strongest and longest and somewhat longer than the third spine (Figure 25); the spines are followed by a soft ray and the imprints of a further 3–4 soft rays. The pterygiophores of the first two spines are very long and strong, of about equal length and strength; distally, they are wider; proximally, they end in a narrow tip; both pterygiophores lie close together and form a long, narrow, club-shaped structure (Figure 25); the third pterygiophore is barely visible, narrow and shorter than the preceding two pterygiophores; these spine-bearing pterygiophores are strongly inclined posteriorly.

Otolith (*sagitta*): The otolith is 1.8 mm long and 1.4 mm high; the ratio of the otolith length to the otolith height is 1.36. It has a roundish shape. The otolith is deepest in the middle (Figure 27). Anteriorly, it is pointed; posteriorly, it is rounded. The rostrum is massive with a rounded tip and with symmetrical margins. The antirostrum is small and indistinct. The excisura is weakly expressed. The inner face of the otolith is convex; the outer face is nearly flat. The dorsal rim is strongly curved and smooth; the ventral rim is regularly curved and slightly undulating (Figure 27). The ventral furrow is indistinct and runs along, but somewhat distant to, the ventral rim. This furrow separates the ventral rim from the distinctly dome-shaped area of the inner face. This dome-shaped area extends dorsally to the ventral boundary of the sulcus. The anterior rim rises steeply. The posterior rim is rounded; there is a slight postcaudal depression (Figure 27).

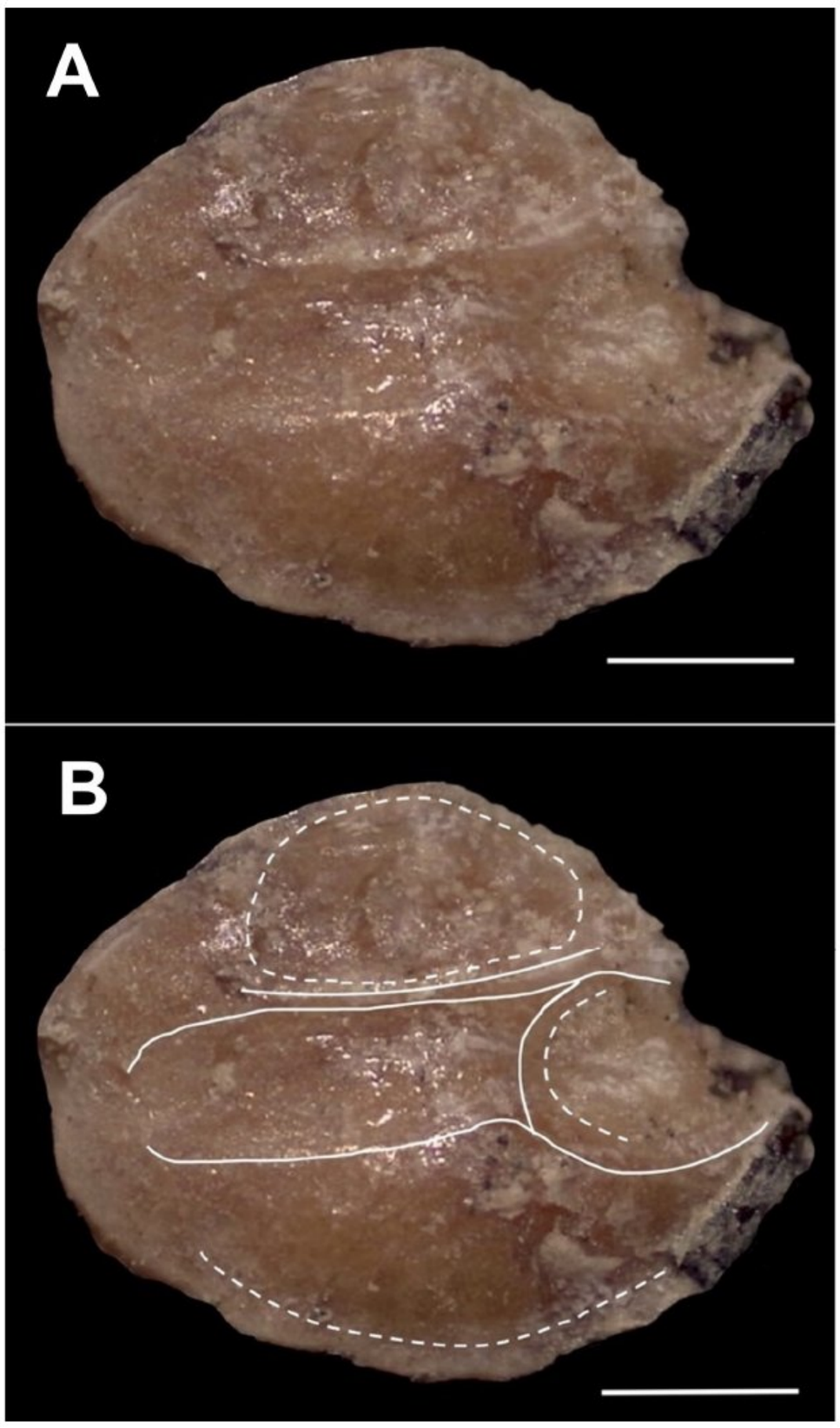

Figure 27. *Dapalis parvus* sp. nov. Otolith GZS-RA34, from holotype (**A**); interpretative outline of inner face (**B**). Scale bars are 0.5 mm. Photo K. Bradić-Milinović.

The overall shape of the well-defined sulcus differs from all other *Dapalis*. The ostium is large and roundish with both rims evenly expanded and wider than the cauda. The wide cauda is straight, is evenly wide along its length, is posteriorly gradually closed and ends distant to the posterior rim; the crista dorsalis, the dorsal boundary of the cauda, is elevated along about two-thirds of its length; the crista inferior, the ventral boundary, is indistinct and just slightly elevated (Figure 27). The ostium is nearly as long as the cauda; the ratio of the ostium length to the cauda length is 0.96. Although ending distantly to the posterior rim, the sulcus is relatively long; the ratio of the otolith length to the sulcus length is 1.22 (Table 4). Dorsal to the sulcus extends the short, oval and uniformly shaped dorsal depression; it reaches its greatest extent in its middle and is anteriorly and posteriorly of the same height; its dorsal boundary runs along but distant from the dorsal rim (Figure 27).

Table 4. Measurements (in mm) and calculations of the otoliths of the genus *Dapalis* from the early Oligocene. The values are from the holotypes, except for *D. macrurus* which are from [13,59]. SuL, OstL and CauL from *D. angustus*, *D. borkensis* and *D. transylvanicus* are calculated from photos of the holotypes; the holotype of *D. borkensis* is shown in Reichenbacher (1995, fig. 2I [47]); OL:OH, OL:SulL and OstL:CauL from *D. macrurus* are calculated from Weiler (1939, fig. 3 [13]) and [59], Figure 4. The vertical line separates measurements (to the left) from calculations (to the right). The new species are shown in bold. OL = length of otolith; OH = height of otolith; OT = width (thickness) of otolith; SulL = length of sulcus; OstL = length of ostium; CauL = length of cauda. [1] [2], [2] [3], [3] [13], [4] [59], [5] [4], [6] [18].

Species	N	OL	OH	OT	OL:OH	OL:OT	OL:SulL	OstL:CauL
D. angustus [1]	1	2.60	1.88	–	1.38	–	1.21	0.70
D. absconditus	**1**	**2.75**	**1.94**	**0.76**	**1.42**	**3.61**	**1.17**	**0.80**
D. borkensis [2]	1	2.10	1.50	–	1.40	–	1.16	0.68
D. macrurus [3]	1	–	–	–	1.39	–	1.24	0.96
D. macrurus [4]	1	1.47	1.03	–	1.43	–	1.15	–
D. octospinus	**1**	**2.10**	**1.32**	**0.50**	**1.59**	**4.20**	**1.17**	**0.82**
D. pauciserratus [5]	1	2.30	1.60	0.54	1.40	4.25	1.21	0.88
D. parvus	**1**	**1.85**	**1.36**	**0.39**	**1.36**	**4.74**	**1.22**	**0.96**
D. quintus	**1**	**2.09**	**1.33**	**0.44**	**1.57**	**5.25**	**1.12**	**0.65**
D. transylvanicus [6]	1	2.50	1.75	0.9	1.43	2.77	1.22	0.77

Dapalis quintus Bradić-Milinović and Ahnelt sp. nov. (Figures 28–31; Tables 2–4).
Holotype: registration number GZS-RA25 (Figure 28).

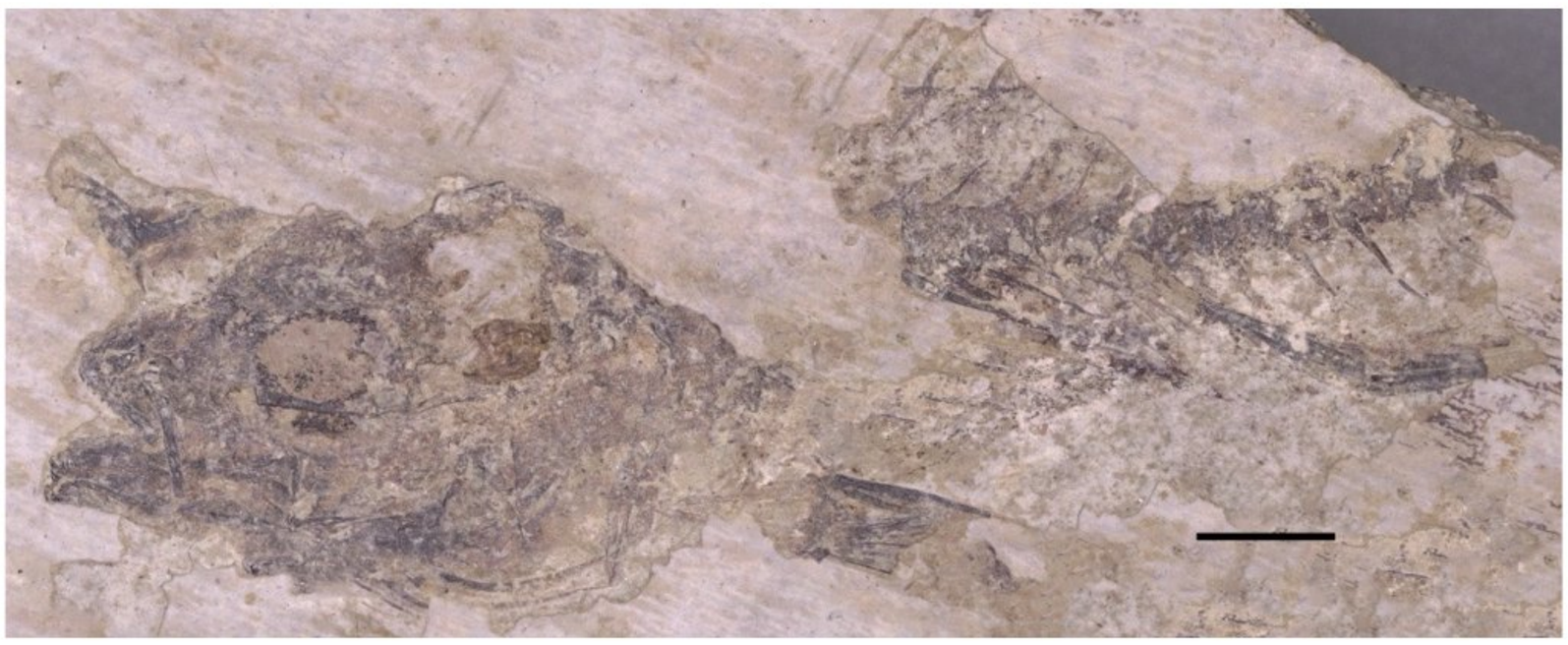

Figure 28. *Dapalis quintus* sp. nov., fragmented skeleton, holotype GZS-RA25. Scale bar is 2 mm. Photo K. Bradić-Milinović.

Type locality: Raljin, Babušnica basin, Serbia: 43°0′1″ N, 22°27′56″ E.
Distribution: only known from Raljin, Babušnica basin; early Oligocene, Rupelian.

Etymology: the new species is named *quintus* (Latin: the fifth), referring to *Dapalis quintus* being the fifth species reported from the Raljin/Strelac locality.

Diagnosis: *Dapalis quintus* is distinguished from its congeners by a combination of the following characters: preopercle with long, narrow and pointed spine-like serrations; otolith elongate (ratio of otolith length to height = 1.57) and thin (ratio of otolith length to otolith width = 5.25); a long sulcus (ratio of ostium length to sulcus length = 1.12) with the ostium distinctly shorter than the cauda (ratio of ostium length to cauda length = 0.65) (Table 4); cauda ending relatively close to the posterior rim; ventral furrow extends distant from ventral rim; and a well-expressed long and high ventral depression.

Dapalis quintus is distinguished from the remaining sympatric species of *Dapalis* from Raljin by (i) a preorbital with narrow and long spine-like serrations pointing anteriorly, (ii) an elongate and thick otolith, (iii) a distinct and pointed antirostrum, (iv) a short, narrow ostium and (v) a well-expressed long and high ventral depression anteriorly reaching to about the middle of the ostium and ventrally nearly reaching the distinct ventral furrow with no elevated area of the ventral field between the sulcus and ventral furrow.

Description: A slender and elongate species. Counts and measurements are reported in Tables 2 and 3. The skeleton of the specimen is only partly preserved, i.e., most of the head and parts of the postcranial skeleton. Most bones of the head are poorly preserved if at all, and the anterior and posterior parts of the postcranial skeleton with most fins are missing (Figures 28 and 29).

Neurocranium: Many bones are fragmented beyond recognition; the parasphenoid, the part in the orbit, is the only discernable bone of the neurocranium. Dorsal to the neurocranium, between the mouth and orbit, a fragment of a premaxilla can be seen, bearing strong canine teeth, which comes from another, unknown, fish species.

Circumorbitalia (suborbitalia + supraorbitalia): Just the preorbital (infraorbital 1 (lacrimal)) is discernable. It is elongated and oval, and its preorbital edge carries three long and narrow spine-like serrations increasing in length ventrally.

Jaws: The premaxilla is in large part preserved; two processes, the narrow ascending process and the wide articulating process, are discernible; tiny, villiform teeth are visible on the ventral edge of this bone (Figures 28 and 29). The maxilla is divided into two parts, a massive head which is partly fragmented and a long, straight shaft which is evenly wide along its entire length; the end of the maxillary shaft is straight (Figure 29).

The lower jaw is somewhat tilted to the left. The dentary carries a series of conical teeth: two small teeth at the symphysis followed by two canines, followed by five small conical teeth decreasing in size posteriorly. From the anguloarticular, the ventral edge and the articular fossa, which receives the articular process of the quadrate, are discernible.

Suspensory: the quadrate is the bone of the suspensory which is relatively well preserved, although just in parts, i.e., the anterior edge of the laminar main body, the articular process and the ventral edge of the laminar body which ends in a short, narrow ventroposterior extension where the quadrate contacts the preopercle (Figure 29).

Opercular series: from the opercular series, only the anterior edge of the opercle and the subopercle are recognizable as well as, in part, the massive preopercle; approximately the ventral half of the vertical arm of the preopercle and, in part, the horizontal arm, which is in close contact with the quadrate, are discernable; both arms incline in a relatively wide angle (>90°); the preopercular ridge is smooth; the ventral part of posterior edge (hind margin) of the vertical arm carries long, narrow and pointed spine-like serrations; the margin of the dorsal part is not discernable (Figure 29).

Hyoid bar and branchial basket: The ceratohyals are not well preserved; the anterior ceratohyal is club-shaped with a long and narrow anterior part and a short, laminar posterior part; the posterior ceratohyal is short and of about triangular shape; the hypohyals are visible at the tip of the anterior ceratohyal (Figure 29). Five branchiostegal rays are preserved; two rays are narrow, and the following three increase in width, with the posterior most of a blade-like shape (Figure 29). Anterior to the preopercle, six narrow and long gill rakers can be seen, which possibly are those of the first gill arch (Figure 29).

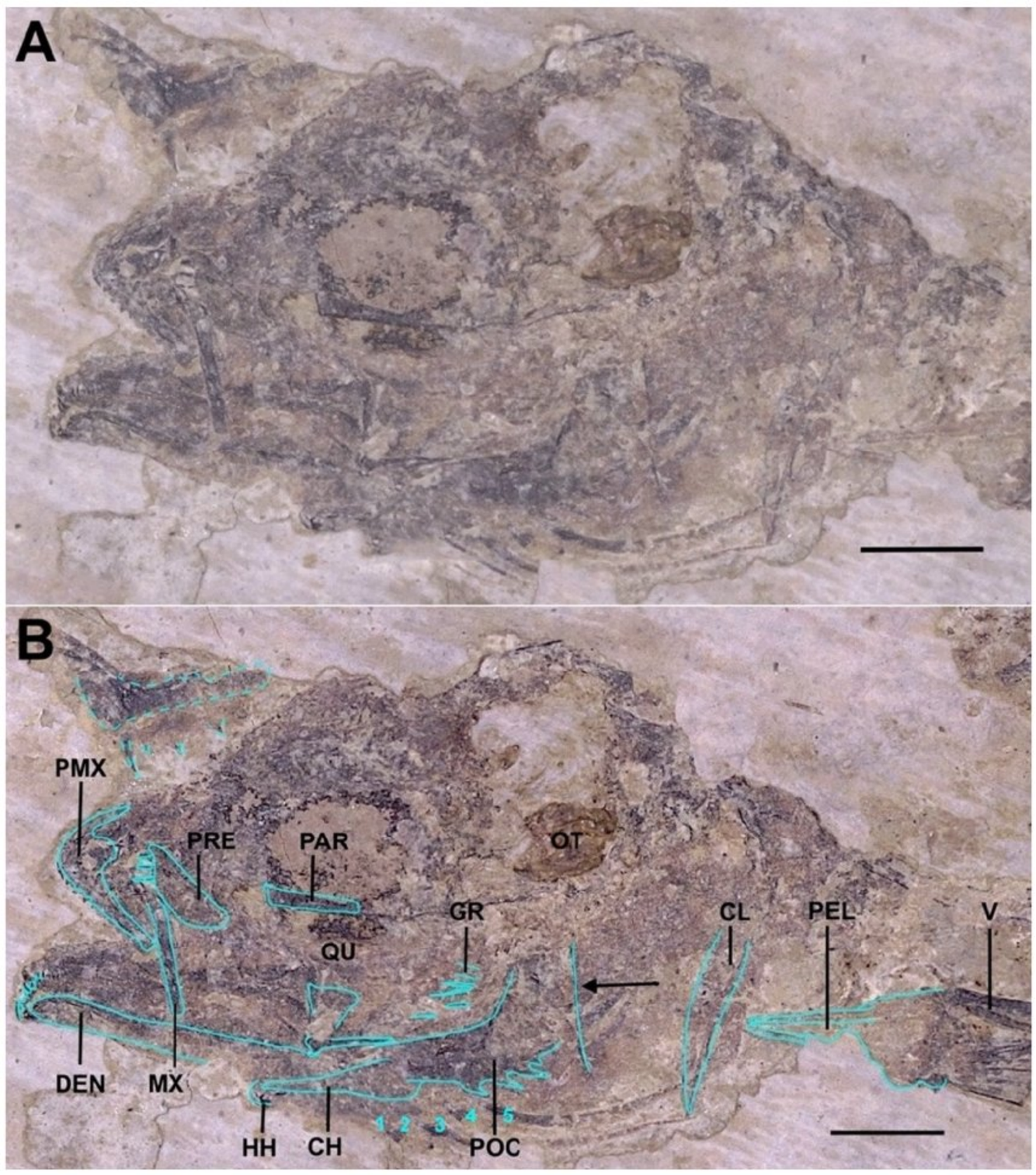

Figure 29. *Dapalis quintus* sp. nov., head of holotype GZS-RA25 (**A**). Outline of the skeletal elements (**B**). CH = ceratohyal; CL = cleithrum; DEN = dentary; GR = gill raker; HH = hypohyal; MX = maxilla; OT = otolith; PAR = parasphenoid; PEL = pelvis; PMX = premaxilla; PRE = preorbital (lacrimal); QU = quadratum; V = pelvic (ventral) fin. 1–5: first to fifth branchiostegal ray. The black arrow points to the anterior edge of the opercle. The premaxilla with large teeth, shown as dashed outline, dorsal to the head, is seemingly from another fish species. Scale bars are 2 mm. Photo K. Bradić-Milinović.

Axial skeleton: The axial skeleton is incompletely preserved; only five precaudal and six caudal vertebrae are visible, at least partly; the parapophysis of the last precaudal vertebra is triangular with the tip directed ventrally; a short pleural rib is attached at this parapophysis (Figure 30); the neural spines of the precaudal vertebrae are narrow and pointed, and the two on the ultimate and penultimate vertebrae are less inclined than the preceding ones; the neural spines of the caudal vertebrae 1–4 are missing, and those of the caudal vertebrae 5–6 are only partly preserved; the hemal spine of the first caudal vertebra is gall-like and widened immediately ventral to its base, possibly a hyperostotic structure; this hemal spine is in close contact with the posterior rim of the second pterygiophore of the anal fin (Figure 30).

Of the pleural ribs, ribs 5–8 are well discernible; imprints and fragments of ribs 1–4 are visible; the last, short pair of these ribs attaches to the triangular parapophysis of the last precaudal vertebra (Figure 30); no epipleural ribs are discernible.

Median fins: Parts of the first dorsal fin and parts of the anal fin are preserved. The spines 4–6 and their pterygiophores of the first dorsal fin are partly preserved (Figure 30).

From the anal fin, three spines and the origin of the first soft ray are partly preserved; from these spines, the tips are missing, and about a third of them are only present as imprints (Figure 30); the pterygiophores of these first two spines are very long and strong, of equal length and strength; distally, they are wider; proximally, they end in a narrow

tip (visible as an imprint); both pterygiophores lie close together and form a long, narrow, club-shaped structure in this way, which is in close contact with the hemal spine of the first caudal vertebra; the third pterygiophore is narrow and shorter than the preceding two pterygiophores; these spine-bearing pterygiophores are strongly inclined posteriorly.

Paired fins and girdles: The pectoral fin is missing; from the pectoral girdle, the long and straight cleithrum with a pointed end is preserved (Figure 29).

The pelvic fin and the pelvic girdle (basipterygia) are preserved, with the latter as an imprint; each basipterygium carries one spine and five soft rays; from the left pelvic fin, the spine and one fin ray are preserved; from the right pelvic fin, the base of the spine and five fin rays are preserved (Figure 30).

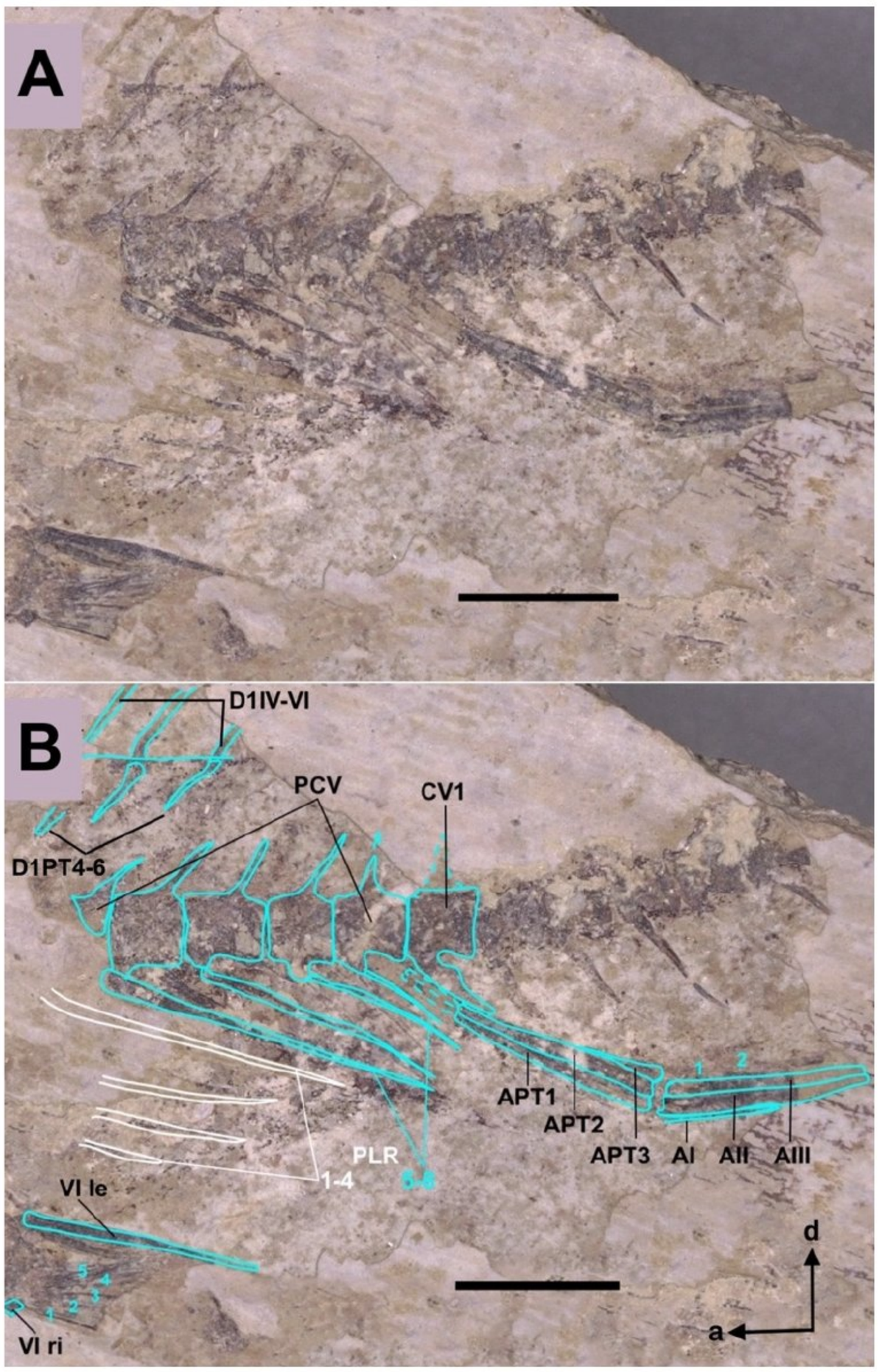

Figure 30. *Dapalis quintus* sp. nov., axial skeleton, GZS-RA25 (**A**). Labeling and outline of skeletal elements (**B**). AI–AIII = first to third anal fin spines; APT1–APT3 = first to third anal fin pterygiophores; CV1 = first caudal vertebra; D1IV-VI = fourth to sixth spines of the first dorsal fin; D1PT4-6 = fourth to sixth pterygiophore of the first dorsal fin; PCV = precaudal vertebra; PLR = pleural rib; VI le = left pelvic spine; VI ri = base of the right pelvic spine. Numbers 1 to 8 refer to the pleural ribs 1 to 8; imprints are shown in white. a = anterior; d = dorsal. Scale bars are 3 mm. Photo K. Bradić-Milinović.

Otolith (sagitta): The otolith is 2.1 mm long and 1.4 mm high; the ratio of the otolith length to the otolith height is 1.57. It has an oval and very elongated shape. It is highest

anteriorly to its middle and decreases in height posteriorly, resulting in a relatively low posterior end (Figure 31). The otolith is anteriorly distinctly pointed and posteriorly rounded. The symmetric rostrum is very pronounced, long and massive with a rounded tip. The antirostrum is short, massive and symmetrical. The excisura is distinct; however, its internal-most margin is marginally chipped. The inner and the outer face are convex, the inner face prominently, the outer face slightly. The dorsal rim rises steeply and continuously falls from the highest point. The ventral rim is regularly curved and undulating (Figure 31). The ventral furrow runs along the ventral rim. This furrow separates the ventral rim from the ventral depression of the ventral field; this depression is long, wide and covers most of the area ventral of the sulcus; anteriorly, it reaches approximately the middle of the ostium; there is no dome-shaped area between the sulcus and the ventral furrow, just a narrow but distinct rim (Figure 31). The posterior rim of the otolith is rounded; there is no postcaudal depression.

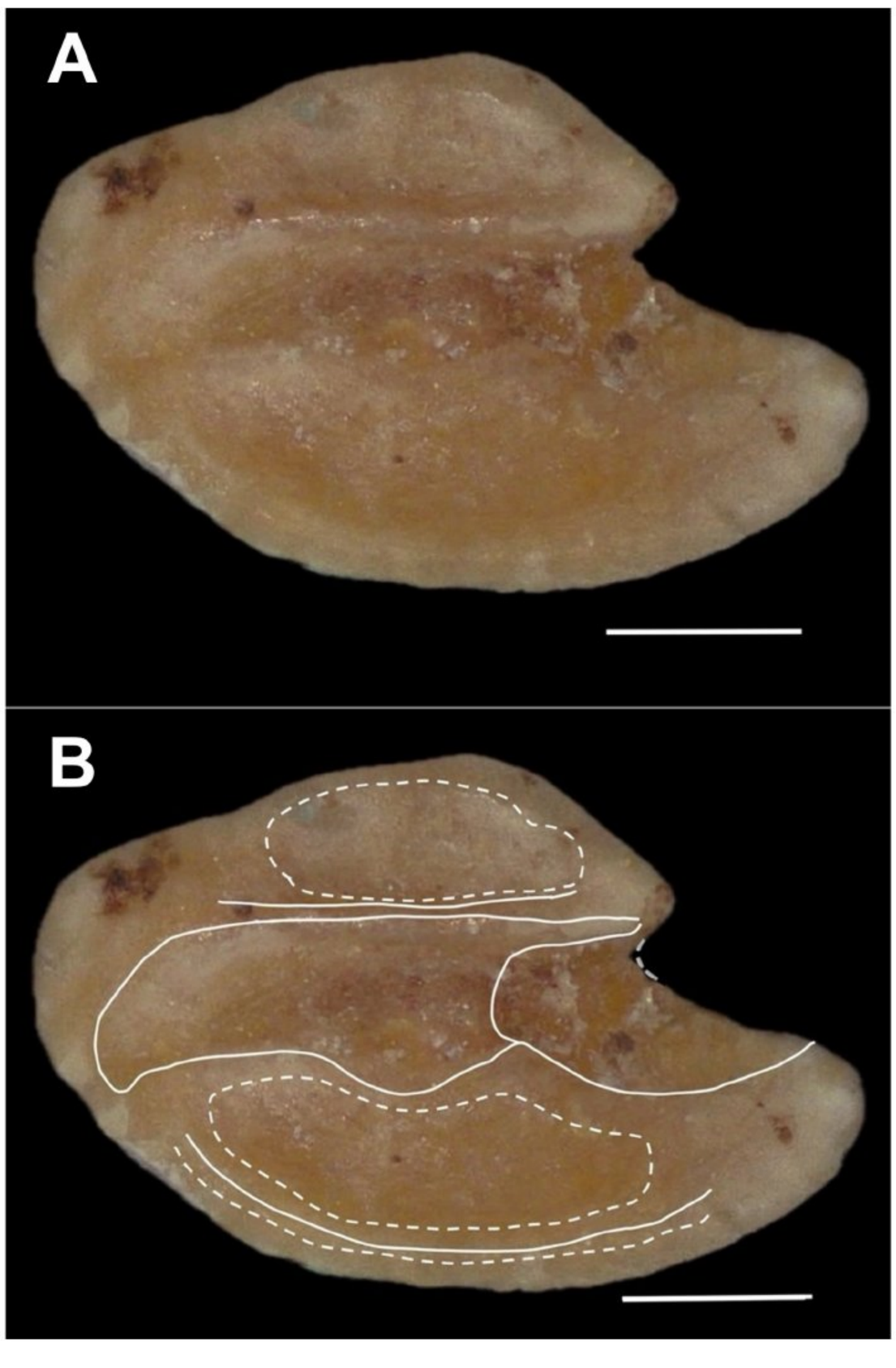

Figure 31. *Dapalis quintus* sp. nov. Otolith GZS-RA25, from holotype (**A**); interpretative outline of inner face (**B**). Dashed grey line is the interpretative outline of the excisura. Scale bars are 0.5 mm. Photo K. Bradić-Milinović.

The overall shape of the well-defined sulcus is characteristic of *Dapalis* [4,18]. The ostium is elongated; its dorsal rim is nearly straight, and its ventral rim is expanded; the ostium is of about the same width as the cauda. The cauda is straight, with a slightly flexed end anteriorly with a distinct ventral expansion following the wavy course of the crista inferior; it is posteriorly closed, ending close to the posterior rim; its terminal part is narrowed ventrally; the crista superior, the dorsal boundary of the cauda, is massive,

bulbous and elevated; the crista inferior, the ventral boundary, is well expressed but not distinctly elevated; about the anterior half of this crista is ventrally expanded (Figure 31). The ostium is shorter than the cauda; the ratio of the ostium length to the cauda length is 0.65. The ratio of the otolith length to the sulcus length is 1.12 (Table 4). On the dorsal field, dorsal to the sulcus, extends the elongated, oval dorsal depression; its dorsal boundary runs along the dorsal rim, anteriorly distant, from the highest point rearwards closer to the rim (Figure 31).

4. Discussion

With the description of the four new species, *D. absconditus*, *D. octospinus*, *D. parvus* and *D. quintus*, a total of twenty-one European *Dapalis* species are now documented, with nine of them from the early Oligocene (Table 1). None of these 21 species are known from marine facies. Species like *D. angustus*, *D. carinatus*, *D. crassirostris*, *D. kuehnior* and *D. rhomboidalis* are euryhaline and known from brackish and freshwater habitats [2,15,46,55]. In addition to the five species from Raljin, only *D. borkensis* (early Oligocene) [18] and *D. paecursor* (middle Miocene) [8] occurred exclusively in freshwater habitats [8]. Most *Dapalis* species were only documented as single species from the respective sites, e.g., [7,8,11,21,60–62]. Only a few species like *D. formosus*, *D. macrurus* or *D. minutus* occur sympatrically [1,2,14,18,19]. Therefore, the locality of Raljin (Babušnica basin) with five species represents the most species-rich assemblage of freshwater *Dapalis*.

The genus *Dapalis* is characterized by a series of similar morphological characters like, e.g., the number of caudal vertebrae, the number of anal fin spines or the otolith type [11,13,21,22] (Table 1). Obviously, a common character which unites *Dapalis* with the extant Ambassidae is the compartmentalization of the internal structure of the fin spines ([4], this study) (Figure 32). However, one challenge with fossil material is that the remains of a species are often incomplete or that traits that are visible in one species are not preserved in other species like, e.g., the squamation, the number of supraneurals or the length of spines in the specimens under study. Nevertheless, the five sympatrically occurring species from Raljin are unambiguously discriminable by a series of morphological characters present in all five species.

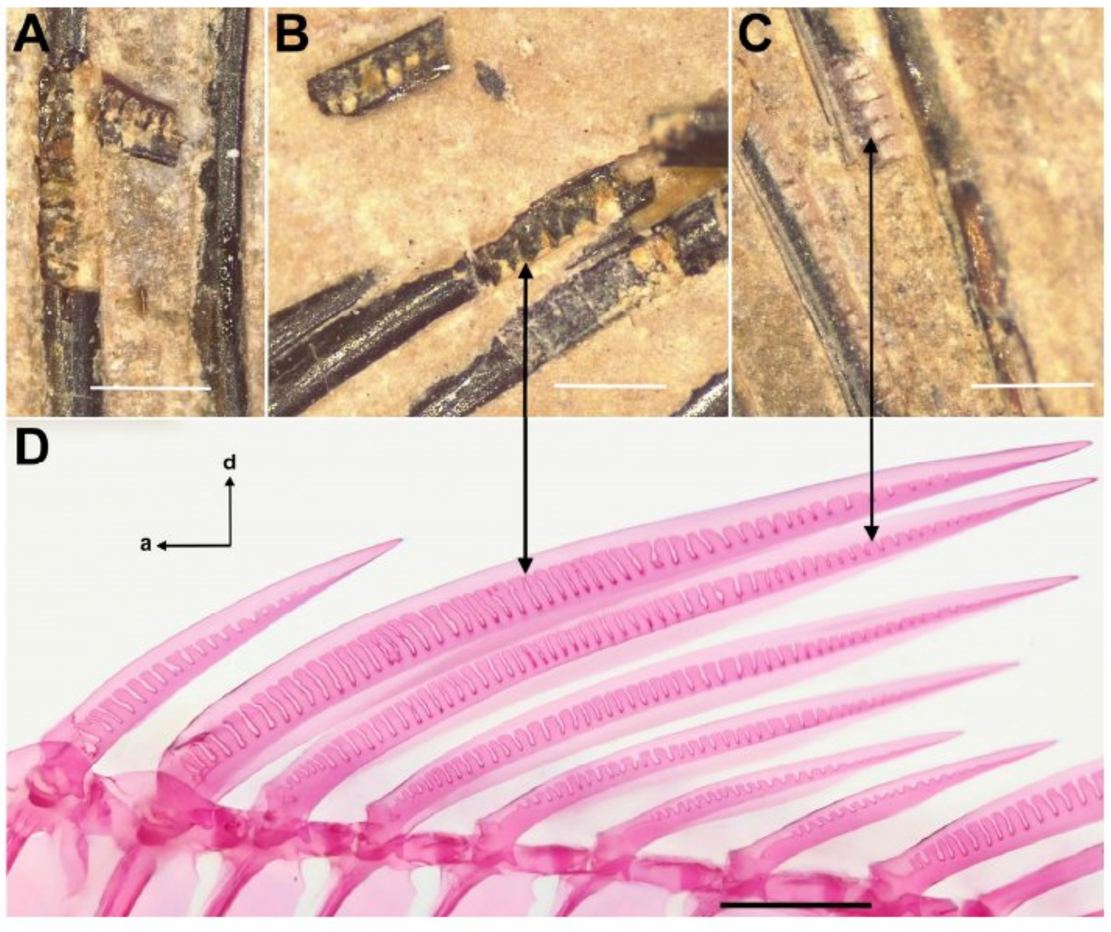

Figure 32. Compartmentalized internal structures of the dorsal fin spines of (**A**–**C**) extinct species of the genus *Dapalis* and (**D**) an extant species of the genus *Parambassis*. (**A**) *Dapalis absconditus* sp. nov. (GZS-RA3), (**B**) *Dapalis octospinus* sp. nov. (GZS-RA21), (**C**) *Dapalis parvus* sp. nov. (GZS-RA34) and (**D**) *Parambassis siamensis* (IE-15611). The arrows point to the compartmentalized internal structures of the dorsal spines. a = anterior; d = dorsal. Scale bars are 2 mm. Photos of (**A**–**C**) K. Bradić-Milinović; photo of (**D**) T. Moritz.

In addition to these five morphological characteristics, there are other traits that help to distinguish between the species, although they are only present in four out of five species: (i) the length of the first spine of the anal fin in relation to the second spine (shortest in *D. absconditus* and longest in *D. pauciserratus*), (ii) the length of the tail (longest in *D. parvus*, shortest in *D. octospinus*) or (iii) the head depth (deepest in *D. absconditus* and most narrow in *D. parvus*) (Table 2).

The new species from Raljin, including *D. pauciserratus* from the same locality, differ in the serration of the preopercle and preorbital and in the morphology of the otoliths from the congeners, *D. angustus*, *D. borkensis*, *D. macrurus* and *D. transylvanicus*. Compared to the only other species from the early Oligocene known from skeletons (*D. macrurus*), the most obvious difference is the serration of the bones of the head. Unfortunately, the specimens from Raljin are missing some of these diagnostic bones such as the interopercle or some circumorbital bones which are serrated in *D. macrurus* and also in extant Ambassidae (Figure 2). Nevertheless, the serration of the preopercle of *D. macrurus* is characteristic, with many densely set and narrow spine-like serrations along its entire length [4,60]. In contrast, these serrations are less numerous, more massive and larger in *Dapalis* species from Raljin. Again, unfortunately, only two otoliths of *D. macrurus* are known so far: an incomplete one with the antirostrum and excisura missing [13] and one of a juvenile specimen which is just figured [59]. Both were (re)classified as *D. macrurus* by [8] but differ distinctly in their morphology from each other (Table 4). A comparison with the otoliths of other *Dapalis* species is therefore problematic. Detailed descriptions of otoliths from adult *D. macrurus* specimens are urgently needed. The other three species from the early Oligocene, *D. angustus*, *D. borkensis* and *D. transylvanicus*, are only known from their otoliths [2,3,18] (Figure 33).

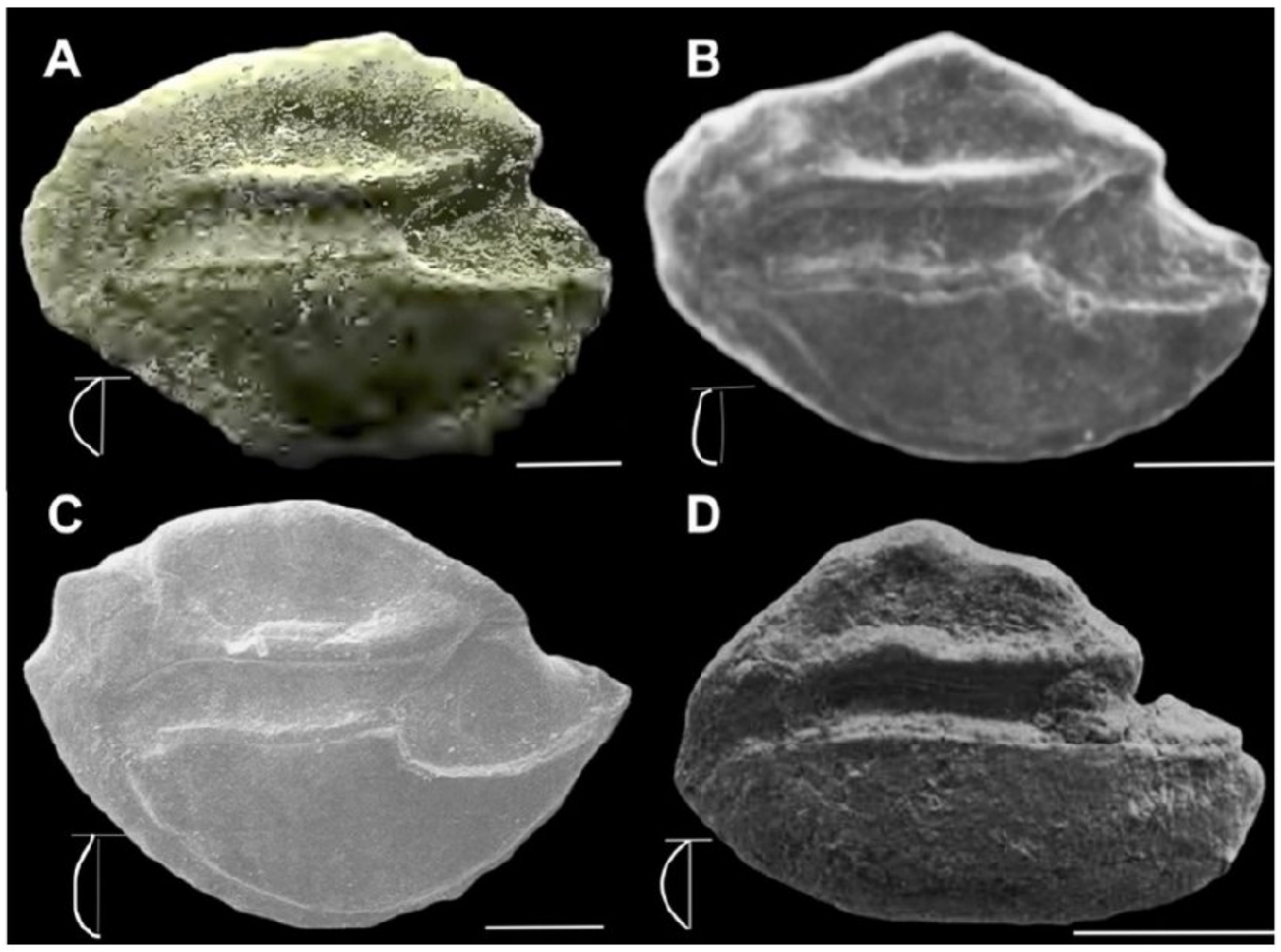

Figure 33. Otoliths from the early Oligocene. *Dapalis angustus* from [2] (**A**); *D. borkensis*, holotype from [3] (**B**); *D. transylvanicus*, holotype from [18] (**C**); and *D. macrurus* [59] (**D**). Sketches estimated from the photographs of the ventral area of the otoliths showing the interpretative surface relief: the horizontal arm of the "T" symbolizes the ventral boundary of the ostium, and the vertical arm of the "T" symbolizes the cross section through the otolith; the thick white line is the interpretative outline of the cross section. Scale bars are 0.5 mm.

The otoliths of *D. absconditus*, *D. octospinus* and *D. quintus* from Raljin are characterized by a unique trait, a ventral depression (Table 5).

This character separates these three species from their early Oligocene congeners which all have a dome-shaped ventral field (Figure 33), also in the sympatrically occurring

D. parvus and *D. pauciserratus* (Figure 34). Nevertheless, the latter two species differ from all other early Oligocene *Dapalis* by the overall shape of the otolith and by the shape of the sulcus (Figure 34C,E).

Additionally, the otolith of *D. transylvanicus* is unique as it is thick [18], the thickest of all nine species from the early Oligocene (Table 4). Its ventral outline is strongly convex, with its deepest point centered, and the antirostrum is indistinct, nearly missing. Like in *D. angustus* and *D. borkensis*, the ostium is shorter than in the congeners from Raljin, with the exception of *D. quintus*, which has the shortest ostium of all nine species (Table 4). With the exception of *D. parvus* with its round otolith, *D. angustus* and *D. transylvanicus* each have a very long sulcus. And, again with the exception of the otolith of *D. parvus*, the otolith of *D. angustus* is the narrowest of all (Table 4).

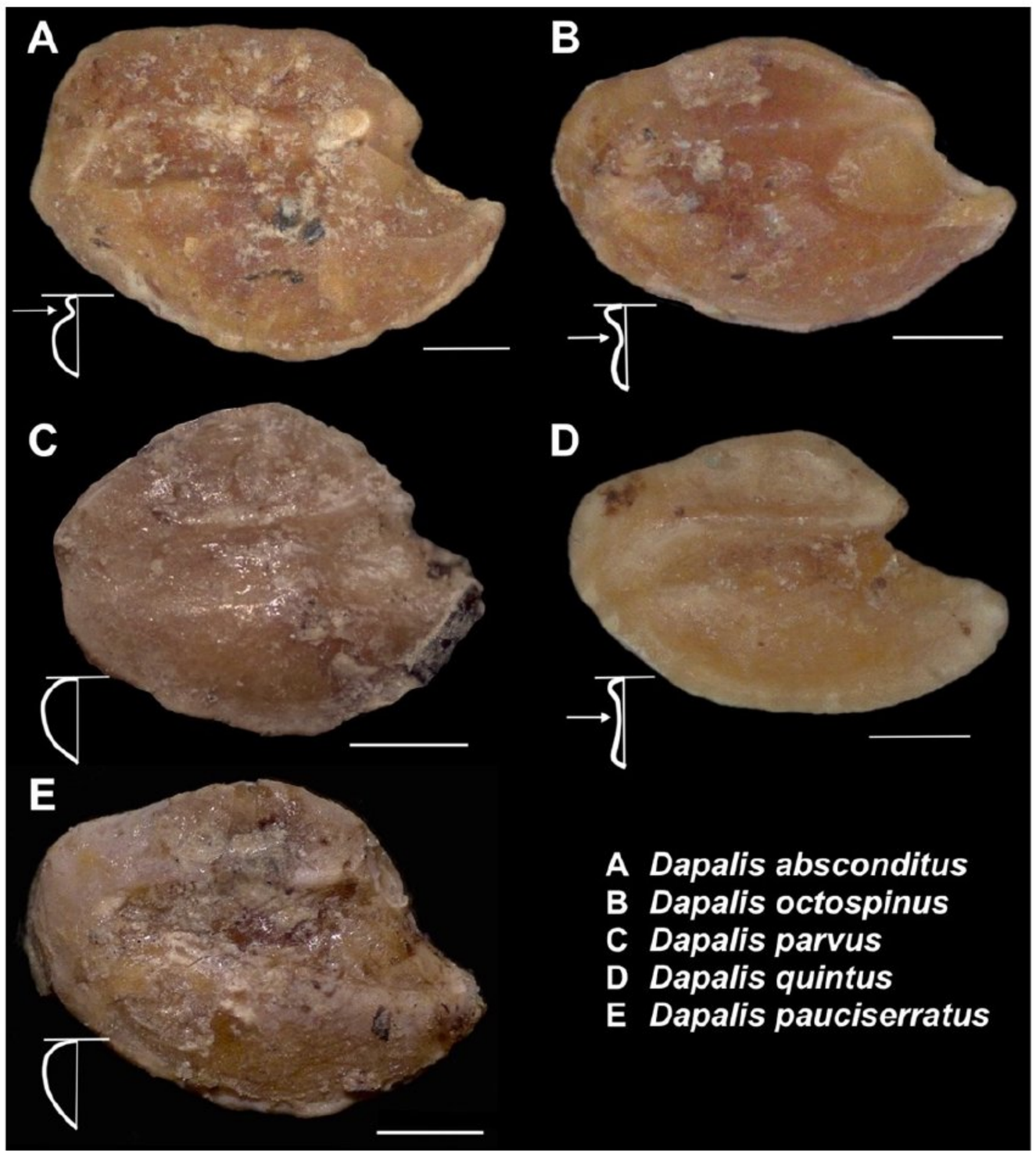

Figure 34. Otoliths of the five species of the genus *Dapalis* from the early Oligocene from Raljin/Strelac (Serbia) (**A**–**D**) and of *Dapalis pauciserratus*, holotype GZS-RA3 (**E**). Sketches of the ventral area of the otoliths showing the interpretative surface relief (**A**–**E**): the horizontal arm of the "T" symbolizes the ventral boundary of the ostium; the vertical arm of the "T" symbolizes the cross section through the otolith; the thick white line is the interpretative outline of the cross section with arrows pointing to the ventral depression (**A**,**B**,**D**). Scale bars are 0.5 mm. Photos K. Bradić-Milinović.

The majority of European *Dapalis* species are only documented from otoliths. Just nine of twenty-one species are described from skeletons, eight of them with otoliths in situ (Table 1). Therefore, the characters of the skeleton (serration of the interopercle, preopercle and circumorbitals and the relative length of the first dorsal and first anal fin spine) are important (summarized in [4]) but finally not key characters in comparing the entire assemblage of European *Dapalis*. Such key characters to distinguish *Dapalis* species are, so far, the characters of the sagittal otolith (shape and thickness, outline of the dorsal, ventral and posterior rim, expression of the rostrum and antirostrum, conspicuousness and

outline of the dorsal depression, shape of the cauda and the end of the cauda relative to the posterior rim).

An additional character is a depression in the ventral field of the otolith, the ventral depression. A survey of the descriptions and figures from the holotypes of the European *Dapalis* revealed that the otoliths of all species have a dorsal depression and that the ventral field, the part between the sulcus and the ventral furrow, is more or less distinctly convex, often dome-shaped (Figures 33 and 34, Table 5). However, in three species from Raljin (*D. quintus*, *D. absconditus* and *D. octospinus*), the ventral field of the otolith has a depression (Figures 10, 20, 31 and 34). This ventral depression is a unique character for these three *Dapalis* species and allows the separation of the Raljin assemblage of *Dapalis* into two species groups: group 1, with a ventral depression, *D. absconditus*, *D. octospinus* and *D. quintus*, and group 2, without a ventral depression and with an entirely elevated ventral field, *D. parvus* and *D. pauciserratus*.

Further otolith traits which support this separation of the Raljin *Dapalis* into two species groups are the length of the rostrum and the length of the sulcus. The rostrum is long in group 1 but shorter in group 2. The sulcus of the otolith of the species of group 1 is long, especially because of the long cauda (Table 4), and all three species have otoliths with long rostra (Figure 34A,B,D); the rostra of the species of group 2 are shorter (Figure 34C,E). According to Reichenbacher and Codrea [18], a "better developed rostrum" is a derived character. This separation into two groups could be supported by two morphometric characters: (i) the relation of the length of the first and second spine of the anal fin and (ii) of the dorsal fin. The first anal fin spine is distinctly shorter in two species of group 1, in *D. absconditus* and *D. octospinus* (the anal fin is missing in *D. quintus*), than in those of group 2 (*D. parvus* and *D. pauciserratus*) (Table 2). However, because these two characters are not present in all five species, they need verification.

Table 5. Presence/absence of a ventral depression of the sagittal otolith in the 21 European *Dapalis*; species in alphabetical order. § = no otoliths are documented. [1] [2], [2] [18], [3] [16], [4] [1], [5] [7], [6] [17], [7] [55], [8] [13], [9] [59], [10] [4], [11] [8].

Species	Ventral Depression
D. absconditus sp. nov.	+
D. angustus [1]	–
D. borkensis [2]	–
D. carinatus [3]	–
D. crassirostris [4]	–
D. curvirostris [4]	–
D. formosus [4]	–
D. hungaricus [5]	–
D. kaelini [6]	–
D. kuehni [7]	–
D. macrurus [8,9]	–
D. minutus	§
D. octospinus sp. nov.	+
D. parvus sp. nov.	–
D. pauciserratus [10]	–
D. praecursor [11]	–
D. quintus sp. nov.	+
D. rhenanus [9]	–
D. rhomboidalis [3]	–
D. transylvanicus [2]	–
D. ventricosus [5]	–

The otoliths of *Dapalis* closely resemble a generalized percoid otolith type [63]. This means that the sulcus is characterized by a wide, more or less rounded and deep ostium, followed by a long, narrow(er), shallow(er) and straight cauda (e.g., Figure 33A–C).

This type of otolith is also characteristic of the species from Raljin. Just the otolith of *D. parvus* differs insofar as the cauda is only slightly longer than the ostium and also relatively wide. The shape of the otolith of teleost fishes is closely linked to habitat and lifestyle, e.g., [64–67]. Since all five species from Raljin were found at the same location, the habitat in general seemingly had no or just a minor influence on the differences in the morphology of their otoliths. On the other hand, roundish otoliths are characteristic of species with a benthic lifestyle, and elongate otoliths with a pronounced rostrum are characteristic of more active swimming species [63,68]. If this holds true also for *Dapalis*, the roundish shape of the otoliths of *D. parvus* and *D. pauciserratus* could point to a less active swimming lifestyle and the elongate shape of the otoliths with a long rostrum of *D. octospinus* and *D. quintus* to a more active swimming lifestyle. Such differences in lifestyle and behavior could explain the high number of sympatrically occurring species in the freshwater habitat of Raljin. But it is likely that this assemblage of freshwater *Dapalis* from Raljin already disappeared early in the Oligocene because no species from younger strata with a ventral depression of the sagittal otolith have been found. However, a possible function of this ventral depression is unknown. Sand and Michelsen [69] showed that the center of the sagittal otolith moves at a lower frequency than the margin. It is possible that the reduction in the mass of the ventral field by a ventral depression influenced the motion of these otoliths. Additionally, otoliths with a smaller mass are believed to have a higher sensitivity to acceleration, e.g., during turns when the fish changes its body position [70]. But the trajectory of an otolith is not only influenced by its mass but also by its shape and by the surface relief. Even with identical mass, the trajectories of the otoliths differ with different surface relief [70]. This relief differs distinctly between species with or without a ventral depression (Figure 34). Comparison with extant taxa of Ambassidae could shed light on the evolution of the otoliths of glassfishes.

A close relationship of *Dapalis* with extant Ambassidae was proposed by [71] based on the morphology of the otoliths and by [71,72] based on osteological characters and is supported by the compartmentalization of the internal structure of the spines [4], as discussed in this study.

Extant species of the family Ambassidae are restricted to the Indo-West Pacific where they occur in marine, brackish and freshwater habitats [73]. Most fossil records of this family were documented from Europe from the early Eocene to the middle Miocene (Table 1). They are from freshwater and/or brackish water environments and are all placed in the genus *Dapalis*. A few records of ambassid fishes, all otolith-based, exist from shallow marine environments of the Eocene of New Zealand and were placed in the genus *Ambassis* sensu lato [74]. Two species from fluvio-lacustrine deposits of the Miocene of Thailand were provisionally placed in the genus *Parambassis* [71].

A recent study on the molecular phylogeny of the extant Ambassidae suggests that this family originated in the early Paleogene age (Paleocene to early Eocene) as marine fishes in the Indo-West Pacific [75]. This is consistent with the fossil records from marine facies of New Zealand [74]. This marine origin of Ambassidae requires multiple adaptation to environments of low salinity and has been found especially in lineages of European *Dapalis* which were confined to brackish and freshwater habitats [4,11,12,16,18,20,55,57].

5. Paleogeographic Considerations

When the first Ambassidae occurred in Europe during the middle and late Eocene [6–8], Europe was fragmented [76] (Figure 35), and freshwater habitats were island-bound with few primary freshwater fishes [5]. These habitats were repeatedly colonized by marine species including Ambassidae [5]. It is well documented that brackish and freshwater habitats are frequently invaded by extant Ambassidae [77]. We assume that the Raljin population under study represents such an isolated freshwater community, as this locality was located on an island covering today's Western Balkans and parts of Bulgaria. This *Dapalis* fauna is very unique in its morphology. It is possible that the Raljin species were a separate lineage of Ambassidae that invaded the Eocene and/or Oligocene of Europe

independently of other lineages. The articulated skeletons and the otoliths from these fishes allow a glimpse of a highly adapted population of a lost ambassid fish assemblage, similar to what has been described for the lost gobiid freshwater fish fauna of the early to middle Miocene of Europe [37].

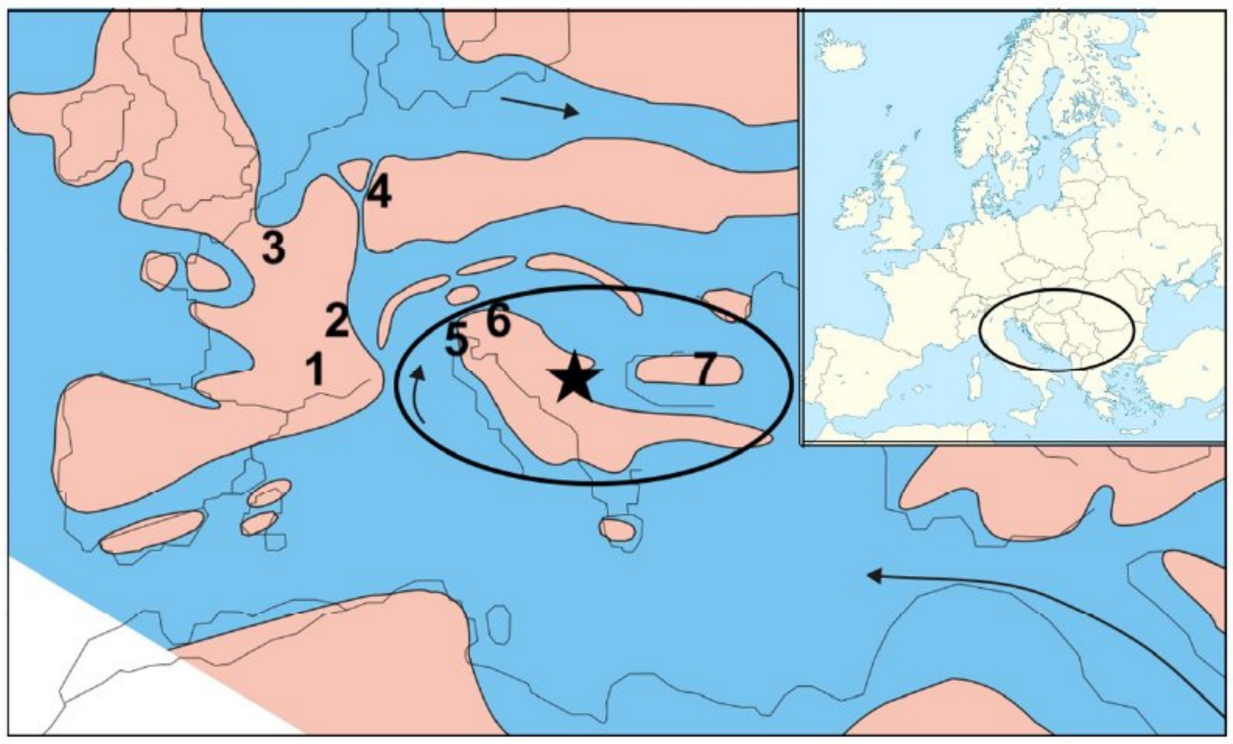

Figure 35. Central and Western Europe during the early Oligocene (Rupelian) based on Rögl [76]. The type localities of the *Dapalis* species described from the middle Eocene and early Oligocene of Europe are indicated. The islands of the early Oligocene shown in the figure are somewhat smaller in the Eocene but still present in a similar configuration in the early Oligocene [76]. Encircled is the island, which covered most of today's Western Balkans and parts of Bulgaria ("Western Balkan Island") and an island covering parts of today's Romania/Black Sea. This encircled area is also shown in the insertion, top right, which shows a political map of Europe. Star = Raljin, *Dapalis absconditus* sp. nov., *D. octospinus* sp. nov., *D. parvus* sp. nov., *D. pauciserratus* and *D. quintus* sp. nov. 1 = d'Apt, *D. macrurus*; 2 = Lovagny, *D. angustus*; 3 = Brasles, *D. praecursor*; 4 = Marburg and Kassel, *D. borkensis*; 5 = Ronca, *D. ventricosus*; 6 = Koșd, *D. hungaricus*; 7 = Cipcheș, *D. transilvanicus*. Black arrows = marine migrating routes [76].

6. Conclusions

Four new species of the extinct genus *Dapalis* (Ambassidae) from the early Oligocene from Raljin, Babušnica basin, Serbia, are described herein. Together with a fifth species, this is the largest assemblage of European freshwater *Dapalis* known so far and the largest assemblage of *Dapalis* with otoliths in situ. Two species groups can be distinguished, most obviously by the presence/absence of a ventral depression on the ventral field of the sagittal otolith. This character, a ventral depression, is unique to three of the new species and separates them from all other eighteen European *Dapalis* described to date. Paleogeographic considerations suggest that the assemblage of *Dapalis* from Raljin was isolated in a lacustrine freshwater habitat and had no close relationship to other congeners of the Eocene and the Oligocene. All these data enhance our understanding of the evolution and migration of *Dapalis* during the Oligocene.

Author Contributions: Conceptualization, K.B.-M. and H.A.; methodology, H.A. and K.B.-M.; validation, K.B.-M. and H.A.; formal analysis, H.A. and K.B.-M.; investigation, H.A. and K.B.-M.; writing—original draft preparation, H.A. and K.B.-M.; writing—review and editing, H.A. and K.B.-M.; visualization, H.A. and K.B.-M. All authors have read and agreed to the published version of the manuscript.

Funding: Open Access Funding by the University of Vienna.

Data Availability Statement: The original contributions presented in the study are included in the article, further inquiries can be directed to the corresponding author.

Acknowledgments: K.B.-M. thanks Žarko Petrović from Niš (Serbia) for assigning material of fossil fishes to the Geological Survey of Serbia and Zoran Marković and Anne van de Weerd for the

localization of the exact sampling locality. H.A. thanks U.B. Göhlich (Naturhistorisches Museum Wien) for making comparative material of *Dapalis minutus* and *Dapalis macrurus* available, E. Maxwell (Staatliches Museum für Naturkunde, Stuttgart), E. Bernard (Natural History Museum, London) and A. Pradel (Muséum national d'histoire naturelle, Paris) for photos of *Dapalis minutus*, *Dapalis macrurus* and *Dapalis formosus* and T. Moritz (Deutsches Meeresmuseum Stralsund), D. Pitassy (National Museum of Natural History, Washington) and Z. Randall (Florida Museum of Natural History, Gainesville) for photos of cleared and stained specimens of *Ambassis buruensis*, *Ambassis agrammus*, *Ambassis dussumieri*, *Ambassis macleayi*, *Gymnochanda ploegi*, *Parambassis piratica*, *Parambassis baculis*, *Parambassis lala* and *Parambassis siamensis*. We thank N. Bogutskaya for radiographs of *Ambassis ambassis*, *Ambassis agrammus*, *Ambassis buruensis*, *Ambassis dussumieri*, *Ambassis macleayi*, *Ambassis nalua*, *Ambassis natalensis*, *Chanda nama*, *Chanda ranga* and *Denariusa australis*. We also thank the three anonymous reviewers for constructive comments, which improved this manuscript.

Conflicts of Interest: The authors declare no conflicts of interest.

References

1. Reichenbacher, B. Die Fischfauna der Kirchberger schichten (Unter-Miozän) an der Typuslokalität Illerkirchberg bei Ulm. *Stuttgarter Beitr. Naturk. Ser. B* **1988**, *139*, 1–53.
2. Reichenbacher, B.; Weidmann, M. Fisch-Otolithen aus der oligo-miozänen Molasse der West-Schweiz und der Haute-Savoie (Frankreich). *Stuttgarter Beitr. Naturk. Ser. B* **1992**, *184*, 1–83.
3. Weiler, W. Die Fischfauna des unteroligozänen Melanientons und des Rupeltons in der Hessischen Senke. *Notizbl. Hess. L. Amtes Bodenforsch. Wiesbaden* **1961**, *89*, 44–65.
4. Ahnelt, H.; Bradić-Milinović, K.; Schwarzhans, W. *Dapalis pauciserratus*, a new species of freshwater glassfishes (Teleostei, Ambassidae) from the Lower Oligocene of the Central Paratethys. *Cybium* **2024**, *48*, 195–209. [CrossRef]
5. Popov, S.V.; Akhmetiev, M.A.; Bugrova, E.M.; Lopatin, A.V.; Amitrov, O.V.; Andreeva-Grigorovich, A.S.; Zherikhin, V.V.; Zaporozhets, N.I.; Nikolaeva, I.A.; Krasheninnikov, V.A.; et al. Biogeography of the Northern Peri-Tethys from the Late Eocene to the Early Miocene: Part. 1 Late Eocene. *Paleont. J.* **2001**, *35* (Suppl. S1), S1–S68.
6. Schubert, R. Die Fischotolithen der ungarischen Tiefebene. *Mitt. Jahrb. Königl. Ungar. Reichsanst.* **1912**, *20*, 117–139.
7. Nolf, D.; Reichenbacher, B. Fisch-Otolithen aus brackischen Faziesräumen aus dem Mittel-Eozän von Norditalien und Ungarn. Bull. l'Inst. *Royal Sci. Nat. Belgique Sci. Terre* **1999**, *69*, 187–196.
8. Gaudant, J. Découverte du plus ancien squelette de *Dapalis* (Poisson téléostéen, Percoidei) dans le Lutétien supérieur du Bassin de Paris. *Bull. Inf. Géol. Bass. Paris* **2007**, *44*, 3–8.
9. Agassiz, L. *Recherches sur les Poissons Fossils*; Petitpierre: Neuchátel, Switzerland, 1833; Volume 4, 296p.
10. von Meyer, H. Fossile Fische aus dem Tertiärthon von Unter-Kirchberg an der Iller. *Palaeontogr* **1952**, *2*, 85–113.
11. Weiler, W. Untersuchungen an der Fischfauna von Unter- und Oberkirchberg bei Ulm vornehmlich an Hand von Otolithen in situ. *Paläont. Z.* **1955**, *29*, 88–102. [CrossRef]
12. Gaudant, J.; Nel, A.; Nury, D.; Véran, M.; Carnevale, G. The uppermost Oligocene of Aix-en-Provence (Bouches-du-Rhône, Southern France): A Cenozoic brackish subtropical Konservat-Lagerstätte, with fishes, insects and plants. *C. R. Palevol.* **2018**, *17*, 460–478. [CrossRef]
13. Weiler, W. Über die systematische Stellung der fossilen Gattung *Smerdis* (Klasse Pisces) auf Grund neuerer Funde im Alttertiär Südwest-Bulgariens. *Zentralbl. Min. Geol. Paläontol. Abt. B* **1939**, *6*, 245–250.
14. Weiler, W. Die Fischfauna des Helvets von Ivančice (Eibenschitz) Mähren. *Paläont. Z.* **1966**, *40*, 118–143. [CrossRef]
15. Brzobohatý, B. Die Fischfauna des Südmährischen Untermiozäns. *Folia Fac. Sci. Nat. Univ. Purkynianae Brunensis 10 Geologia* **1969**, *17*, 1–49.
16. Stinton, F.C.; Kissling, D. Quelques otolithes de téléostéens de la Molasse oligocène de suisse occidentale. *Compt. Rend. Séanc. Soc. Phys. D'hist. Nat. Genève* **1968**, *3*, 140–154.
17. Reichenbacher, B. Mikrofaunen, Paläogeographie und Biostratigraphie der miozänen Brack-und Süßwassermolasse in der westlichen Paratethys unter besonderer Berücksichtigung der Fisch-Otolithen. *Senckenb. Lethaea* **1993**, *73*, 277–374.
18. Reichenbacher, B.; Codrea, V. Fresh- to brackish water fish faunas from continental Early Oligocene deposits in the Transsylvanian Basin (Romania). *Bull. L'Inst. Royal Sci. Nat. Belgique Sci. Terre* **1999**, *69*, 197–207.
19. Martini, E. Die Fischfauna von Langenau bei Ulm (Unter-Miozän, Ottnang-Stufe). *Stuttgarter Beitr. Naturk.* **1983**, *91*, 1–25.
20. Reichenbacher, B. Preliminary otolith-zonation in continental Tertiary deposits of the Paratethys and adjacent areas. *Neues Jahrb. Für Geol. Und Paläontologie Abh.* **1999**, *214*, 375–390. [CrossRef]
21. Bránkin, K.; Obrhelova, N.; Dimitrov, I. A find of *Dapalis macrurus* in the Oligocene sediments of West Marica coal basin. *Rev. Bulg. Geol. Soc.* **1983**, *64*, 194–197.
22. Gaudant, J. Présence des genres *Dapaloides* Gaudant et Dapalis Gistel (Poissons téléostéens, Percoidei) dans l'Oligo-Miocène lacustre de la Limagne bourbonnaise. *Bull. Mus. Natl. Hist. Nat. Paris* **1992**, *14*, 289–300.
23. Gaudant, J. Présence d'un Osmeridae: *Enoplophthalmus schlumbergeri* Sauvage, 1880 dans l'Oligocène inférieur des environs de Céreste (Alpes-de- Haute-Provence, France). *Geodiversitas* **2013**, *35*, 345–357. [CrossRef]

24. Bieńkowska-Wasiluk, M.; Paldyna, M. Taxonomic revision of the Oligocene percoid fish *Oligoserranoides budensis* (Heckel, 1856), from the Paratethys and paleobiogeographic comments. *Geol. Acta* **2018**, *16*, 75–92. [CrossRef]
25. Argyriou, T. The fossil record of ray-finned fishes (Actinopterygii) in Greece. In *Fossil Vertebrates of Greece*; Vlachos, E., Ed.; Springer Nature: Berlin/Heidelberg, Germany, 2022; Volume 1, pp. 91–142. [CrossRef]
26. Schultz, O. Ein Zackenbarsch (*Epinephelus*, Serranidae, Pisces) aus dem Mittel-Miozän von Retznei, Steiermark. *Joannea Geol. Und Paläontologie* **2000**, *2*, 5–56.
27. Gaudant, J. Mise aupoint sur les Vertebras inferieurs de l'Oligocene de Sieblos (Hesse, Allemagne). *Compt. Rend. L'Acad. Sci. Paris (II)* **1985**, *300*, 185–188.
28. Pantić, N. Biostratigraphy of the Tertiary floras from Serbia. *Ann. Geol. Pénin. Balkanique* **1956**, *24*, 199–317. (In Serbian)
29. Anđelković, J. Tertiary fishes of Serbia. *Ann. Geol. Penin. Balkanique* **1970**, *35*, 281–366.
30. Anđelković, J. On the fossil fish from the freshwater sediments of the Valjevo-Mionica Basin. *Ann. Geol. Penin. Balkanique* **1978**, *42*, 393–403, (In Serbian with English Summary).
31. Anđelković, J. Tertiary fishes of Yugoslavia. A stratigraphic-paleontologic-paleoecological study. *Palaeontol. Jugoslav.* **1989**, *38*, 1–121.
32. de Bruijn, H.; Marković, Z.; Wessels, W.; Milivojević, M.; van de Weerd, A.A. Rodent faunas from the Paleogene of south-east Serbia. *Palaeobio. Palaeoenv.* **2018**, *98*, 441–458. [CrossRef]
33. Wessels, W.; van Weerd, A.A.; de Bruijn, H.; Marković, Z. Dipodidae (Mammalia, Rodentia) from the Paleogene of south-east Serbia. *Palaeodiv Palaeoenv.* **2020**, *100*, 841–848. [CrossRef]
34. van de Weerd, A.A.; de Bruijn, H.; Wessels, W.; Marković, Z. New late Oligocene rodent faunas from the Pannonian basin. *Palaeodiv. Palaeoenv.* **2022**, *102*, 465–492. [CrossRef]
35. Marković, Z.; Wessels, W.; Weerd, A.; Brujin, H. Pseudocricetodontinae (Mammalia, Rodentia) from the Paleogene of south-east Serbia. *Palaeobiodiv. Palaeoenv.* **2020**, *100*, 251–267. [CrossRef]
36. Gaudant, J. L'ichthyofaune des eaux continentals miocènes de Serbie (Yougoslavie): Un revision. *Neues Jahrb. Für Geol. und Paläontologie-Abh.* **1998**, *207*, 107–123. [CrossRef]
37. Bradić-Milinović, K.; Ahnelt, H.; Rundić, L.; Schwarzhans, W. The lost freshwater goby fish fauna (Teleostei, Gobiidae) from the early Miocene of Klinci (Serbia). *Swiss J. Plaeont.* **2019**, *138*, 285–315. [CrossRef]
38. Marović, M.; Toljić, M.; Rundić, L.; Milivojević, J. *Neoalpine Tectonics of Serbia*; Serbian Geological Society: Belgrade, Serbia, 2007; pp. 1–87.
39. Zagorchev, I. Introduction to the geology of SW Bulgaria. *Geol. Balcan.* **2001**, *31*, 3–52. [CrossRef]
40. Anđelković, M.; Pavlović, M.; Eremija, M.; Anđelković, J. Palaeogeographic-stratigraphic development of the Oligocene and Miocene lacustrine basins in Eastern Serbia. *Ann. Geol. Pénin. Balkan.ique* **1988**, *52*, 1–35.
41. Mihajlović, D.S. Paleogene fossil flora of Serbia. *Ann. Geol. Penins. Balkan.* **1985**, *49*, 399–434, (In Serbian with English Summary).
42. Petcović, K. *On the Tectonic Composition of Eastern Serbia*; Herald SKA: Southampton, UK, 1930; 140p.
43. Dimitrijević, M.; Karamata, S.; Sikošek, B.; Veselinović, D. Basic Geological Map of SFRY 1:100000, Vlasotince Sheet (K34-45). *Fed. Geol. Surv. Belgrade* **1973**, 1–69. (In Serbian)
44. Dimitrijević, M.; Dragić, D.; Karamata, S.; Sikošek, B.; Veselinović, D. Basic Geological Map of SFRY 1:100000, Pirot Sheet (K 34-34) and Breznik Sheet (34-46). *Fed. Geol. Surv. Belgrade* **1977**, 1–69. (In Serbian)
45. Dimitrijević, M.; Dragić, D.; Karamata, S.; Sikošek, B.; Petrović, B.; Veselinović, D. Basic Geological Map of SFRY 1:100000, Bela Palanka Sheet (K 34-33). *Fed. Geol. Surv. Belgrade* **1980**, 1–69. (In Serbian)
46. Pirkenseer, C.; Berger, J.-P.; Reichenbacher, B. The position of the Rupelian/Chattian boundary in the southern Upper Rhine Graben based on new records of microfossils. *Swiss J. Geosci.* **2013**, *106*, 291–301. [CrossRef]
47. Reichenbacher, B. Unteroligozäne Fische (Otolithen) aus dem Neuwieder Becken (Rheinisches Schiefergebirge, West-Deutschland). *Paläont. Z.* **1995**, *69*, 241–255. [CrossRef]
48. Martini, E. Die Fischfauna von Sieblos/Rhön (Oligozän). *Senckenb. Lethaea* **1965**, *46*, 291–314.
49. Fraser-Brunner, A. A synopsis of the centropomid fishes of the subfamily Chandidae, with description of a new genus and two new species. *Bull. Raffles Mus.* **1954**, *25*, 185–213.
50. Martin, T.J.; Heemstra, P.C. Identification of *Ambassis* species (Pisces: Perciformes, Ambassidae) from South Africa. *S. Afr. J. Zool.* **1988**, *23*, 7–12.
51. Ahlstrom, E.H.; Butler, J.L.; Sumida, B.Y. Pelagic stromateoid fishes (Pisces, Perciformes) of the Eastern Pacific: Kinds, distributions, and early life histories and observations on five of these from the Northwest Atlantic. *Bull. Mar. Sci.* **1976**, *26*, 285–402.
52. Reichenbacher, B. Biota, Palaeoenvironments and biostratigraphy of continental Oligocene deposits of the southern German Molasse basin (Penzberg Syncline). *Palaeontology* **2004**, *47*, 639–677. [CrossRef]
53. Reichenbacher, B.; Krijgsman, W.; Lataster, Y.; Pippérr, M.; Van Baak, C.G.C.; Chang, L.; Kälin, D.; Jost, J.; Doppler, G.; Jung, D.; et al. A new magnetostratigraphic framework for the Lower Miocene (Burdigalian/Ottnangian, Karpatian) in the North Alpine Foreland Basin. *Swiss J. Geosci.* **2013**, *106*, 309–334. [CrossRef]
54. Reichenbacher, B.; Cappetta, H. First evidence of an early Miocene marine teleostean fish fauna (otoliths) from La Paillade (Montpellier, France). *Palaeovertebrata* **1999**, *28*, 1–46.
55. Weinfurter, E. Die miozäne Otolithenfauna von St. Veit an der Triesting, NÖ. *Ann. Naturhist. Mus. Wien* **1967**, *71*, 381–393.

56. van Hinsbergh, W.M.V. Fish otoliths from euryhaline Oligocene deposits in Belgium (Atuatuca Formation) and the Netherlands (Goudsberg Deposits) and their paleoecological importance. *Meded. Werkgr. Tert. Kwart. Geol.* **1980**, *17*, 199–223.
57. Reichenbacher, B. Das brackisch-lakustrine Oligozän und Unter-Miozän im Mainzer Becken und Hanauer Becken: Fischfaunen, Paläoökologie, Biostratigraphie, Paläogeographie. *Cour. Forsch. Inst. Senckenberg* **2000**, *222*, 1–143.
58. Weiler, W. Die Fischfauna des Tertiärs im ober-rheinischen Graben, des Mainzer Beckens, des unteren Maintales und der Wetterau, unter besonderer Berücksichtigung des Untermiozäns. *Abh. Senckenberg. nuturforsch. Ges.* **1963**, *504*, 1–75.
59. Malz, H. Aquitane Otolithen-Horizonte im Untergrund von Frankfurt am Main. *Senckenb. Lethaea* **1979**, *58*, 451–471.
60. Gaudant, J.; Guillevin, Y. Découverte de *Dapalis* (=*Smerdis*) *macrurus* (Ag.) (Poisson téléostén) dans l'Oligocène du Bassin de Valence (Drôme): Implications stratigraphiques et paléoécologiques. *Bull. Mus Natn. Hist Nat. Paris* **1979**, *1*, 25–33.
61. Gaudant, J. Sur les conditions de Gisement de l'Ichthyofaune Oligocene d'Aix-en-Provence (Bouches-du-Rhone): Essai de definition d'un modele paleoecologique et paleographique. *Géobiosis* **1978**, *11*, 393–397. [CrossRef]
62. Uhlig, U.; Reichenbacher, B.; Bassler, B. Säugetiere, Fisch-Otolithen und Charophyten aus den Unteren Cyrenen-Schichten (Oligozän) der bayrischen Faltenmolasse (Murnauer Mulde). *Ecol. Geol. Helvet.* **2000**, *93*, 503–516. [CrossRef]
63. Nolf, D. A survey of perciform otoliths and their interest for phylogenetic analysis, with an iconographic synopsis of Percoidei. *Bull. Mar. Sci.* **1993**, *52*, 220–239.
64. Schwarzhans, W. Otolith-morphology and its usage for higher systematical units, with special reference to the Myctophiformes s.l. *Meded. Werkgr. Tert. Kwart. Geol.* **1978**, *15*, 167–185.
65. Schulz-Mirbach, T.; Ladich, F.; Plath, M.; Heß, M. Enigmatic ear stones: What we know about the functional role and evolution of fish otoliths. *Biol. Rev.* **2019**, *94*, 457–482. [CrossRef] [PubMed]
66. Bose, A.P.H.; Zimmermann, H.; Winkler, G.; Kaufmann, A.; Strohmeier, T.; Kolblmüller, S.; Sefc, K.M. Congruent geographic variation in saccular otolith shape across multiple species of African cichlids. *Scientif. Rep.* **2020**, *10*, 12820. [CrossRef] [PubMed]
67. Schwarzhans, W.; Gerringer, M.E. Otoliths of the deepest-living fishes. *Deep-Sea Res.* **2023**, *198*, 104079. [CrossRef]
68. Volpedo, A.; Echeverría, D.D. Ecomorphological patterns of the sagitta in fish on the continental shelf off Argentine. *Fish. Res.* **2003**, *60*, 551–560. [CrossRef]
69. Sand, O.; Michelsen, A. Vibration measurements of the perch saccular otolith. *J. Compar. Physiol.* **1978**, *123*, 85–89. [CrossRef]
70. Kasumyan, A.O. The vestibular system and sense of equilibrium in fish. *J. Ichthyol* **2004**, *44* (Suppl. S2), 224–268.
71. Roberts, T.S.; Jumnongthai, J. Miocene fishes from lake Phetchabun in north-central Thailand, with descriptions of new taxa of Cyprinidae, Pangasidae and Chandidae. *Nat. Hist. Bull. Siam Soc.* **1999**, *47*, 153–189.
72. Gaudant, J. Sur la présence de Chandidae (Possions téléostéens, Percoidei) das le Cénozoïque européen. *C. R. Acad. Sc. Paris* **1987**, *304*, 1249–1252.
73. Anderson, M.E.; Heemstra, P.C. Review of the glassfishes (Perciformes: Ambassidae) of the Western Indian Ocean. *Cybium* **2003**, *27*, 199–209.
74. Schwarzhans, W. Reconstruction of the fossil marine bony fish fauna (Teleostei) from the Eocene to Pleistocene of New Zealand by means of otoliths. *Mem. Soc. Ital. Sci. Nat. Mus. Stor. Nat. Milano* **2019**, *46*, 3–326.
75. Ghazali, S.Z.; Lavoué, S.; Jamaluddin, J.A.F.; Abu Hassan Alshari, N.F.M.; Zain, K.; Azizah, M.N.S. Phylogenetic niche conservatism hypothesis in the fish family Ambassidae (Teleostei; Percomorphaceae). In Proceedings of the 2nd ICFAES 2019 International Conference on Fisheries, Aquatic and Environmental Sciences 2019, Syiah Kuala University, Darussalam, Banda Aceh, Indonesia, 19–20 June 2019. [CrossRef]
76. Rögl, F. Palaeogeographic considerations for Mediterranean and Paratethys seaways (Oligocene to Miocene). *Ann. Naturhistorischen Mus. Wien. Ser. A Für Mineral. und Petrogr. Geol. und Paläontologie Anthropol. und Prähistorie* **1998**, *99*, 279–310.
77. Roberts, T. Systematic revision of the tropical Asian freshwater glassperches (Ambassidae), with descriptions of three new species. *Nat. Hist. Bull. Siam Soc.* **1994**, *42*, 263–290.